Expression and Allosteric Regulation of Calcium Channel and Effect of Ulip-1 on Neurogenesis in the Adult Hippocampus

By

Shirin Manouchehri

A Thesis submitted in conformity with the requirements
For the degree of Doctor of Philosophy,
Graduate Department of Physiology
University of Toronto

ABSTRACT

Expression and Allosteric Regulation of Calcium Channel and Effect of Ulip-1 on Neurogenesis in the Adult Hippocampus

Shirin Manouchehri Supervisor: Dr. M. J. Wojtowicz

This thesis is an investigation of factors involved in the processes of neurodegeneration and neurogenesis in the brain. Three aspects of research were chosen for study in detail. Voltage-dependent calcium channels (VDCCs) are diverse heteromeres that mediate various cellular functions. One major VDCC- the L-type (L-VDCC), is thought to play a role in neurodegeneration and is essential in regulating the influx of calcium into the aging neurons. The expression level of L-VDCCs was investigated in rat aged hippocampus, cortex and cerebellum using specific antibodies, and 3H-isradipine binding assay. The expression level of the $\alpha_2\delta$ subunit was increased in the aged hippocampus. However, the expression levels of β_3 did not change significantly in the studied regions. The overall density of L-VDCCs did not change. The second topic in this thesis is, the allosteric regulation of calcium channels. Affinity chromatography in conjunction with other techniques such as spectrofluorimetry, radiolabelling, and circular dichroism were used to detect ATP binding and allosteric regulation of the channel. The results indicate that there is no affinity between the fusion protein and Mg-ATP. The third topic in this thesis is the mechanism underlying adult neurogenesis in the hippocampus of Ulip-1 knockout mouse. Ulip-1 protein is highly expressed during neurogenesis in hippocampus. Immunolabelling with Ki67 (a proliferative marker) revealed differences in hippocampal cellular proliferation between -

/-, -/+ and +/+ mice. An increased number of Ki67+ cells was found within the proliferative zone (SGZ) of the DG of Ulip-1 knockout mice. Using doublecortin, a marker of immature neurons, it was shown that the number of the cells was markedly increased in -/- mice. Calbindin a marker for mature neurons, showed that intrapyramidal mossy fibers have a defasiculated appearance in CA3 region in -/- mice. These results suggest the involvement of Ulip-1 in cell proliferation and axonal development within the hippocampus.

ACKNOWLEDGEMENT

I would like to thank my supervisor Dr. Martin J. Wojtowicz for his academic guidance and support during the course of this thesis. I would also like to thank my supervisory committee members professor Harold Atwood; and Dr. Linda Mills for their critical comments, guidance and helpful discussions. I am very grateful for the advice and assistance of Dr. Maire Percy for the final revision of this thesis. I am indebted to Drs. Jennifer Griffin, Roman Pekhletski, John Glover, D.E. Isenman, Massimo Marcone and Thetin Nguyen for their technical guidance and help for the second chapter of this thesis.

A special thanks to Dr. Susan Rainey for her friendship, support and comments. Many thanks to my entire lab members, past (Sharon) and present (Marianne, Jason, Nohjin, Seri, Heather, Jennifer, Arash) for help and/or friendship. I also thank all those who are not mentioned, but not forgotten.

Finally, these studies would not be possible without unconditional support and encouragement of my husband Dr. Firouz Jahaniaval and understanding, and patience of my sons Araz and Taymaz Jahaniaval.

Table of Contents

CHAPTER TWO: Allosteric Regulation of Cardiac L-VDCCs by Mg-ATP

CHAPTER FOUR: Adult Neurogenesis in Ulip-1 Knockout Mice

List of Figures

List of Tables

Abbreviations

Adenosin Triphosphate (ATP)

A kinase Anchoring Protein (AKAP)

Alzheimer Disease (AD)

ATP-binding Cassette (ABC)

5-bromo-3-deoxyuridine (BrdU)

BL21 (DE3) plysS (strain of E.coli bacteria)

Calcium binding protein (CaBP)

Calcium currents (I_{Ca})

Calf Intestine Alkaline Phosphatase (CIAP)

Central Nervous System (CNS)

Circular dichroism(CD)

Collapsin response mediator protein (CRMP)

Cyclic ADP-ribose (cADPR)

Cystic fibrosis transmembrane conductance regulator (CFTR)

Cyclic adenosine monophosphate (cAMP)

C-elegans

CA1 neurons

Dentate Gyrus (DG)

Dihydropyridin (DHP)

Doublecortin (DCX)

Enhanced chemiluminescence (ECL)

Ethylene glycol tetra acetic acid (EGTA)

Granular cell layer (GCL)

Green Fluorescent Protein (GFP)

Human embryonic kidney cells (HEK cells)

High voltage activated (HVA)

Horseradish peroxidase conjugated goat anti-mouse (HRP GAM)

Heat shock protein 70 (Hsp70)

Sarcoplasmic Reticulum (SR)

Inositol tri phosphate (IP_3)

Isopropyl-D-thiogalactopyranoside (IPTG)

Kir 6.2 (pore-forming subunit)

Ki67 protein (proliferative marker)

L-type voltage dependent calcium channels (L-VDCCs)

Nicotinamide adenine dinucleotide (NAD)

Neuronal cell adhesion molecule (PSA-NCAM),

Nerve growth factor (NGF)

National Institute of Health (NIH)

Neuronal nuclei (NeuN)

Neuronal Growth Factor (NGF)

N-methyl-D-aspartate (NMDA)

Non-fat dry milk (NFDM)

Nucleotide Binding Folds (NBF-1 and NBF-2)

N',N'-methylene-bis-acrylamide (BIS)

Olfactory bulbs (OB)

Plasma membrane (PM)

Polymerase chain reaction (PCR)

Polyvinyl difluoride (PVDF)

Protein kinase A (PKA)

Rostral migrating stream (RMS)

Ryanodine receptor (RyR)

Sodium Dodecyl Sulphate (SDS)

SDS-polyacrylamide Gel Electrophoresis (SDS-PAGE)

Semaphorin 3 (Sema-3)

Sub ventricular zone (SVZ)

Subgranular zone (SGZ)

TBS (Tris buffered saline)

TNT-ATP (2'-(or 3')-o-(trinitrophenyl) adenosine-5'- triphosphate trisodium salt)

TTBS [Tween-20- Tris buffered saline]

Ulip-1 (Unc-33 like protein-1)

Phosphate Buffered Saline (PBS)

Chapter One: General Introduction

1.1 Summary of Thesis

This thesis is an investigation of factors involved in the mechanisms of neurodegeneration and neurogenesis in the adult brain. The region of the brain chosen for study is the hippocampus, since it is one of the regions of the brain that exhibits significant neurogenesis during adulthood and neurodegeneration in aged related diseases. My studies cover three major areas.

1. It is known that calcium levels in neurons have a significant effect on both neurodegeneration and neurogenesis. Calcium channels are essential in regulating the influx of calcium into the neurons. It has previously been shown by electrophysiological experiments that in aging the level of expression of calcium channels is altered in the hippocampus. Thus, in my first study, the expression of L-type calcium channels (known to be the major source of calcium influx to the cells) in the hippocampus in aged rats was examined. This study found that effect of aging on L-type calcium channels expression in the brain is subunit- and region-specific.

2. The allosteric regulation of these L-type calcium channels is also important in regulating the influx of calcium to cells and thus regulating the processes of neurodegeneration and neurogenesis. It has been suggested by electrophysiological experiments that ATP is involved in the allosteric regulation of these L-type calcium channels. In my second study, I examined the regulation of these channels by ATP at a molecular level, by examining a proposed binding site for ATP on the C-terminus of this calcium channel. This study was performed using cardiac myocytes as an experimental

preparation. The results of this study indicated that no allosteric regulation is involved in modulation of L-VDCCs.

3. Another protein that has recently been proposed to be important in neurogensis is Ulip-1 (Unc 33 like protein). Ulip-1 is a cytoplasmic phosphoprotein that is implicated in axonal collapse and pathfinding. In peripheral nervous system tumours, the expression of Ulip-1 has been shown to be significantly downregulated. This suggests that Ulip-1 plays an inhibitory role in the process of cell division and possibly in neurogenesis. In my third study, I examined the levels of neuorgenesis in the hippocampus of Ulip-1 null mice. These studies found that in these mice, neuronal proliferation is significantly increased, supporting an inhibitory role of Ulip-1.

These studies have provided new information about the involvement of calcium channels and Ulip-1 on the regulation of processes of neurodegeneration and neurogenesis. It will be interesting to consider for future studies whether there is a common link between calcium channels and molecular machinery involved in neurogenesis.

Chapter one will present a general introduction which discusses the concepts of neurodegeneration and neurogenesis, including pathologies related to these processes. This introduction will then be continued to outline the importance of calcium and the mechanisms by which calcium enters and leaves cells, as well as discussion of calcium channels, their subtypes, and diversity, including their molecular biology, structure, and function. I will also discuss the regulation of calcium channels, and overview the role of calcium in neurogenesis and neurodegeneration. A discussion of the Ulip-1 protein will also be presented.

In chapters 2-4, the experimental works that I performed will then be presented. Each of these chapters contains a more specific introduction to the work, methods and results, and a specific discussion of these results.

Chapter 5 presents a general discussion of these experiments, and their relevance to neurodegeneration and neurogenesis. A discussion of limitations and future work is also presented.

1.2 Introduction

Most tissues in adults, such as liver and skin, contain multipotent stem cells which are capable of differentiating into new components of these tissues in adult animals. However, until the late twentieth century, it was assumed that in the central nervous system (CNS), no new neurons could be generated (neurogenesis) in the adult (Alvarez-Buylla, 2001). This lack of neurogenesis was attributed to the depletion of stem cells in the adult brain (CNS). But, the discovery in 1967 of progenitor cells in the CNS with the ability to generate new neurons and glia in the adult brain overturned this concept of CNS stability throughout life (Altman and Das, 1967). These neuronal progenitor cells are referred to as "stem cell-like cells", since they do not display exactly the same characteristics as stem cells from other tissues. The progenitor cells in the brain are more heterogeneous and have more limited capabilities. However, since they do have self-renewal capability, they are assumed to be a kind of stem cell (Temple, 2001). It has now become clear that the adult brain retains these progenitor cells in at least two regions; the sub ventricular zone (SVZ) and the dentate gyrus. New neurons are generated in these regions throughout an animal's life (Alvarez-Buylla, 2001).

Neurogenesis in the adult CNS allows for the possibility of regeneration in the adult brain (Doetsch et al., 1999; Temple, 2001), as damaged or dying neurons may be replaced with new neurons. The regeneration of new neurons by neurogenesis to replace damaged or dying cells has recently been shown in the ischemic hippocampus (Nakatomi et al., 2002). Moreover, new young neurons may provide a greater degree of plasticity in the brain. Therefore, factors such as learning and the environment may affect them and their connectivity, even in adults (van Praag et al., 2002).

Initially, questions were raised about the functionality of these newborn neurons; it was unknown whether these new neurons actually became functional. Direct and indirect evidence have now shown that these newborn neurons do function. For example, an enriched environment, exercise, and learning, are known to enhance neurogenesis and synaptic plasticity and also to improve memory. In contrast, other factors, such as stress (via glucocorticoid hormones and NMDA receptors), impair neurogenesis and memory. Additionally, insults to brain, such as ischemia, seizure, and selective lesions, are associated with enhanced neurogenesis (Sharpe et al., 2000). Recently van Praag et al. (2002) provided direct evidence that newly generated neurons are functional in the adult brain. They used a GFP (green fluorescent protein) labelled retroviral vector, which specifically labels dividing cells, to visualize new neurons in *in situ* hippocampal slices during electrophysiological assay. They reported that newly born cells in the adult mouse hippocampus not only show neuronal morphological specifications but also display similar functions, such as passive membrane properties, generation of action potentials, and functional synaptic inputs (van Praag et al., 2002).

The brain is highly vulnerable to insults, because most neurons cannot undergo cell division. This vulnerability is increased with advancing of age, perhaps because of failing protective mechanisms in aging (Ansari et al., 1989). Also, in the aged brain, neurogenesis declines ((Kuhn et al., 1996) and diseases such as Alzheimer disease (AD) and Parkinson's increase in frequency with age. These diseases are associated with massive neuronal loss and neurodegeneration, while at the same time neurogenesis declines. An important question is whether knowledge of the neurogenesis and neurodegeneration can help with the development of strategies to treat neurodegenerative diseases.

It has been argued that the "microenvironment can enhance the acquisition of neuronal stem cell fates" (Temple, 2001). For example, in the postnatal chick retina after damage, Muller radial glia, which are maintained throughout life, can re-enter the cell cycle, re-express retinal progenitor cell markers and generate new neurons and glia (Fischer and Reh, 2001). Moreover, type C progenitor cells in the adult subventricular zone (SVZ) are stimulated to convert to stem cells by epidermal growth factors (Temple, 2001). Also, type B and C progenitor cells produce neurospheres *in vitro*. It has also been shown that various insults can stimulate the proliferation of endogenous progenitors, either in known neurogenic sites (Magavi et al., 2000), or in regions where neurogenesis normally does not occur, for example adult rat spinal cord (Yamamoto et al., 2001). The above processes might occur through an alteration of endogenous factors in their microenvironment, that then stimulate neurogenesis.

In aging and age-related diseases, neurogenesis may be reduced due to an altered microenvironment. For example, an excess influx of calcium ions through L-type voltage

dependent calcium channels (L-VDCCs) may affect the progenitor cells and the proliferation of new neurons in the aged brain. In diseases like Alzheimer disease, the profound loss of neurons (neurodegeneration) is associated with accumulation of ß-amyloid protein and neurofibrillary tangles. These accumulations may create a microenvironment that can affect neurogenesis or lead to neurodegeneration. Interestingly, it has been shown that the regeneration of hippocampal neurons after ischemic insult can occur by changing the internal environment and manipulating endogenous progenitors using neurotrophic hormones (Nakatomi et al., 2002). This strategy could be further developed for use as a prevention or possible cure for neuropathological diseases (Nakatomi et al., 2002).

1.3 Neurodegeneration and Calcium Concentration

Over the last few decades considerable emphasis has been placed on elucidating mechanisms underlying neurodegenerative. Such degeneration is a hallmark of the age-related neurodegenrative diseases, and its prevalence in areas of the brain responsible for cognition and memory, notably the cortex and hippocampus, leads to the most serious effects of Alzheimer disease (AD) (Clark and Goate, 1993; Roses, 1996; Lendon et al., 1997). In AD there is a profound loss of neurons that correlates well with the decrease in learning abilities and memory function (Roses, 1996). In addition, a key element of AD pathology, the ß- amyloid protein, has been shown to disrupt neuronal $[Ca^{2+}]i$ homeostasis (Mattson et al, 1993). It is now clearly established that a primary mode of neurodegeneration is through an excess of intracellular calcium ($[Ca^{2+}]i$) ions (Schnne et al., 1979; Gibson and Peterson, 1987; Choi, 1988; McEntee and Rook, 1993). Agents that

that act to increase $[Ca^{2+}]i$ levels, such as agonists for amino acid receptors, are extremely cytotoxic to cells both in culture and *in vivo* (McEntee and Rook, 1993; Schanne et al., 1979). Moreover, agents that act to suppress Ca^{2+} influx or buffer $[Ca^{2+}]i$ are neuroprotective (Krinke et al., 1995). However, it is also known that Ca^{2+} is essential for a variety of neuronal functions (Llinas, 1988; Bading et al.,1993) such as neurotransmitter release (Verkhratsky and Toescu, 1998), while removal of Ca^{2+} is also cytotoxic (Mills and Kater, 1990). Such observations have led to the proposal that Ca^{2+} levels in neurons are maintained within a concentration window which allows Ca^{2+} signaling but where the levels are neither too low or too high to be cytotoxic (Carafoli, 1987; Tsien and Tsien, 1990).

In healthy resting adult neurons, the $[Ca^{2+}]$ window appears to be set so that the $[Ca^{2+}]i$ is approximately 100 nM, i.e. approximately 10,000 fold lower than the extracellular Ca^{2+} ion concentration (Mills and Kater, 1990). The steep concentration gradient of Ca^{2+} between the outside and inside of the cell appears to allow Ca^{2+} signalling through activated voltage and ligand-gated Ca^{2+} channels (Llinas, 1988; Tank et al.,1988; Bading et al.,1993; Llinas et al., 1992). After signalling, or when signalling is absent (and other mechanisms such as leakage or Na^{+} - Ca^{2+} exchangers contribute to Ca^{2+} influx) three distinct mechanisms are used to return the $[Ca^{2+}]i$ to, or maintain it at, its low resting level: first, Ca^{2+} buffering by specific cytosolic proteins such as calbindin-D28k and parvalbumin (Celio, 1990); second, Ca^{2+} sequestration by organelles such as the endoplasmic reticulum (Tsien and Tsien, 1990; Henzi and McDermott, 1992); third, the active extrusion of Ca^{2+} by ATP-dependent Ca^{2+} pumps (Carafoli, 1992). Consequently, any events which perturb the activity of the influx, efflux, buffering or

sequestration mechanisms underlying Ca^{2+} homeostasis are likely to be cytotoxic. Thus, it has been proposed that a disruption in Ca^{2+} homeostasis underlies age related changes seen in brain aging (Khachaturian, 1984 and 1994).

It is unclear whether perturbations in Ca^{2+} homeostasis actually occur in aging. There have been numerous attempts to measure $[Ca^{2+}]i$ in aging, many of which suggest that the free Ca^{2+} level rises in an age-dependent fashion (Landfield, 1994; Landfield and Pitler, 1984). However, this has not been confirmed by other workers (Reynolds and Carlen, 1989). Such discrepancies have been suggested to reflect regional differences in the tissues analyzed or different methodologies for determining Ca^{2+} levels (Campbell, 1996). A similar picture has also emerged when possible changes in the events underlying Ca^{2+} homeostasis during aging were examined (Landfield and Pitler, 1984; Landfield, 1994). In general, the aging literature is plagued by inconsistencies, raising doubt about the validity of the calcium hypothesis of brain aging. However, reports have emerged suggesting changes arise in voltage dependent calcium channels (VDCCs) during brain aging (Landfield, 1994; Landfield and Pitler, 1984). Among the most convincing are studies by Landfield's group showing an increase in currents through high voltage activated (HVA) Ca^{2+} channels in hippocampal CA1 neurons (Landfield, 1994; Landfield and Pitler, 1984). Such an increase is reported to arise primarily via L-type channels (L-VDCCs) since it can be blocked by dihydropyridines such as nimodipine (Thibault and Landfield, 1996). Owing to their slow inactivation kinetics and large conductances (27pS for Ba^{2+} ions), L-VDCCs mediate much larger rises of Ca^{2+} influx into neurons than other VDCCs (Hofmann et al, 1994). To define how an increase in L-VDCC currents may arise, Landfield's group examined single channel currents in CA1

neurons in brain slices using patch clamp electrophysiology (Thibault and Landfield, 1996). The results from this study show an age-dependent increase in the density of L-VDCCs in the CA1 nerve cell surface (Thibault and Landfield, 1996). To test this possibility, the expression of mRNA encoding L-VDCCs was assayed through the polymerase chain reaction (PCR) (Porter et al, 1997). While these studies suggested an age-dependent increase in L-VDCC mRNA, they suffer from the serious criticism that they were conducted using hippocampal neurons in "long-term" (4 wk) culture as a model of aging (Porter et al, 1997). Moreover, it is tempting to speculate that any increase in L-VDCC currents reflects enhanced gene expression. This view is rather simplistic as the electrophysiological data could also be rationalized in several ways: 1) via an increase in mRNA translation, 2) a decrease in mRNA degradation, 3) enhanced insertion of L-VDCC proteins into the membrane or 4) reduced endocytosis or turnover (Porter et al, 1997). In addition, there are evidence that ion channels may be unmasked through conversion of silent (i.e. non-functional) ion channels to functional ones at the cell surface (Landfield and Pitler, 1984; Landfield, 1994); this could occur, for example, through second messenger regulation. To date, none of these mechanisms have been explored for any channel in aging, let alone L-VDCCs. This picture is further complicated by previous evidence for a decrease in HVA Ca^{2+} currents in aging (Reynolds and Carlen, 1989). However, these latter studies examined neurons from the dentate gyrus so it is conceivable that changes in L-VDCCs, or at least HVA current levels, are region specific. Region-specific changes of VDCCs expression in rat cerebellum have been examined recently by immunohistochemistry and Western blot analysis (Chung et al., 2001). Increases in α1C subunits immunoreactivity in the

dendrites as well as in the cell bodies of Purkinje cells were observed. In contrast, immunoreactivity for α1A and α1D subunits decreased in the molecular or granular layers. The exact significance of such channel re-distributions is uncertain. One possibility is that these alterations in the distribution of VDCCs in the aged rat cerebellum may contribute to impairments of Ca^{2+} homeostasis during aging (Chung et al., 2001).

1.4 Regulation of Calcium in Neurogenesis

Previously in this chapter (1.3) it was stated that in the past few decades considerable attention has been placed on elucidating the mechanisms underlying neurodegeneration which occurs in the hippocampus and cortex of aged brain and during AD. On the other hand, Altman (1967) rejected the dogma that there is no neurogenesis in the adult brain. It was shown that in regions of brain like hippocampus, neurogenesis occurs in adulthood. The same region is vulnerable to neurodegeneration in aging and in cognitive diseases such as AD. These findings raised the question: What is the relationship between neurogenesis, and neurodegeneration? In aged hippocampus, neurogenesis is diminished but neurodegeneration increased. Whether neurogenesis and neurodegeneration employ some of the same pathways and mechanisms is not known. The calcium hypothesis suggests that altered calcium homeostasis underlies neurodegeneration in age-related diseases (Khachaturian, 1984 and 1994). It has also been shown that perturbation of calcium influx or altered regulation of VDCCs occurs in aged brain (Landfield, 1994; Landfield and Pitler, 1984).

It has been recognized that calcium influx is necessary for all aspects of neurogenesis such as cell division, neuronal outgrowth, pruning and cell polarity (Purves et al., 1986; Johnson and Deckwerth, 1993). During mitosis, calcium is released from intracellular stores through inositol triphosphate (IP_3) channels by autonomous oscillation (Ciapa et al., 1994). Furthermore, calcium enters the cytosol through various calcium channels embedded in the plasma membrane during different phases of the cell cycle. Mitogen factors activate plasma membrane channels and cause elevation of cytosolic calcium selectively (Kuga et al., 1996; Munaron et al., 1997). Ca^{2+}-induced $[Ca^{2+}]i$ release is critical to differentiation of cultured embryonic spinal cord neurons (Holliday and Spitzer, 1990; Spitzer, 1995).

The role of Ca^{2+}- channel expression in the development of hippocampus pre- and postnatally is important. *In situ* hybridization studies indicated that mRNAs encoding VDCCs that mediate high voltage activated (HVA) Ca^{2+} current appear in the regions of brain undergoing active proliferation and migration post- and prenatally (Tanaka et al., 1995). How VDCCs contribute to these events is not well defined. However, recent research suggests that VDCCs can play critical roles in hippocampal development pre- and post-natal. For example, it has been shown that the expression of VDCCs is necessary for neuroblast migration in the cerebellum (Komuro and Rakic, 1996). It has also been shown that expression of N-VDCCs before birth is consistent with their role in migration and proliferation, and their high level of expression after birth coinciding with synaptogenesis in the hippocampus. Taken together VDCCs can have a role in key developmental events in the brain and also in neurogenesis of the adult dentate gyrus (Jones et al., 1997). The mechanisms underlying these events and how these channels

may contribute to them are complicated due to the diversity of VDCCs and the diversity of mechanisms modulating calcium influx (signalling). In addition, as described in detail early in this chapter (section 1.4) neurodegeneration may be related to the altered regulation of L-VDCC which produce the major route of calcium influx into the cell (Hess, 1990). Therefore, knowledge about all aspects of calcium channels and their regulation and also neurogenesis may help to determine the mechanisms underlying neurodegeneration and therapeutic strategies for preventing it in aging and Alzheimer's disease (AD).

1.5 Ulip/CRMP and Neurogenesis/Neurodegeneration

The Ulip/CRMP family of phosphoproteins is thought to play key roles in growth cone guidance during development and in the adult brain regions capable of neurogenesis. The proteins in this family are widely expressed before birth in the developing brain but their expression is downregulated two weeks after birth and limited only to the regions with adult neurogenesis where they are thought to be associated with neuronal migration/differentiation (reviewed in Quinn et al., 1999).

One member of the family of Ulip proteins is a component of the Semaphorin-3 (Sema-3) signalling pathway for axonal collapse (Nakamura et al., 2000). Both calcium channels and the Ulip family are also involved in neuronal migration and differentiation and contribute to the cytoarchitecture of the brain. For example, the deletion of *unc 33* gene (the homologue of Ulip-1 gene in C-elegans) has led to the defects in axonal targeting, egg laying and abnormal movement (Siddiqui, 1990; Siddiqui et al., 1991). *In vitro* experiments have also supported the importance of CRMPs in neuronal

development. In PC12 cells, a common *in vitro* model for neuronal differentiation, treatment with neuronal growth factor (NGF) induced rapid changes in the phosphorylation state of CRMPs, as well as changes in their expression (Minturn et al., 1995; Byk et al., 1996). CRMP-4 is strongly upregulated in response to NGF treatment, whereas CRMP-1 and –2 were slightly upregulated, and CRMP-3 was strongly downregulated (Byk et al., 1998). In another *in vitro* experiment, human CRMP-4 expression was found to be upregulated when neuroblastoma cells were induced to differentiate with the application of retinoic acid (Gaetano et al., 1997). The involvement of this protein family together with calcium channels has also been shown in brain neurodegeneration. Interestingly, members of Ulip/CRMP family have been implicated in neurodegenerative diseases such as AD. In AD, increased levels of highly phosphorylated Ulip/CRMP2 are associated with neurofibrillary tangles (Yoshida et al., 1998; Gu et al., 2000). Extracellular deposition of ß-amyloid and intracellular accumulation of neurofibrillary tangles are hallmarks of AD. These results suggest a possible role of CRMP family in AD via abnormal regulation of microtubule assembly in neurons (Fukata et al., 2002)

1.6 Importance of Calcium in Signalling

Calcium was one of the earliest recognized signal transduction molecules (Busa, 1996). Signal transduction by calcium was first observed in cardiac cells by Ringer in 1887, and the role of calcium influx in skeletal muscle contraction and neurotransmitter release was shown later (Heilbrunn, 1965; Katz and Miledi, 1965).

Calcium signalling is critical for almost all aspect of cellular functions. Some significant functions among these are neuronal excitability and the generation of action

potentials (Llinas, 1988) and release of neurotransmitters at synapses (Dunlop et al., 1995). Calcium signalling also mediates the activation of genes encoding transcription factors, (Bading et al., 1993). In addition, calcium signalling is involved in activation of diverse cytosolic and nuclear enzymes, such as kinases and calcium dependent proteases and phospholipases (Ghosh and Greenberg, 1995). Calcium signalling can also affect broad cellular events such as neuronal survival (Ghosh et al., 1994), axonal ougrowth and adaptive response (plasticity) in the nervous system (Ghosh and Greenberg, 1995).

Calcium is unique among chemical messengers in that it cannot be generated or degraded in the cells (Busa, 1996). Calcium signalling is accomplished by a transient change in the intracellular calcium concentration. Both a concentration gradient of calcium across the plasma membrane and cytoplasm, as well as intracellular calcium stores are necessary for this calcium signalling. The intracellular calcium concentration $[Ca^{2+}]_i$ is maintained in the normal range (70-100 nM), i.e., approximately 10,000 fold lower than the extracellular calcium concentration (Mills and Kater, 1990) by homeostatic mechanisms (Bading et al., 1993; Tank et al., 1988; Llinas et al., 1992). These are diverse, flexible and complex for this important ion. If the concentrations are outside of this range, calcium ions appear to be neurotoxic. High calcium influx is well associated with neuronal cell death in prolonged seizure activity and global hypoxia/ischemia (Choi, 1988; Lobner and Lipton, 1993), while low calcium inhibits neuronal outgrowth (Mills and Kater, 1990).

Due to diversity and importance of cellular functions that depend on calcium signaling it is not surprising that diverse intracellular homoestatic mechanisms have been developed inside cells to maintain a high concentration gradient of calcium across

membranes. These mechanisms include calcium extrusion, sequestering by intracellular stores such as mitochondria and endoplasmic reticulum (Blaustein, 1988; Werth and Thayler, 1994) and bufferring via the binding of calcium to specific proteins such as calbindin, calmodulin and parvalbumin (Celio, 1990; Baimbridge et al., 1992). Calcium entering the cells must eventually be exported to prevent saturation of the cell's buffering system. This is accomplished by two means: a Na^{+}/Ca^{2+} exchanger (antiporter), which does not directly require ATP, and a Ca-ATPase, which utilizes ATP for the active transport of calcium (Nachshen et al.. 1986; Carafoli, 1992).

Transient change in the intracellular calcium concentration (calcium signalling) for signal transduction occurs in two ways: first, through the influx of calcium by voltage and ligand-activated ion channels (Tsien, 1986; Catteral, 1994); and second, through its release from intracellular stores (Blaustein, 1988)

1.7 Calcium Entry through Plasma Membrane

Transient passive influx of calcium through the plasma membrane occurs in response to diverse stimuli such as plasma membrane depolarization, the binding of Ca^{2+}-mobilizing hormones, growth factors, neurotransmitter binding, cell-cell interactions and mechanical forces. This function regulates, in whole or in part, important physiological processes as neurotransmission, muscle contraction, secretion, egg activation, cell mobility, ciliary beating, cell growth, gene expression, and memory (Busa, 1996). The major classes of plasma membrane channels mediating the influx of calcium may be classified into two groups based on their gating mechanisms: voltage dependent calcium channels (VDCCs) and ligand dependent calcium channels (Busa, 1996). Since VDCCs

is the focus of this thesis, the structure and function of these channels will be discussed in detail below.

1.7.1 Diversity and Structural Properties of VDCCs

In the heart, VDDCs play a very important role in calcium signalling. They are involved in generating the plateau in the cardiac action potential, triggering excitation-contraction (E-C) coupling in cardiac myocytes, and determining the force of cardiac muscle contraction (Rougier et al., 1969). In other cells, VDCCs are important for functions such as neurotransmitter release and gene expression in neurons (Dunlap et al., 1995; Bading et al., 1993) and insulin secretion from pancreatic ß cells (Smith et al., 1989). The influx of calcium through VDCCs is critical to nerve function. At a cellular level, VDCCs orchestrate neurotransmitter release, modulation of Ca^{2+}- dependent enzymes, nerve excitability, apoptosis, and the morphological and growth patterns of the cells. At the level of brain function, VDCCs are key to changes seen in learning and memory, aging, and pathologies such as epilepsy and ischemic cell death. Thus, the structure and function of these channels and their mode of regulation is very important in cellular function.

Given the wide range of cell types that possess VDCCs and the variety of physiological functions that they are involved in, it is not surprising that diverse types of VDCCs have been discovered. These channels are classified as L, N, P/Q, T and R type based on their pharmacological and biophysical properties (Nowycky et al., 1985; Fox et al., 1987 a, b; Bean, 1989; Llinas et al., 1988; Hess, 1990; Hillman et al., 1991; Miller et al., 1992; Randall and Tsien, 1995) and the molecular identity of the pore forming and

sensor subunit (α1 subunit) (Mikami et al., 1989; Snutch et al., 1990; Snutch and Reiner, 1992; Soong et al 1993; Zhang et al., 1993). However, molecular cloning has shown that this classification is too simplistic. The cloning of α1 subunit cDNAs has revealed an unexpected diversity of these proteins. Calcium channel structural diversity is the consequence of different genes and alternative splicing of their primary transcripts.

VDCCs can also be classified into two major groups based on electrophysiological characteristics: high voltage activated (HVA) and low voltage activated (LVA) Ca^{2+} - channels . The L-VDCC, which is focus of this thesis, is a member of the HVA Ca^{2+} - channels. This is a major type of calcium channel found in cardiac cells. HVA calcium channels are heterologous proteins made of 5 subunits: α1, ß, α2, δ, and γ (only found in skeletal muscle) which are encoded by 4 distinct genes, in a 1:1:1:1 stoichiometry. The structural analysis of VDCCs has been performed in two ways: 1) purification of the channels to identify their subunit composition; and 2) molecular cloning to identify the genes encoding these proteins (Nakafuku et al., 1997).

Studies by Fosset et al (1983) revealed that calcium channels are composed of several subunits and also indicated that the α1 subunit forms a pore in the membrane and has sites for drug binding. Heterologous expression studies of the α1 subunit revealed that it demonstrates all the characteristics of the calcium channel complex (Mikami et al., 1989; Perez-Reyes et al., 1989; Campbell et al., 1988), including pore formation, selectivity of this pore, voltage sensitivity and dihydropyridin (DHP) binding, and interaction sites for the ß subunit and other subunits and proteins (Mikami et al., 1989; Perez-Reyes et al., 1989; Biel et al., 1990; Ellinor et al., 1995). The α1 subunit shares a common ancestry with Na+ and K+ channels (Schmidt and Catterall, 1986; Tanabe, et

al., 1987). The α1 subunits have four homologous domains and each domain (I-IV) consists of six transmembrane segments (S1-S6), containing four negatively charged glutamate residues within the pore region (Figure 1.1). Mammalian α1 subunits are encoded by at least ten distinct genes. These genes are homologous to one another and encode proteins with predicted molecular weights of 190-250 kDa. Four of these genes code for L-type calcium channels α1 subunit (i.e α1C, α1D, α1S, α1F) (Figure 1.2). The others code for α1A (P/Q-type), α1E (R-type), α1B (N-type), and α1G, α1H, α1I (T-type).

Cardiac calcium channels contain the α1C subunit. The cDNA encoding the α1C subunit has been isolated from the heart (Mikami et al., 1989), lung (Biel et al., 1990), brain (Snutch et al., 1991), aorta (Koch et al., 1990) and bone (Barry, 2000). However, this subunit is mainly expressed in the cardiovascular system. Molecular cloning has revealed several splice variants for α1 subunit such as α1C-a, α1C-b, α1C-c. Alternative splicing sites are located in the N-terminal portion, repeat II in the vicinity of S6, the region between repeat I and II (I-II loops), II-III loops, IIIS2, IVS3 and its vicinity and in the carboxyl terminal region (Pere-Reyes et al., 1990; Biel et al., 1990; Snutch et al., 1991; Soldadov, 1992; Diebold et al., 1992).

The ß subunits, like α1 subunits, are diverse and encoded by four distinct genes called ß1, ß2, ß3, ß4 (Hullin et al., 1992; Perez-Reyes et al., 1992; Castellano et al., 1993; Pragnell et al., 1994). Further diversity arises through the existence of alternative splicing (Hullin et al., 1992). The ß subunit is completely cytoplasmic and binds to the α1 subunit through cytoplasmic linker in the region I-II (Pragnell et al., 1994). The ß2 subunit is the most abundant ß subunit in the heart. 80 % of DHP receptors are

immunoprecipitated by using specific antibodies against ß2. However, other variants of the ß subunit such as ß1 and ß3 have been detected in heart tissue by cDNA cloning (Hullin et al., 1992; Collin et al., 1993). The ß subunits play various roles, including modulation of channel activity by protein kinases. Co-expression of this subunit with the α1 results in a 10 fold increase in currents and affects the number of DHP receptors, and their activation /inactivation kinetics (reviewed by Catterall, 1995).

Both the α_2 and δ subunits are encoded by the α_2 gene (Kim et al., 1992). The product of this gene is degraded by proteolytic processes to generate a large α_2 and a smaller δ subunit which are linked through disulfide bonds. Several isoforms of the α_2 subunit have been detected, including α_2a in skeletal muscle, α_2b in brain α_2c and α_2d in heart. Co-expression of $\alpha_2\delta$ with α1C causes an approximate two-fold increase in expression of DHP sites, gating currents and ionic currents (Hullin et al., 1992; Gurnett et al., 1996).

Figure 1.1. Schematic topology of L-VDCCs. L-VDCCs are comprised of two transmembrane spanning subunits ($\alpha 1$, δ), an intracellular (β) and an extracellular ($\alpha 2$) subunit. The $\alpha 1$ subunit consists of four domains (I-IV) and each domain contains six transmembrane segments (S1-S6 not shown here); cytoplasmic loops are labelled according to the domains they link. This Figure is adapted from Walker and De Waard, 1998.Tins, 21(4):148-154.

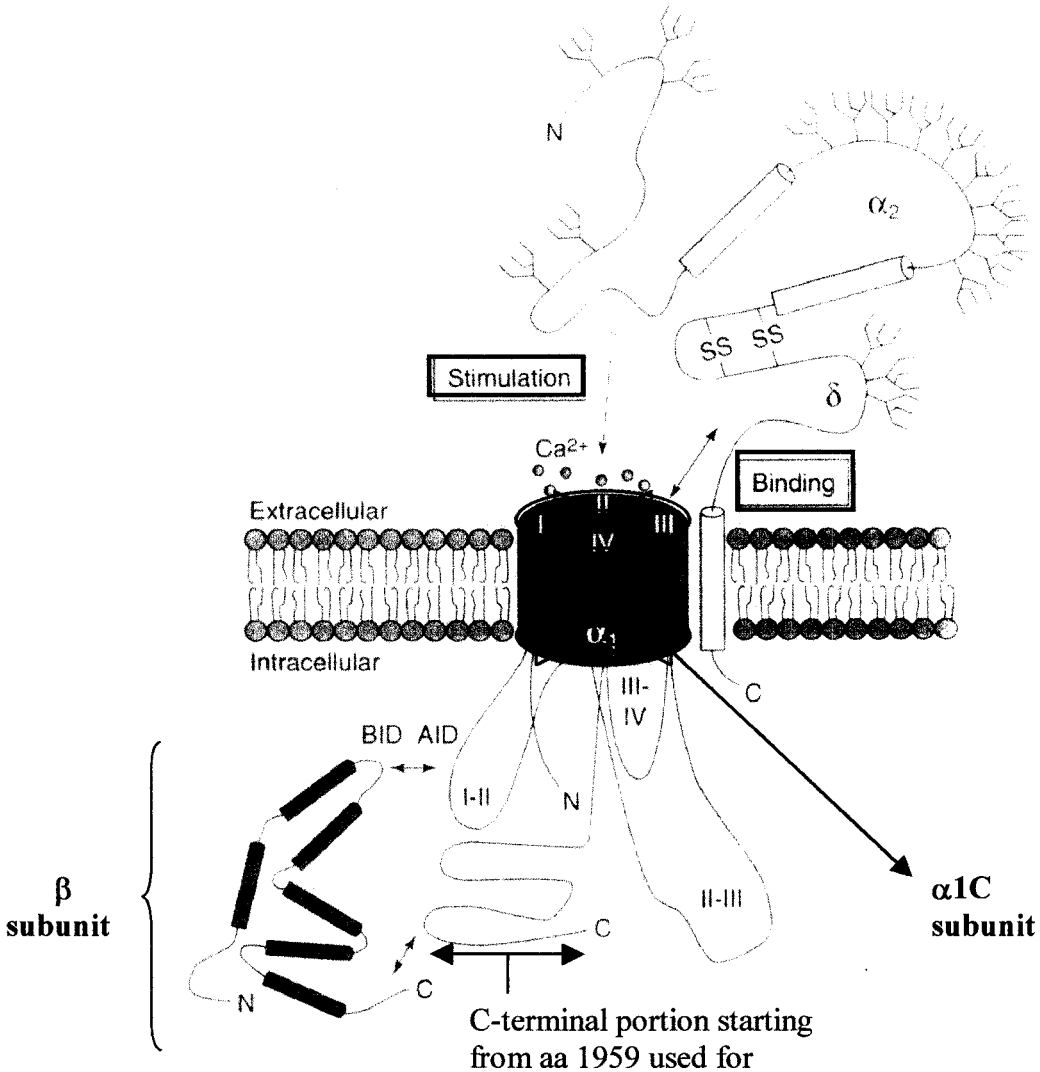
N
α2
SS SS
δ
Stimulation
Ca2+
Binding
Extracellular
I
II
III
IV
α1
Intracellular
III-IV
C
BID AID
I-II
N
II-III
C
C
N
β subunit
α1C subunit
C-terminal portion starting from aa 1959 used for making 1959- GST fusion protein

Figure 1.2. Summary of cloned VDDC α1 subunits. VDCCs are distributed among two main categories, high- or low-voltage threshold, depending on their biophysical and pharmacological characteristics. This chart, though not exhaustive, demonstrates the breakdown of cloned α1 subunits and respective tissue distribution. Medline unique identifier numbers are indicated.

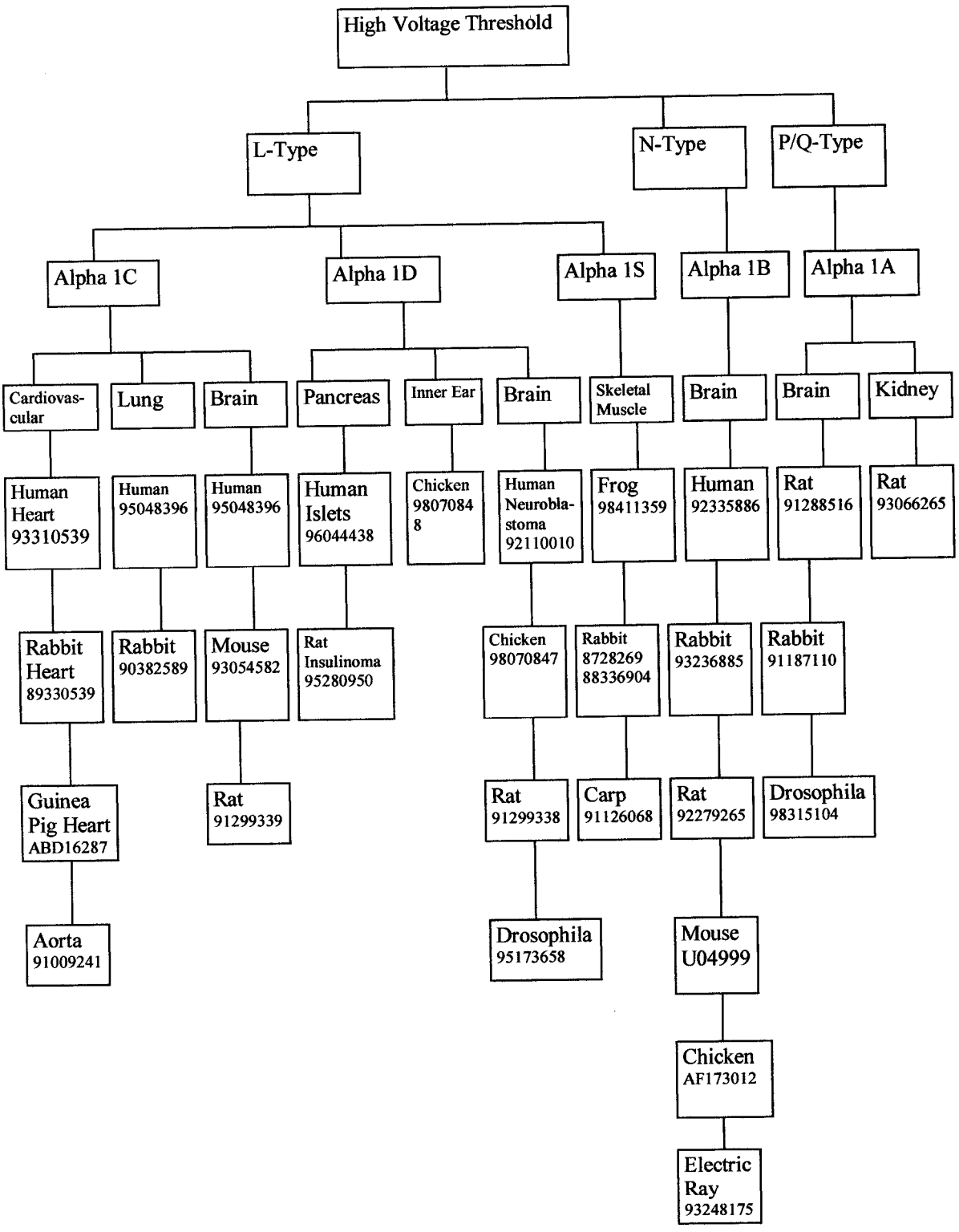
High Voltage Threshold
L-Type
N-Type
P/Q-Type
Alpha 1C
Alpha 1D
Alpha 1S
Alpha 1B
Alpha 1A
Cardiovas-cular
Lung
Brain
Pancreas
Inner Ear
Brain
Skeletal Muscle
Brain
Brain
Kidney
Human Heart 93310539
Human 95048396
Human 95048396
Human Islets 96044438
Chicken 98070848
Human Neurobla-stoma 92110010
Frog 98411359
Human 92335886
Rat 91288516
Rat 93066265
Rabbit Heart 89330539
Rabbit 90382589
Mouse 93054582
Rat Insulinoma 95280950
Chicken 98070847
Rabbit 8728269 88336904
Rabbit 93236885
Rabbit 91187110
Guinea Pig Heart ABD16287
Rat 91299339
Rat 91299338
Carp 91126068
Rat 92279265
Drosophila 98315104
Aorta 91009241
Drosophila 95173658
Mouse U04999
Chicken AF173012
Electric Ray 93248175

1.8 Mechanisms of Ca^{2+} Efflux (Calcium Homeostasis)

The steep electrochemical gradient between the cytosol and the extracellular and intracellular spaces necessitates sophisticated homeostatic mechanisms to keep $[Ca^{2+}]i$ within the physiological range at rest and when Ca^{2+} influx increases during cellular activity. Two parallel mechanisms are employed by cells to extrude the calcium from cytosol: Na+/ Ca^{2+} exchanger and Ca^{2+} ATPase. In addition, the buffering properties of cytosolic proteins and organelles like the mitochondria and the endoplasmic reticulum (ER) help to maintain $[Ca^{2+}]i$ within a physiological range. Eukaryotic cells rely on all of the above mentioned mechanisms. These homeostatic mechanisms are described in detail below.

1.8.1 Ca^{2+} -ATPase

The Ca^{2+} pump is a member of the plasma membrane (PM) ATPases such as the Na^{+}/ H^{+} ATPase. This pump is ubiquitously distributed among eukaryotic cell types (Blaustein, 1988); at least four genes code for this PM protein. It is distinguished from other ATPases by its sensitivity to calmodulin. Binding to calmodulin creates a 30 fold increase in the affinity of the pump to $[Ca^{2+}]i$ (Ghosh and Greenberg, 1995). It is also regulated by cAMP and PKA. However, extrusion of calcium through this pump is too slow to contribute significantly to the fast recovery after a large Ca^{2+} overload. The small capacity of the pump and its high affinity for Ca^{2+} makes it more suitable for fine tuning the resting intracellular calcium concentration rather than the fast recovery required after a large Ca^{2+} load.

1.8.2 Na^+/Ca^{2+} Exchanger

Unlike the Ca^{2+} -ATPase, the Na^+/Ca^{2+} exchanger antiport has a very high capacity for extrusion mechanism. It has a low affinity for binding to Ca^{2+} (Blaustein, 1988). Biochemical studies show that this protein is an electrogenic pump; this bidirectional pump exchanges 3 Na^+ for 1 Ca^{2+}. This exchange can happen in both sides of the PM depending on the concentration of Na^+ on each side. The Na^+/Ca^{2+} exchanger is a 100 kDa single polypeptide strand with 12 putative transmembrane domains. No details of the regulation of these molecules have been revealed based on their primary structure. However, it is allosterically regulated by $[Ca^{2+}]i$ (Dipolo and Beaug, 1993).

1.8.3 Buffering

As Ca^{2+} enters the cytosol, it encounters very large high affinity binding proteins including calmodulin, paravalbumin and calbindin (CaB) (Celio, 1990). These proteins regulate the biochemical effects of Ca^{2+}. Many authors have pointed out that physiochemical buffering plays a minor role in Ca^{2+} homeostasis quantitatively. To maintain a steady state (resting concentration) all Ca^{2+} entering the cell must be exported again; chemical buffers are saturated rapidly whereas the extrusion mechanism is not. Some E-F hand proteins such as camodulin bind to a number of enzymes (for example CaM kinase), and modulate their activity, whereas others such as parvalbumin act primarily as a cytosolic Ca^{2+} buffer.

1.8.4 Organelles

Intracellular organelles like mitochondria and ER are required to sequester Ca^{2+} until the Ca^{2+} can be extracted across the PM.

1.8.4.1 Mitochondria

Mitochondria can accumulate a large amount of Ca^{2+} within their cytosol. Nevertheless, their large sequestering capacity depends on $[Ca^{2+}]i$. Their rate of re-uptake and their affinity for Ca^{2+} are very low under resting conditions (Blaustein, 1988). Mitochondria start to sequester calcium when $[Ca^{2+}]i$ exceeds 5 micromoles. Excess mitochondrial calcium can be slowly released to the cytosol after the other calcium regulatory mechanisms restore $[Ca^{2+}]i$ to below set point levels; this leads to signal prolongation due to delay in returning back to the resting condition.

1.8.4.2 Endoplasmic Reticulum

The endoplasmic reticulum is another organelle whose involvement in sequestering Ca^{2+} from cytosol has been implicated. It has a lower capacity for the accumulation of calcium ion compared to mitochondrial stores (Blaustein, 1988). However, its diffuse subcellular distributions in submembrane and synaptic terminal regions as well as dendrites have been shown (Mcgraw et al, 1980 (a, b)). Synaptic vesicles are also involved in sequestering calcium ion from the cytosol by ATP-driven mechanisms (Smith and Augustine, 1988). However, with their low affinity for Ca^{2+} the contribution of synaptic vesicles in the regulation of intracellular calcium can not be major.

1.9 What Is the Goal of This Study?

The focus of this study has been on L-type VDCCs regulation in the heart and their expression in aged brain, and also on the mechanisms of neurogenesis in the hyppocampus of the adult brain.

The allosteric regulation of L-type VDCCs by ATP in the rabbit cardiac model was studied. A central hypothesis of this part of thesis (chapter 2) was that Mg-ATP binds directly to the C-terminal portion of the α1C subunit of the rabbit L-type calcium channel and this regulation is independent of phosphorylation. My specific goals were: **A)** To generate fusion proteins from the C-terminal portion of the α1C subunit of the cardiac rabbit L-type calcium channel. **B)** To investigate the allosteric binding of Mg-ATP to the α1C subunit of this fusion protein using affinity chromatography in conjunction with other techniques such as radiolabelling, spectrofluorimetry and circular dichroism analysis by using the above fusion protein.

The expression levels of L-VDCCs have been studied in aged brain. My hypothesis in chapter three was that the level of expression of L-VDCCs increases in aged brain. My specific aims were: **A)** To detect the levels of the expression of the ß3 and α2δ and α1C subunits of L-VDCCs in the hippocampus, cortex, and cerebellum of aged rat brain by Western blotting analysis. **B)** To determine the overall expression of the L-VDCCs in hippocampus of aged rat brain by radioligand labelling.

I have also examined the mechanism of neurogenesis in Ulip-1/CRMP-4 knockout mouse model. A central hypothesis of chapter four is that Ulip/CRMP expression modulates neurogenesis in the adult brain. My specific goals were: **A)** To detect the genotype of each mouse by PCR analysis and to determine its phenotype by

immunohistochemistry using anti CRMP-4 antibody. **B)** To define neurogenesis in the dentate gyrus of the adult -/-, -/+ and +/+ mice using the proliferative marker Ki67. **C)** To investigate the state of neuronal differentiation/migration in the dentate gyrus of the adult -/-, -/+ and +/+ mice, using the immature neuronal marker DCX. **D)** To define the morphology of mature neurons and gross anatomy of hippocampus in adult -/-, -/+ and +/+ mice using markers for mature neurons such as NeuN (Neuron nucleus) and Calbindin.

Chapter Two: Allosteric Regulation of Cardiac L-VDCCs by Mg-ATP

2.1 Introduction

2.1.1 Calcium Channels in Cardiac Cells

The influx of calcium through voltage dependent calcium channels (VDCCs) plays a critical role in the function of both excitable and non-excitable cells. L-type calcium channels are required for excitation-contraction (E-C) coupling in cardiac cells (Morad and Cleemann, 1987). An influx of calcium through these channels, however, is not sufficient to trigger cardiac contraction (Morad and Cleemann, 1987; Callewaert et al., 1988). The rise in intracellular calcium levels leads to the release of calcium from intracellular stores via the ryanodine receptor (RyR) of the sarcoplasmic reticulum (SR) through a process called "calcium-induced calcium release" (Fabiato, 1985; Fabiato, 1989). The movement of calcium from the RyR of the SR into the cytoplasm raises the intracellular calcium $[Ca^{2+}]_i$ sufficiently to trigger the contraction of cardiomyocytes (Wier, 1990; Nabauer and Morad, 1990; Niggli and Lederer, 1990). The cardiac isoform of RyR is known as a RyR2. Single channel recordings of isolated RyR2 indicate that the cardiac isoform is activated at much lower calcium concentrations than the skeletal muscle isoform (Hymel et al., 1988). Calcium is not the only physiological activator of RyR2. Cyclic ADP-ribose (cADPR) (a metabolite of NAD) can also trigger the release of calcium from RyR2s (Clapper et al., 1987; Galione et al., 1991; Koshiyama et al., 1991 Takasawa et al., 1993).

The influx of calcium via calcium channels and the subsequent release of calcium from intracellular stores is the most prominent model for calcium-induced calcium release in cardiac cells. Skinned fibers experiments (Fabiato, 1985) and voltage clamp studies provide key evidence which demonstrate the correlation between calcium currents

(I_{Ca}) and calcium transients as a function of voltage (Wier, 1990; Bers, 1991). Further support comes from observations showing that activation of calcium channels without calcium influx could not induce SR calcium release. In contrast, the abrupt release of caged calcium by photolysis triggers the release of calcium from the SR membrane (Nabauer and Morad, 1990). It has also been shown that E-C coupling can be re-established in dysgenic skeletal muscle, where calcium channels are missing, after injection with cardiac dihydropyridine (DHP) receptor cDNA (Tanabe et al., 1990). There are also other forms of "calcium induced calcium release" in addition to the calcium channel, such as the IP3 receptor (Berridge and Irvine, 1989; Berridge, 1993). However, there is strong evidence which supports calcium-induced calcium release mediated by L-type calcium channels.

2.1.2 ATP and Calcium Concentration in Cardiomyocytes

The systole phase in the cardiac ventricle is accompanied by a dramatic increase in the intracellular calcium concentration $[Ca^{2+}]_i$. It is this increase that triggers the contraction of cardiac myocytes and the ventricle (Blinks et al., 1982; O'Rourke et al., 1992a; O'Rourke, 1993). It is well established that the function of cardiac cells is highly dependent on energy release from the breakdown of ATP. This cellular energy is required for myocardial contraction and for maintaining the ionic gradient across the cell membrane, i.e., the gradient required for the influx of calcium from the extracellular matrix (Suga, 1990).

Thus the cardiac function is dependent on the regulation of both $[ATP]_i$ and $[Ca^{2+}]_i$ (O'Rourke et al., 1990; Hansford, 1991; Goldhaber et al., 1991; O'Rourke et al.,

1992a ; Di Lisa et al., 1993). Their relationship has been primarily investigated in the ischemic and anoxic myocardium. It was expected that depletion of $[ATP]_i$ would lead to an elevation of $[Ca^{2+}]_i$ in the cell resulting in damage to the cardiac cells. Surprisingly, it was shown that the depletion of cellular ATP stores via either anoxia or metabolic inhibitors was not immediately associated with large elevations in resting $[Ca^{2+}]_i$, even if the ATP concentration dropped to such low levels as seen in the rigor state (Cobbold and Bourne, 1984; Allshire et al., 1987). One possible explanation for the small changes in $[Ca^{2+}]_i$ observed during this period is that calcium influx is reduced during this period of time. Experiments involving ATP depletion and excitation have been undertaken to study this issue. It has been shown, for example that rat myocytes become ATP depleted during anoxia, the action potential duration shortens (Hamada et al., 1998), and the cells eventually become inexcitable (Payat et al., 1978 ; Kimura et al., 1991). It is well known that the excitability of cardiac myocytes and other excitable cells (including pancreatic ß cells and neurons) are affected by the metabolic state of the cells, i.e., hypoxia, which leads to a depletion of ATP, and affects cellular excitability by shortening the action potential (Payat et al., 1978 ; Kimura et al., 1991). This effect can be reversed by the addition of substances, which give rise to the production of ATP or ADP such as glucose (Vereecke et al., 1981). In cardiac myocytes the plateau phase of the action potential is prolonged following the injection of ATP or related substances like ADP and AMP (Taniguchi et al., 1983). In guinea pig cardiac myocytes a 40-60 % prolongation of the plateau phase has been observed after injection of ATP, in a dose dependent manner. Reduction or prolongation of the action potential plateau in cardiac myocytes, as a result of ATP depletion or enhancement, suggests that VDCCs are involved in cellular

excitability and alteration of the action potential. This has been established by Irisawa and colleague (1983) who showed that this prolongation of action potential by ATP in perfused guinea pig myocytes was related to augmented calcium current through L-type calcium channels ($I_{Ca,L}$).

The question is now raised as to what are the underlying mechanisms of these events. There are several possibilities. The electrophysiological changes probably result from the opening of ATP sensitive K^+ channels (Deutsch et al., 1991). Depletion of ATP can open the ATP sensitive K^+ channels and the resulting K^+ efflux leads to a shortening of the action potential and a reduction in the excitability and contractility of the cardiomyocytes. An elevation of ATP can also result in the phosphorylation of the VDCCs by cAMP dependent protein kinase A (PKA) (Kameyama et al., 1985; Walsh et al., 1989). Finally, allosteric regulation of channel without ATP hydrolyzation, which is the focus of this thesis, is another possibility for the regulation of calcium channels by Mg-ATP (Backx et al., 1991; O'Rourke et al 1992b).

2.1.3 Regulation of Calcium Channels by cAMP Dependent Phosphorylation, via Protein Kinase A

ATP regulates intracellular calcium concentrations through phosphorylation of L-type calcium channels by cAMP dependent PKA, which increases the influx of calcium and the rate and contractility of the heart (Tsien et al., 1986; Trautwein and Heschler, 1990; Peltzer et al., 1990). Calcium channels become phosphorylated by cAMP in response to ß-adrenergic agonists, which stimulate adenylate cyclase (Figure 2.1) and increase cAMP levels in cardiomyocytes (Tsien, 1977). This has been verified by a large

number of experiments performed using a variety of direct and indirect methods. External application of cAMP analogs, such as 8-bromo-cAMP, resulted in an increase in the calcium current (I_{Ca}) in multicellular preparations from heart (Tsien et al., 1972; Reuter, 1974; Morad et al., 1981; Cachelin et al., 1983), with even larger effects being observed in atrial (Charnet et al., 1991; Ono and Giles, 1991) and ventricular single cell preparations (Bean, 1990; Parsons et al., 1991). This effect was also imitated by the intracellular application of cAMP or cAMP-dependent protein kinase (Tsien, 1972). Other methods such as photolysis or direct injections were also employed to elevate the intracellular concentration of cAMP, leading to an increase in I_{Ca}. In addition, elevation of cAMP production by the addition of an adenylate cyclase activator such as forskolin, which stimulates cAMP production have been shown to increase I_{CaL} in the rabbit, guinea pig and rat (Wahler and Sperelakis, 1986; Hartzell and Fischmeister, 1987). It has been shown that the enhancement of I_{Ca} by increasing the level of cAMP is regulated by cAMP dependent-PKA (Trautwein and Pelzer, 1985; Trautwein and Osterreider, 1986; Trautwein and Cavalie, 1985). The stimulation of ß receptors or treatment with PKA activators induces a 3-10 fold increase in the peak calcium currents observed in dissociated cardiac myocytes. It has also been shown that a competitive inhibitor of phosphorylation such as AMP-PNP, reduces stimulation of $I_{Ca,L}$ by isoprenaline (Kameyama et al., 1985), whereas ATP-[γ S], which irreversibly phosphorylates calcium channels, potentiates the effect of isoprenaline. Further proof for the effects of cAMP on $I_{Ca,L}$ that is in channel phosphorylation can be achieved by manipulating the dephosphorylation pathway. Internal perfusion of cardiac cells with catalytic subunits of protein phosphatase and isoprenaline decrease the stimulating effect of isoprenaline on

I_{CaL}, however, this does not have any effect on the basal I_{CaL} levels. In contrast, phosphatase inhibitors e.g. okadaic acid lead to an increase in I_{CaL} (Hescheler et al., 1987 and 1988).

It has been demonstrated in rabbit cardiac myocytes that both the α1C and ß2 subunits are substrates for phosphorylation by cAMP-dependent protein kinase *in vitro* (Curtis and Catterall, 1987). The rabbit cardiac L-type calcium channel is phosphorylated by cPKA on the α1C subunit possibly on the serine 1928 residue (De Jong et al., 1996; Bunemann et al., 1999). The phosphorylation of serine 1928 on the α1C subunit requires an A kinase anchoring protein (AKAP) while phosphrylation on the ß2a subunit does not (Bunemann et al., 1999). Co-transfection of cardiac AKAP with calcium channels can increase the PKA regulation of the channel by 18%-38% in heterologous cells (Gao et al, 1997; Bunemann et al., 1999). However few studies have been undertaken to establish regulation of cloned channels by PKA. In addition to serine 1928, there are several other phosphorylation sites on the α1C subunit, but their roles have not been identified.

Figure 2.1. Representation of the cAMP cascade. Gs, coupling stimulatory G protein that has α, β and γ subunits; PDE, phosphodiesterase; PKA, protein kinase A.

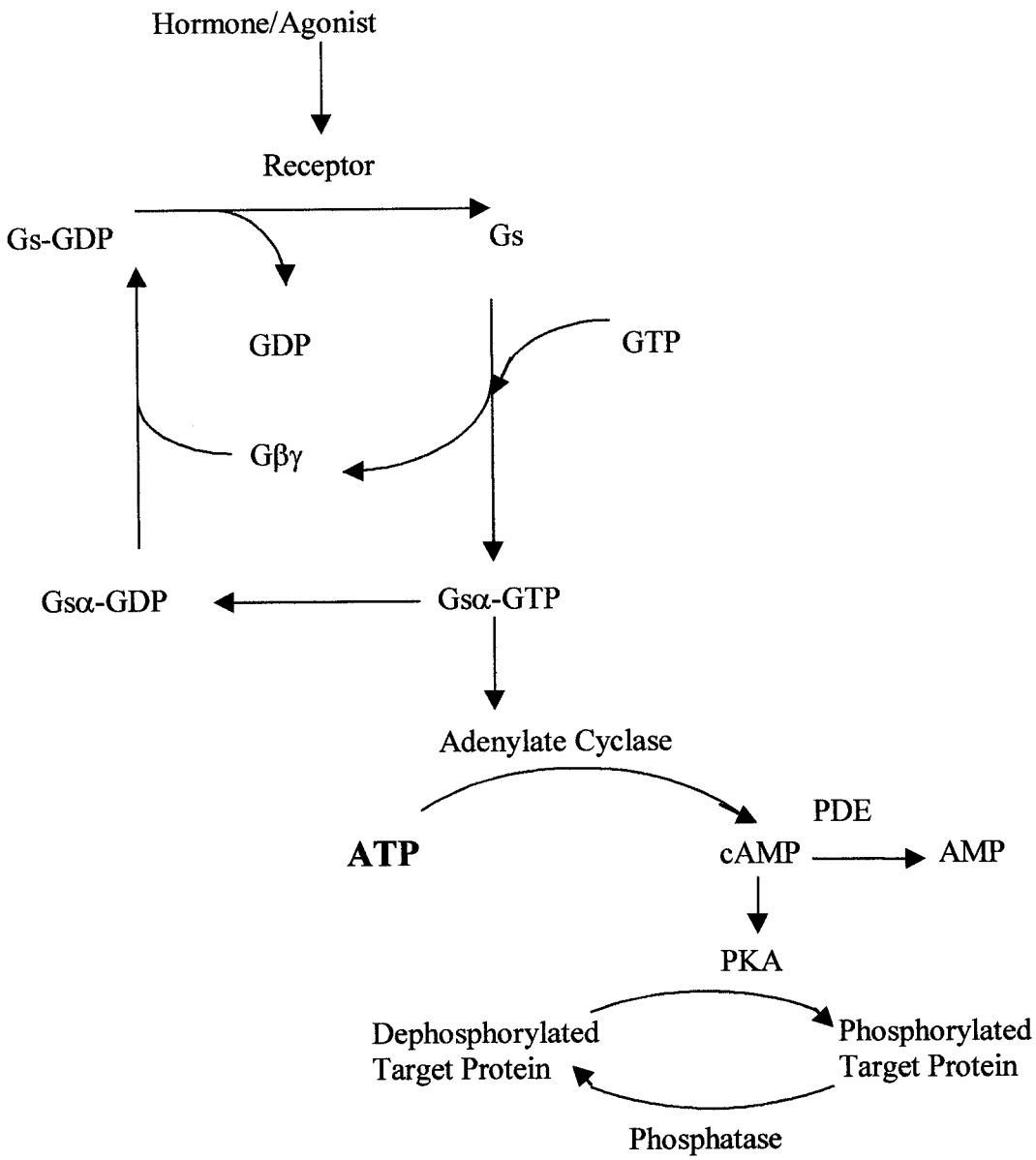
Hormone/Agonist
Receptor
Gs-GDP
Gs
GDP
GTP
Gβγ
Gsα-GDP
Gsα-GTP
Adenylate Cyclase
ATP
PDE
cAMP
AMP
PKA
Dephosphorylated
Target Protein
Phosphorylated
Target Protein
Phosphatase

2.1.4 Allosteric Regulation of Calcium Channels

An elevation or depletion of intracellular ATP can affect calcium channel current ($I_{Ca,L}$). ATP regulates calcium channels in two ways: 1) cAMP levels trigger PKA-dependent phosphorylation of the channel. In this pathway the channel is phosphorylated using the energy released from the hydrolyzation of an ATP molecule (Kameyama et al., 1985; Walsh et al., 1989); 2) Direct binding of ATP or other nucleotides can also regulate calcium channels in a non-hydrolyzable manner (Backx et al., 1991; O'Rourke et al 1992b). While the phosphorylation pathway has been well characterized, the allosteric regulation has not, and research in this field is not abundant. However, this type of regulation has been demonstrated in CFTR (cystic fibrosis transmembrane conductance regulator) chloride channels (Randak et al., 1995), Na^+/H^+, exchangers (Demaurex et al., 1997), and K_{ATP} channels (Tanabe et al., 1999).

Allosteric regulation of calcium channels has been shown in guinea pig cardiac myocytes. Mg-ATP or nonhydrolyzable compounds like PCP-AMP or PNP-AMP in the presence of a PKA inhibitor resulted in a 2-fold increase in the peak of calcium current. This effect is independent of the phosphorylation induced by cAMP (O'Rourke et al., 1992b). The source of ATP used in the allosteric regulation of I_{Ca} in rabbit cardiac myocytes is the glycolysis pathway (Losito et al., 1998).

In vascular smooth muscle isolated from rat mesenteric arteries, a decrease in the intracellular concentration of ATP reduces Ba^{2+} current through calcium channels and an increase in ATP concentration enhances the maximal peak for Ba^{2+} current (I_{Ba}). A dissociation constant (Kd) which was detected by the dose response relation between I_{Ba} and ATP was 0.53 mM (Yokoshiki et al., 1997) which, is close to the Kd of cardiac

myocytes (0.5) (O'Rourke et al, 1992b) and also is close to the Kd measured for guinea pig vascular smooth muscle (0.34 mM) (Ohya and Sperelakis, 1989). The Kd value of vascular smooth muscle (0.53) (Yokoshiki et al., 1997) is higher than the value of Kd for phosphorylation (0.15) (Francis and Corbin, 1994), suggesting the involvement of allosteric regulation of vascular smooth muscle calcium channels by ATP. In contrast to cardiac cells, allosteric regulation of vascular smooth muscle is not dependent on Mg^{2+} (Yokoshiki et al., 1997).

K_{ATP} channels are also regulated allosterically through direct binding of ATP to the Kir 6.2 subunit. These channels open when intracellular ATP is depleted, and the elevation of ATP levels inhibits the channels rapidly. K_{ATP} channel is a member of the ATP-binding cassette (ABC) protein family. They are formed from the sulfonylurea receptor and a pore-forming channel (Kir 6.2). It has been shown that the cytoplasmic domain of the Kir 6.2 subunit is involved in the inhibitory role of ATP through direct binding (Drain et al., 1998). A photoaffinity analog of ATP (8-azido-[α^{32}P] ATP) was used in studies of heterologously expressed channels in COS-7 cells to prove direct binding of ATP to this subunit (Tanabe et al., 1999).

CFTR, like K_{ATP}, is a member of the ABC protein family. Both nucleotide binding folds (NBF-1 and NBF-2) were identified to contain Walker A and B sites. These channels are regulated by both phosphorylation through cAMP dependent protein kinases, using cytoplasmic Mg-ATP for hydrolysis, and by allosteric regulation. A recombinant protein made from NBF-2 acts as an allosteric switch between channel opening and closing, and is inhibited by AMP. It has been shown in enzymatic assays that NBF-2 does not have any hydrolyzing activity on ATP (Randak et al., 1995).

2.1.5 Goal of This Chapter of Thesis

A central hypothesis of this chapter of this thesis is that Mg-ATP binds directly to the C-terminal portion of the α1 subunit of the rabbit L-type calcium channel and this regulation is independent of phosphorylation. This hypothesis was formulated on the basis of electrophysiological experiments that were conducted in our laboratory (unpublished) and elsewhere (O'Rourke et al., 1992b). To address this hypothesis I generated fusion proteins from the C-terminal portion of the α1C subunit, as this region has been correlated with allosteric regulation of calcium channels by electrophysiological experiments previously performed in the laboratory (unpublished). This region has also been involved in regulation of cardiac channels by cAMP-PKA phosphorylation.

My specific goals were:

A) To generate recombinant proteins from the C-terminal portion of the α1C subunit of the cardiac rabbit L-type calcium channel.

B) To investigate the allosteric binding of Mg-ATP to the α1 subunit of this fusion protein using affinity chromatography in conjunction with other techniques such as radiolabelling, spectrofluorimetry and circular dichroism analysis by using the above fusion protein.

2.2 Materials and Methods

2.2. 1 Construction of Expression Vector

A construct carrying the full length coding sequence of the α1C subunit from the rabbit cardiac L-type calcium channel was provided by Dr. Hofmann, (GenBank accession # 0058866, Mikami et al., 1989). From this, the construct Xa-1-1959 (ct-1959),

which contains the coding sequence of the C-terminal portion of this α1C subunit (spanning amino acids 1959-2171) was prepared. This construct was then used as the template for construction of the expression vector pGX-2T1959, as follows. BamHI-HindIII fragments of ct-1959 were excised, blunt ended, and subcloned into the SmaI site of the vector pGEX-2T (kindly provided by Dr. J. Griffin (Pharmacia)) to produce the expression vector pGX-2T1959. The pGX-2T vector digested with SmaI was first incubated with calf intestine alkaline phosphatase (CIAP) for 1 h at 37 °C to prevent self-ligation by removing phosphate groups at 5' ends. Competent cells produced from BL21 (DE3) plysS (see section 2.2) were transformed with pGEX-2T1959 to produce a GST-1959 fusion protein.

2.2.2 Making Competent Cells

The ice cold calcium method was used for the preparation of competent cells, as follows. Overnight cultures of XL-1 or BL21 (DE3) plysS strains of E.coli were used to innoculate 30 mL LB media. For BL21 (DE3) plysS cultures, the LB media was supplemented by 30 μL chloramphenicol (34μL/mL). Diluted overnight cultures (1:100 dilution) were grown to a density of OD_{600} = 0.4, then placed on ice to stop bacterial growth. Cultures were centrifuged at 2500 rpm in a 4 °C rotor (Sorvall 6001) for 10 min, the resulting pellets resuspended in 10 mL ice cold 100 mM $CaCl_2$, then kept on ice for 20 minutes. After a further 10 min centrifugation at 4 °C, the pellets were resuspended in 1.8 mL ice cold $CaCl_2$ (100 mM), and placed on ice for 40 minutes. These competent cells were used fresh for transformation of ligation mixtures or were frozen in liquid

nitrogen, after adding glycerol to a final concentration of 30 %, and stored in 200 μL aliquots at –70 °C.

2.2.3 Transformation

Competent cells were transformed either with ligation mixtures or the pGEX-2T1959 construct, according to the following procedure. Cold Qiagen purified expression vector DNA (0.3 μL) or cold ligation mixture (10 μL) were added to 200 μL competent cells on ice, placed on ice for 40 min, then heat shocked for 2 min in a 37 °C water bath. LB medium (1 mL) was added to each tube, and after a 40 min incubation in a 37 °C air incubator, 400 μL of each transformed bacteria mixture was spread on LB ampicillin-chloramphenicol agarose plates. The plates were dried and incubated (37 °C air incubator) overnight, at which time the degree of transformation was detected and calculated in comparison to the control plate (vector only).

2.2.4 Fusion Protein Generation

A GST-1959 fusion protein, corresponding in sequence to the final 211 amino acid residues of the C-terminal portion of the α1C subunit of the rabbit cardiac L-type calcium channel, was generated as follows (Figure 2.2).

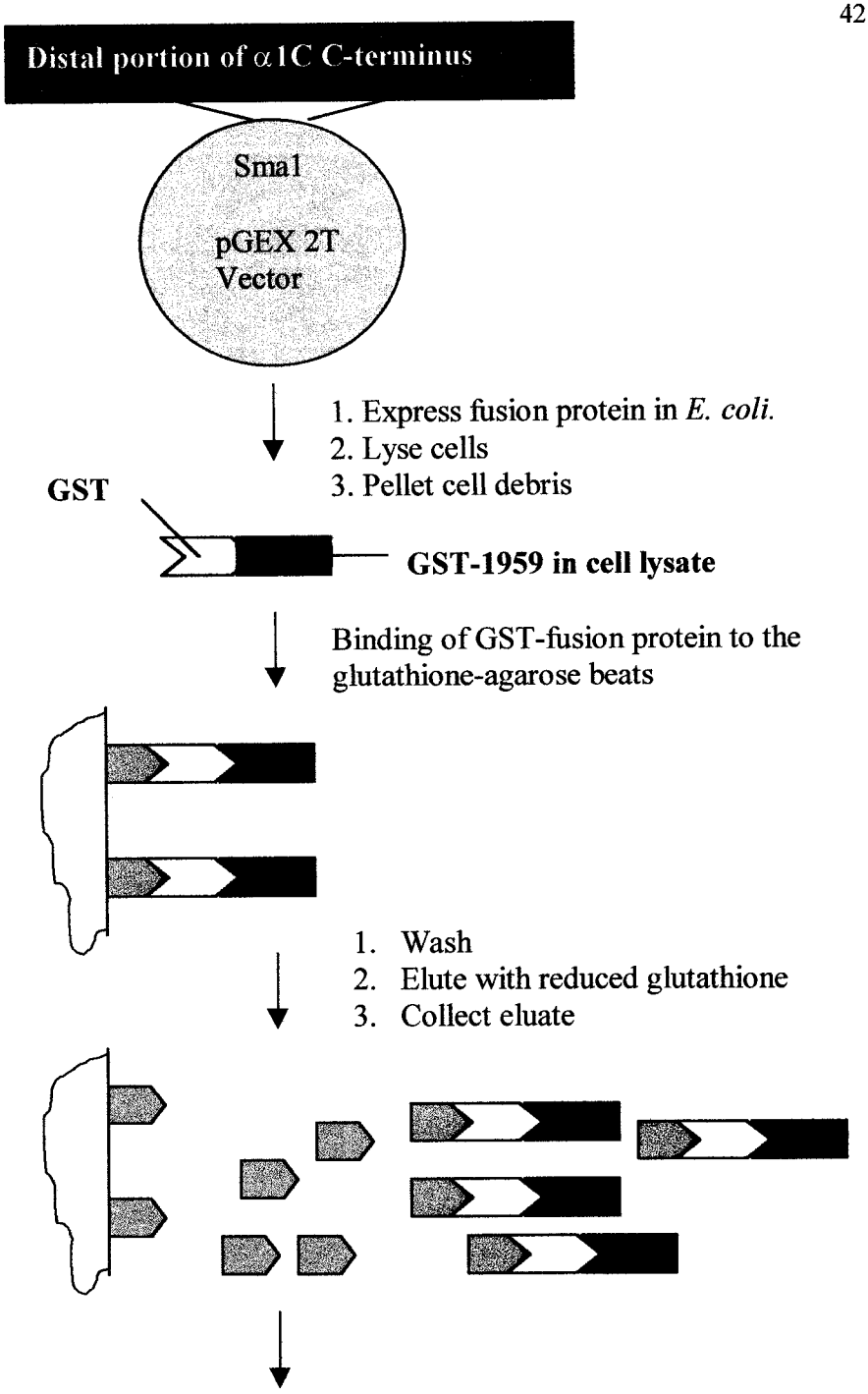

Figure 2.2. Schematic diagram of recombinant protein expression and purification using the glutathione-agarose

2.2.4.1 Large Scale Culture and Protein Induction

Overnight cultures of the E.coli host strain (BL21 (DE3) plysS) transformed with pGEX-1959 constructs were grown in 20 mL of LB medium supplemented with 100 μL/mL ampicillin and 34 μL/mL chloramphenicol. These cultures were used to innoculate 500 mL of LB media containing 0.4 % glucose (purified using a 0.4 micron filter) plus 100μL/mL ampicillin and 34 μL/mL chloramphenicol. These cultures were then incubated at 37 °C with shaking at 260 rpm (Orbital Incubator, Lab Equip Ltd.), or were frozen by the addition of glycerol to a final concentration of 30%. The rate of cell growth was detected by spectrophotometry (Ultraspec 2000, UV/visible, Pharmacia Biotech) at OD_{600} nm. Fusion protein synthesis was induced by the addition of isopropyl-D-thiogalactopyranoside (IPTG) (100 mM final concentration) at mid log growth (OD_{600}= 0.6). Induced cell cultures were incubated for an additional 2.5-3 hours (37 °C, 260 rpm) before being harvested by centrifugation at 3000 rpm for 20 min. Bacterial pellets were either frozen at –70 °C or lysed (see section 2.4.2). The induction and expression of fusion proteins was verified by examining 1 mL of non-induced and induced cell cultures by SDS-PAGE and Western blotting.

2.2.4.2 Bacterial Lysis

Frozen bacterial pellets (thawed on ice) or freshly prepared were resuspended in cold phosphate buffered saline (PBS) plus a protease inhibitor cocktail tablet (1 tablet/10 mL buffer) (Complete, Mini tablet, Boehringer Manneheim) to minimize protein degradation. Mild sonication was used to lyse the bacterial cells (10 second pulse, 10 second rest, for 2 min). During sonication the tubes were placed in a beaker of ice water.

The mixture was then adjusted to 1% TritonX-100 and centrifuged at 10000g for 10min. The supernatant, containing the GST fusion protein (called "clear lysate") was collected for protein purification by affinity chromatography. The insoluble material was re-suspended in PBS. The presence, solubility and yield of protein were determined by analyzing 10 μL of clear lysate and insoluble material by SDS-PAGE and Western blotting.

2.2.5 Isolation of GST Fusion Protein using Affinity Chromatography

2.2.5.1 Resin Preparation

The GST fusion protein was purified by affinity chromatography using glutathione agarose (Sigma Catalogue # G4510). The binding capacity of this resin is 5-10 mg/mL. The glutathione agarose beads were prepared according to the instructions provided, briefly as follows. The lyophilized powder was soaked in deionized water (200 mL/g) for 1 hour at room temperature (RT). The swollen beads (gel) were washed with approximately 10 column volumes of the beads to remove lactose. The beads were then used either in a column or batchwise.

2.2.5.2 Protein Purification

For batchwise use, the beads were washed and equilibrated with several column volumes of washing buffer (PBS), then diluted to a 50% slurry. Cleared lysate was incubated with this slurry for 20 min at RT with rotation. After low speed centrifugation, the supernatant was discarded and the protein-bound beads were washed 3X with PBS. After washing, protein-bound beads were either resuspended in glycerol (20% in PBS)

and frozen at –70 °C, or proteins were immediately eluted in elution buffer (10mM glutathione in 10 mM Tris-HCl, pH 8.0). Samples of bound protein (20μL) as well as samples of each wash (20μL) were collected for SDS-PAGE and Western analysis, to verify the purification of the GST-fusion protein. Before being used in protein binding assays, glycerol was washed out of the beads using 3X 1mL PBS and then proteins were eluted with elution buffer. The elution process was repeated 4 times, and eluted fractions were frozen at -70 °C. Samples for gel analysis were collected from all fractions.

2.2.5.3 Thrombin Cleavage of GST-1959

The GST-1959 fusion proteins eluted from the beads were resuspended in 300μL of PBS plus 1mM $CaCl_2$. Cleavage with thrombin protease (approximately 6U) (Sigma, Catalogue # T3010) was carried out at RT with gentle agitation for 1 h. The reactions were stopped by adding 0.5M EGTA, pH 7.7, to a final concentration of 5 mM. The supernatant from the thrombin cleavage reactions, as well as 2X 300 μL washes (with PBS), were collected for each sample and the yield was determined by analyzing 10 μL of supernatant by SDS-PAGE and Western blotting.

2.2.6 Gel Electrophoresis and Immunoblotting

Protein samples were prepared by adding one part protein to one part 10x sodium dodecyl sulphate (SDS) electrophoresis sample buffer of the following composition: 0.0625 M Tris-HCl (pH 6.8); 10% (v/v) glycerol; 2% (w/v) (SDS); 5% 2-mercaptoethanol; and 0.001% (w/v) bromophenol blue. However, very diluted protein samples were mixed 5 parts protein to 1 part 10X sample buffer. Protein samples were

boiled (100°C) for 5 min. in sample buffer, and resolved by SDS-polyacrylamide gel electrophoresis (SDS-PAGE) (Laemmli, 1970). The samples were electrophoresed in a Mini-Cell II (XCell) or Bio-Rad Mini-Protean II gel apparatus using an EC Apparatus Inc. power supply (model E-C 105). Discontinuous polyacrylamide gels (1.5 mm X 7.3 mm, made up of an initial 4% stacking gel followed by a 12% separating gel) were prepared as follows. Stacking gel: 4% (w/v) acrylamide monomer and N,N'-methylenebisacrylamide (BIS) crosslinker; 0.125 M Tris-HC1 buffer (pH 6.8); 0.1% (w/v) SDS; 0.05% (w/v) ammonium persulfate; and 0.05% (v/v) TEMED. Separating gel: 12% (w/v) acrylamide monomer and N, N'-methylenebisacrylamide (BIS) crosslinker; 0.375 M Tris-HCI (pH 8.8); 0.1% (w/v) SDS; 0.05% (w/v) ammonium persulfate and 0.05% (v/v) TEMED. Pre-cast gels (20% gradient Tris-glycine gels (1.5 mm X 80 mm X 80 mm, NOVAX) were also used for radiolabelled photoaffinity experiments. The electrophoresis running buffer consisted of 0.025 M Tris-HCl (pH 8.3), 0.192 M glycine and 0.1% (w/v) SDS. Electrophoretic separation of the 4% stacking/15% separating gel occurred at 120-150V, run at constant voltage (45-60'). Pre-stained (broad range) molecular mass standards (New England BioLabs) containing MBP-3-galactosidase (175 kDa), MBP-paramyosin (83 kDa), glutamic dehydrogenase (62 kDa), aldolase (47 kDa), triphosphate isomerase (32 kDa), lactoglobulin A (25 kDa), lysozyme (16 kDa), and aprotinin (6.5 kDa) were also separated on each gel. Each standard lane contained 10 μL of mass marker. The gel resolved fusion proteins were either stained by coomassie brilliant blue or transferred onto membranes for detection by immunoblotting.

2.2.6.1 Immunoblotting

To visualize protein bands by staining with coomassie blue, SDS gels were soaked in staining solution (1% (w/v) coomassie blue in 10% acetic acid and 40% ethanol) for 30 minutes, then destained (10% acetic acid in 40% ethanol) overnight. For immunodetection, proteins were transferred electrophoretically (Towbin et al., 1979) onto nitrocellulose or polyvinyl difluoride (PVDF). Prior to transfer, PVDF membranes were presoaked in 100% methanol for 2 seconds, then equilibrated in transfer buffer (0.025 M tris-HCl (pH 8.3), 0.192 M glycine and 20% (v/v) methanol) for 3 min. Nitrocellulose sheets were equilibrated directly in transfer buffer for 20 min. The gels were also equilibrated in transfer buffer for 15 min before transfer. Transfer occurred at a constant voltage of 100V, in transfer buffer, for 1 hour in a Bio-Rad Mini Trans-Blot Electrophoretic Transfer Cell with an EC Apparatus Inc. power supply (model E-C 105). Non-specific binding sites were blocked following transfer by incubating the membranes overnight at 4° C in 5% (w/v) non-fat dry milk (NFDM) (Carnation) plus 0.1% (v/v) Tween 20 in PBS.

Blots were washed (3 brief followed by 3 long washes) in PBS-T (PBS + 20mM Tris, 500 mM NaCI, 0.05% (v/v) Tween-20 (pH 7.5), and then 3 brief followed by 3 long washes in PBS at 20 °C. Blots were then incubated in the presence of the primary antibody (Mouse anti-GST, Serotec U.K.), which was diluted (1:100) in PBS-T, for 1 hour at RT on an orbital shaker. After repeated washings (3 brief followed by 3 long washes in PBS-T, and 3 brief followed by 3 long washes in PBS), the blots were exposed to the secondary antibody (horseradish peroxidase conjugated goat anti-mouse (HRP GAM) diluted 1:10000 in PBS-T. The blots were then re-washed. The enhanced

chemiluminescence (ECL Plus) method (Amersham Pharmacia Biotech) was used for the detection of immobilized specific antigens conjugated to HRP labelled antibodies as follows. Blots were incubated with detection reagents (A and B, mixed in a ratio of 40:1) (0.1 ml of mixture/cm^2 of nitrocellulose) for 5 min, then drained, covered in plastic wrap (Saran Wrap), placed in autoradiography cassettes (Fisher Biotech; FBXC 810, 8 x 10 inches) protein side up and exposed to Kodak scientific imaging film (X-Omat AR, 8 x 10 inches). The films were developed using a developer (M35 AX-Omat Developer, Kodak).

2.2.6.2 Determination of Protein Concentration

Protein concentration was determined using the Bradford Assay. Briefly, the dye reagent was prepared by diluting 1 part Dye Reagent Concentrate (Bio-Rad No. 500-0001) with four parts of distilled and deionized water. Then, the dye reagent was filtered through a Whatman # 1 filter to remove particulate. Three to five dilutions of a standard protein (bovine serum albumin (BSA)) were prepared and used as a standard protein solution. Then, 100 µl of each standard and sample solution was transferred into a clean, dry test tube, and was assayed in duplicate. Diluted dye reagent (5.0 ml) was added to each tube and was mixed by vortexing. Absorbency was measured at 595 nm.

2.2.7 ATP Binding Assay

2.2.7.1 ATP-agarose Resin Preparation

ATP-agarose beads (Sigma Catalogue #A9268) were used to detect the level of binding of the GST-fusion protein (GST-1959) to ATP. Adenosine 5'-triphosphate (ATP)

is attached to the agarose beads through the adenine N-6 position, and the concentration of the immobilized ATP ligand is 1-5 moles/mL of packed resin. The resin was hydrated in an excess of water (approximately 50 mL per gram of resin) for 2 hours at 4 °C. The swollen ATP-agarose beads were washed 3X by adding 10 column volumes of deionized distilled H_2O. The washed, swollen beads were equilibrated with several column volumes of Tris-HCl buffer with or without $MgCl_2$. The concentration of Mg^{2+} in the buffer was estimated using Chelator Software (Schoenmakers et al., 1992). This concentration was equal to the concentration of free Mg^{2+} in a solution of 20 mM Mg^{2+} -ATP in 50 mM Tris-HCl buffer, which was used as a competitor solution in the ATP binding assays.

2.2.7.2 Affinity Chromatography using ATP-agarose Beads

2.2.7.2.1 Binding Protocol

The ATP binding ability of the distal portion of the α1C C-terminus (amino acids residues 1959-2171) fused with the GST tag (named GST-1959) was examined using ATP-agarose beads. The fusion protein (100 μg) was incubated with 100 μL of packed ATP-agarose beads (ligand immobilized 1-5 M/1mL packed resin) in 500 L of 50 mM Tris-HCl, 150 mM NaCl, 0.9 mM $MgCl_2$, pH 7.5, for 3 hours with rotation at 4 C. The beads were washed 3 X with 100 μL incubation buffer, and proteins were eluted with 20 mM Mg^{2+} -ATP. The beads were dissolved in SDS sample buffer, boiled for 5 minutes, and centrifuged. The supernatant was collected for gel analysis (Figure 2.3).

2.2.7.2.2 ATP Competition Assay

Non-specific binding of GST-1959 to ATP agarose beads was determined by carrying out the binding assay described in 2.7.2.1 in the presence of 20 mM Mg-ATP as a competitor. The GST-1951 fusion protein (100 μg) was incubated with 20 mM Mg-ATP in tris buffer with $MgCl_2$ for 2 hours on ice prior to incubation with 100μL packed ATP-agarose for 3 hours. Unbound, bound, samples from 3 washes, and eluted fractions were collected for SDS-PAGE analysis (Figure 2.3).

2.2.7.2.3 Role of $MgCl_2$

To test the possible role of Mg^{2+} ($MgCl_2$ Tris buffer) on the ability of the GST fusion protein to bind the ATP-agarose beads, binding assays were carried out in the absence of $MgCl_2$. The assay procedure was similar to the procedure that used for binding assay in the presence of $MgCl_2$ (Figure 2.3).

For quantitative analysis of proteins stained with coomassie brilliant blue, gels were scanned using a Bio-Rad Model GS-670 (Bio-Rad, Richmond, CA) imaging densitometer (scan mode: transmittance, pixel density: 8 bit precision, max. resolution: 64μm) with image analysis software (Molecular Analyst/MacIntosh software for Bio-Rad) within the range where the relationship between the protein loaded and the densitometric response was linear. Binding assay experiments were repeated 5 times and the data were analyzed using paired t-tests.

Figure 2.3. ATP-agarose binding assay diagram.

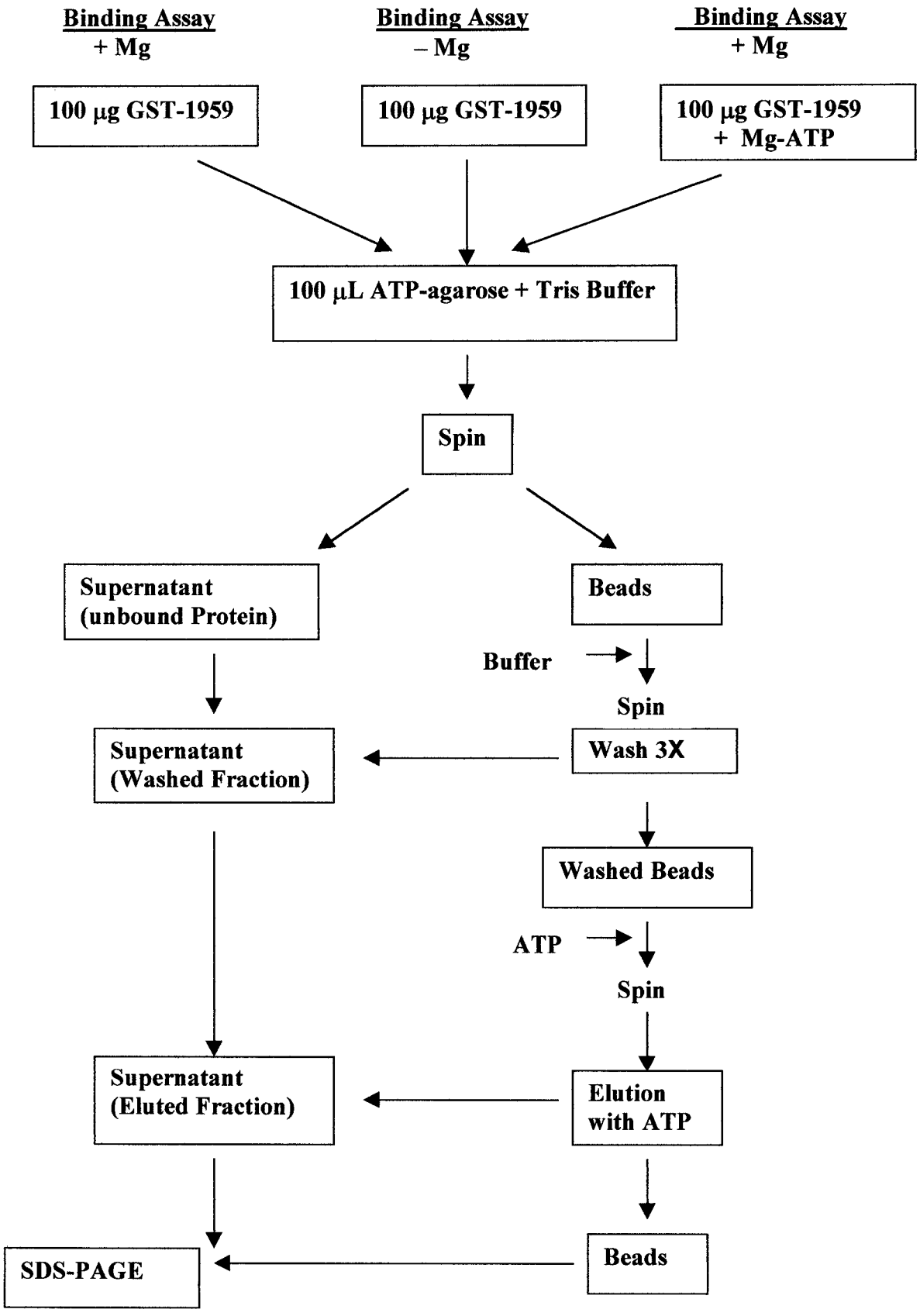

2.2.8 Photoaffinity Radiolabelling

As an alternative method for ATP binding direct interaction of the GST-1959 fusion protein with ATP was investigated using the photoaffinity ATP analog, 8-azido-α [^{32}P] ATP. The GST-1959 fusion protien (5 g/L) (3.2 μL) was incubated on ice with 25 pM of 8-azido-α [^{32}P] ATP at pH 7.4 for one hour. The reaction mixtures were exposed to UV irradiation (using an inverted UV box at a fixed position) for 0.5, 1, 2, and 10 min, on ice, to facilitate cross-linking. After addition of SDS sample buffer to the tubes, the tubes were mixed and incubated at RT for 30 min prior to analysis by SDS-PAGE. Samples were electrophoresed in precast 20% SDS gels. Gels were washed, wrapped in plastic wrap, placed in autoradiography cassettes, and exposed to X ray film for 15 min, 2 h and overnight, at –70 °C. Experiments were carried out in triplicate.

2.2.8.1 Competition of Photoaffinity Labelling by ATP

The specificity of photoaffinity labeling of GST-1959 was examined by pre-incubation of the GST-1959 fusion protein with various concentrations (1, 3, and 5 mM) of unlabelled ATP, prior to incubation with 8-azido-α [^{32}P] ATP.

2.2.9 Binding Assay using TNT-ATP

Binding of ATP to the GST-1959 fusion protein was investigated using a fluorescent ATP (TNT-ATP) and scanning fluorimeter (Florke et al., 1994). Two sets of experiments were conducted to perform the binding assay. In one set of experiments, the TNT-ATP compound 2'-(or 3')-o-(trinitrophenyl) adenosine-5'- triphosphate trisodium salt (Molecular Probe, Eugene, Oregon, USA) at three different concentrations (0.0 mM,

0.35 mM , 0.5 mM) was added to the tubes containing Tris-HCl buffer (150 mM, pH 7.5, plus $MgCl_2$) and 2 nM GST-1959 fusion protein. In another set of experiments, TNT-ATP (0.0 mM, 0.35 mM and 0.5 mM) were added to the tubes containing only Tris-HCl buffer and used as a control to compare the enhancement of fluorescent intensity. The fluorescent intensity of experimental samples was detected using scanning fluorimeter. The excitation wavelength was 415 nm and the emission was scanned in a various wavelength (500- 600 nm) with the maximum emission at 550 nm.

2.2.10 Far-UV Circular Dichroism Spectroscopy

Circular dichroic measurements were carried out in the far-UV range (190-250 nm) at 20°C under constant nitrogen purge using a Jasco J-600 Spectropolarimeter (Japan Spectroscopic Co. Ltd., Tokyo, Japan) with a cell length of 1 mm. The GST-1959 fusion protein (0.5 mg) samples were diluted in tris HCl buffer (pH 7.5) and assayed in the presence and absence of 0.5 mM Mg-ATP. The secondary structure fractions were calculated using the Jasco-SSE program, which was based on the algorithm of Chang et al. (1978) and the database of Hennesseg and Johnson (1981). Analyses were performed in triplicate with four scans per replicate.

2.3 Results

2.3.1 Generation of Fusion Protein

The GST-1959 fusion protein was generated by subcloning the cDNA from the C-terminal portion of the rabbit cardiac α1C subunit of the L-type calcium channel, consisting of amino acid residues 1959-2171 into a pGEX-2T (Figure 2.4) to form the

pGEX-1959 construct (Figure 2.4). Competent E.coli (BL21 (DE3) plysS) were transformed with this construct and induced by IPTG to express a 48-kDa GST-1959 fusion protein. The expression of fusion proteins was verified by SDS-PAGE and Western blotting using antibodies against the GST tag. As shown by SDS-PAGE analysis (Figure 2.5), a major 48 kDa band (equal to the molecular weight of the GST-1959 protein) appeared in each lane loaded with the preparation of the bacterial cultures induced with IPTG (lanes 2-9). This band was not observed in the bacterial culture prior to induction with IPTG (lane 1). Furthermore, Western blot analysis using an anti-GST antibody proved that this 48 kDa band was a GST-tagged protein which was induced by IPTG and was eluted by a competitor of 10 mM glutathione (Figure 2.6). In addition to the 48kDa protein band, which represents the expression of the GST-1959 fusion protein, there are several minor bands at molecular weights below the 48 kDa GST-1959 fusion protein (Figure 2.5, lanes 8 and 9) that are recognized by anti-GST antibodies (Figure 2.6, lanes 3, 4). These minor bands may represent truncated or degraded recombinant proteins. All possible precautions were employed, such as using protease inhibitors and carrying out all bacterial lysis and protein purification steps on ice, to prevent degradation of the GST protein. These minor bands may also be preterminated proteins, which can occur when eukaryotic proteins are expressed in a prokaryotic system such as E.coli. This pretermination may be due to the different codon bias between species. However, the majority of the protein expressed is the 48kDa GST-fusion protein and the expression of the minor bands is trivial.

Figure 2.4. The pGEX-1959 construct. pGEX-2T vector (4.9 Kb) plus cDNA fragment cut by BamHI- Hind III restriction enzymes from ct-1959 construct and inserted into SmaI site of pGEX-2T. The direction of cloning and open reading frame of GST + cDNA Tanabe was verified by restriction enzyme analysis and sequencing.

1959 cDNA codes for amino acids 1959-2171

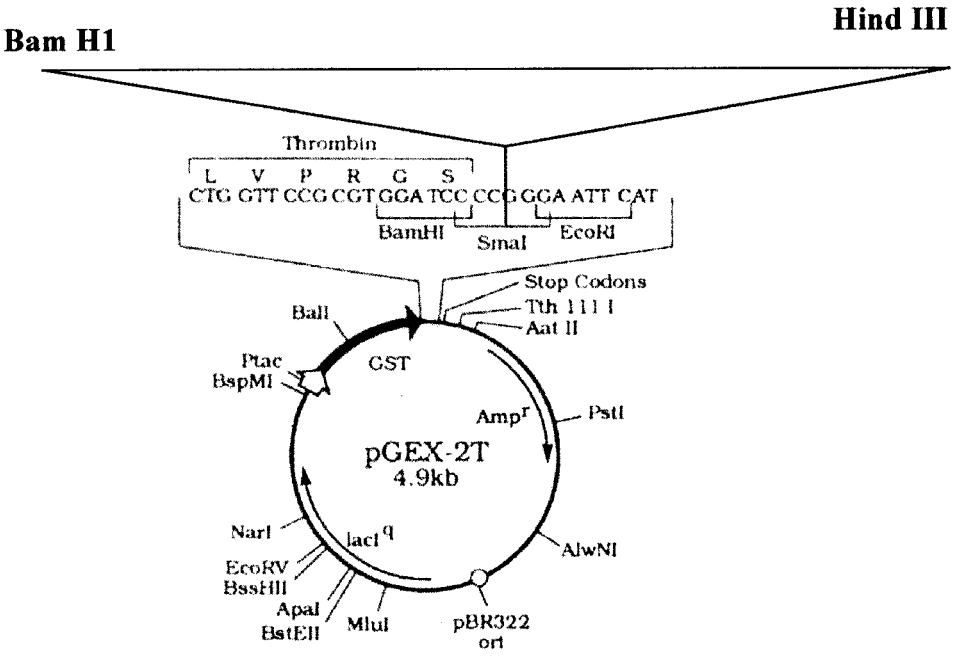

Figure 2.5. Expression and purification of recombinant fusion protein GST-1959 (12% SDS-PAGE gel stained with coomassie blue). Lane M, molecular weight standard; lane 1, lysate of uninduced E.coli transformed with expression vector pGX-1959; lanes 2-9 lysate of E.coli transformed with pGEX-1959 and induced for 2.5 h with 1mM IPTG; lane 3, lysate of induced E.coli after sonication; lane 4, cleared lysate (soluble protein after centrifugation of induced lysate); lane 5, first wash; lane 6, insoluble protein (cell debris); lane 7 supernatant after incubation of cleared lysate with glutathione agarose beads and centrifugation; lane 8, purified GST-1959 fusion protein bound to the glutathione-agarose beads; lane 9, purified GST-1959 fusion protein and concentrated by ultrafiltration.

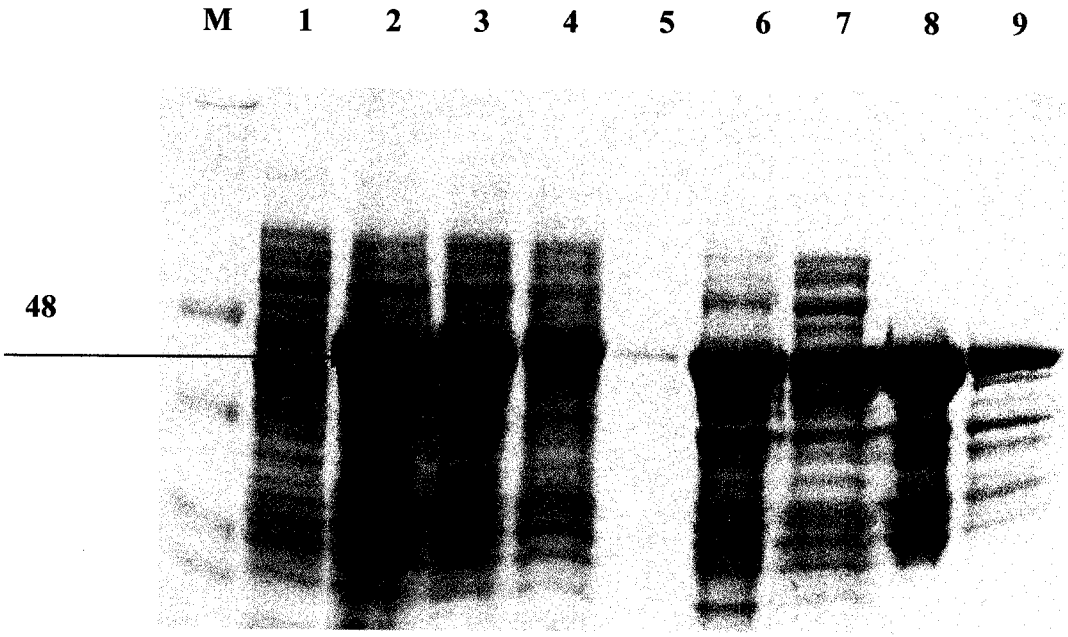
M
1
2
3
4
5
6
7
8
9
48

Figure 2.6. Expression and purification of recombinant fusion protein GST-1959 by Western blotting using an antibody against the GST tag. Lane 1, lysate of E.coli transformed with pGEX-1959 construct and induced for 2.5 h with 1mM IPTG; lane 2, lysate of uninduced E.coli transformed with pGX-1959 construct; lane 3,4, GST-1959 fusion protein purified by affinity chromatography using glutathione-agarose and concentrated by ultrafiltration using Centricon 10.

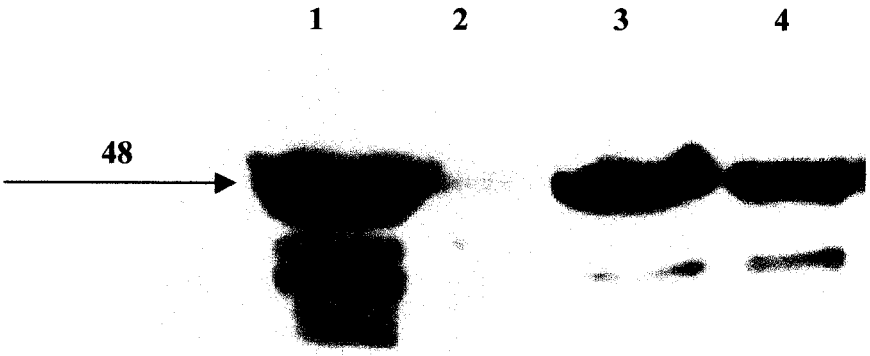
1
2
3
4
48

After elution the purified GST-1959 fusion protein was concentrated by ultrafiltration. The concentration of protein was determined prior to and after ultrafiltration. The GST-1959 fusion protein was then incubated with thrombin enzyme to cleave the GST tag. The results of cleavage were analyzed by SDS-PAGE and Western blotting. SDS-PAGE of the cleaved samples (Figure 2.7A) showed that the 48 kDa band (GST-1959) (lane 2) disappeared, and two new bands appeared (lanes 3-5). One band represents the 26 kDa GST fragment, and the other band represents the 22 kDa 1959 C terminus fragment. However, both bands were recognized by a GST-antibody using Western blot analysis (Figure 2.7B).

Figure 2.7

A) Cleavage of the GST-1959 fusion protein by thrombin while bound to the glutathione agarose beads. 12% SDS-PAGE, stained with commassie brilliant blue. Lane 1, GST-1959 fusion protein before cleavage by thrombin; lane 2, GST-1959 fusion protein eluted from beads after cleavage by thrombin; lanes 3 and 4, bead washes after cleavage by thrombin.

B) Cleavage of the GST-1959 fusion protein by thrombin Western blot analysis using an antibody against the GST tag, 1 minute exposure. Lane 1, GST-1959 fusion protein before cleavage by thrombin; lane 2, GST-1959 fusion protein remaining bound to the agarose beads after cleavage by thrombin; lanes 3 and 4, beads washes after cleavage by thrombin; lane 5, GST-1959 fusion protein eluted from beads after cleavage by thrombin.

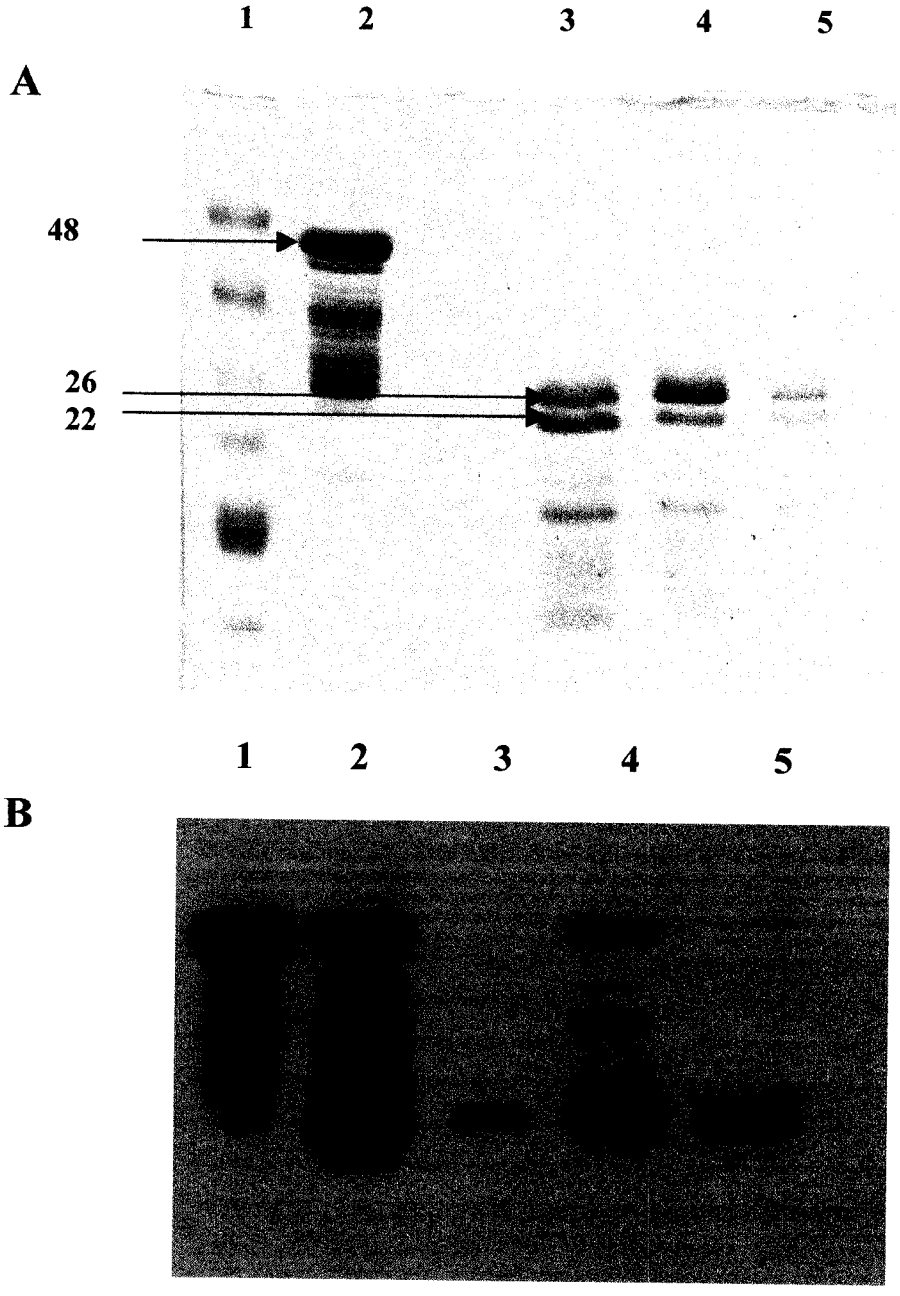
1
2
3
4
5
A
48
26
22
1
2
3
4
5
B

2.3.2 Allosteric Regulation of Calcium Channels by Mg-ATP

The hypothesized allosteric regulation of calcium channels by ATP was investigated by examining the ability of the GST-1959 fusion protein to bind Mg-ATP using affinity chromatography, (ATP-agarose), photoaffinity radiolabelling (azido-ATP), spectrofluorimetry, and circular dichroism.

2.3.2.1 Binding Assay

2.3.2.1.1 Affinity Chromatography using ATP-agarose Beads

2.3.2.1.1.2 Rational for using Affinity Chromatography

Affinity chromatography is a powerful technique for protein purification. This method is based on the interaction of proteins with specific ligands. In this technique, the ligand is chemically attached to a suitable solid support (insoluble or porous); the site on the ligand that attaches to the solid support does not participate in binding to the desired protein. More importantly, a spacer group is usually inserted between the ligand and the solid support to prevent interference with binding of proteins to the ligand (Creighton, 1984). The desired protein binds to the ligand-resin. Other proteins do not bind; instead they pass through the column. After washing the column to remove all non-specific proteins, those proteins bound tightly are eluted by adding soluble ligand to compete with that of protein already bound.

Affinity chromatography using ATP-agarose resin has previously been used successfully for detection of the ATP binding ability of proteins containing nucleotide binding sites, such as heat shock protein 70 and 110 (hsp70, hsp110) (Oh et al., 1999), voltage dependent anionic channels (VDAC) and the cystic fibrosis transmembrane

conductance regulator (CFTR) (Florke et al., 1994). Thus this method was chosen to detect the binding ability of the GST-1959 fusion protein to ATP.

2.3.2.1.1.3 ATP Binding

To investigate the binding of Mg-ATP to GST-1959, 100 μg (2 nM) GST-1959 fusion protein was incubated with 200 μL ATP-agrose beads, and centrifuged to remove the unbound protein (in the supernatant). The bound protein (in the pellet) was eluted with 20 mM free Mg-ATP, after 3X washing with washing buffer. The unbound protein, protein in 3 washes, eluted protein, and protein that remained bound to the beads were analyzed by SDS-PAGE followed by staining with coomassie brilliant blue (Figure 2.8). The experiment was also conducted in the presence of excess amount of Mg-ATP as a competitor to detect any non-specific binding to the ATP-agarose beads. A similar experiment was performed in the absence $MgCl_2$ to detect the role of Mg^{2+} on the binding of ATP. The results of these three parallel experiments are shown in Figure 2.8.

Lane 2 (UB) (Figure 2.8A) represents the protein that remained unbound to the beads and was recovered in the supernatant, after 3 hours of protein incubation with the ATP-agrose beads (in the presence $MgCl_2$). Densitometric quantification of this band showed that most of the protein incubated with ATP-agrose beads did not bind to the beads and was recovered in this supernatant portion (Figure 2.9, lane 5). Quantification of the bands representing unbound proteins isolated from the supernatant in the competition experiments (to determine non-specific binding) (Figure 2.8B, lane UB and Figure 2.9, lane 6) carried out in the presence of Mg-ATP or in the absence of $MgCl_2$

(Figure 2.8C, lane UB and Figure 2.9, lane 4) revealed that the amount of the unbound proteins was not different from that recovered in the presence of Mg-ATP.

The ATP-agarose beads were typically washed 3X's with washing buffer after incubation with GST-1959 fusion protein. Most of the ATP-agarose bound protein was recovered in washing fractions (Figure 2.8 A,B,C, lanes w1-w3 and Figure 2.9 lanes 7-9). That may suggest the binding of GST-fusion protein to the ATP agarose beads was non-specific or the binding affinity was very low which resulted in easily dissociation of protein from ATP-agarose beads by washing.

No visible band was detected in the eluted fraction in the presence of $MgCl_2$ (specific binding assay) (Figure 2.8A, lane E), or in the assay for detecting non-specific binding (competition assay) (Figure 2.8 B, lane E) or in the absence of $MgCl_2$ (Figure 2.8C, lane E). These results suggest that there may not be any detectable specific binding between ATP-agarose beads and GST-1959 fusion protein and Mg^{2+} does not have positive role in the binding. However, if there was any affinity between Mg-ATP and GST-1959 fusion protein, it was expected to have a visible band in the lane E of Figure 2.8 A.

Finally in these three experiments equal amounts of protein remained bound (called bound protein) to the ATP-agarose beads even after 3X's washing and elution with 20 mM free ATP as a competitor (Figure 2.8, lane 1B, and Figure 2.9, lanes 1,2,3). Since there was no difference in the amount of protein remained bound to the ATP-agarose beads after washing and elution, it can also be the indicative of non-specific binding. Otherwise, the density of the bound protein band would be different in those experiments.

All experimental conditions including pH, buffer system, ionic strength and Mg^{2+} concentration were chosen to be the same as the physiological conditions and that were employed for electrophysiological experiments conducted in the laboratory and my hypothesis was formulated based on them (*in vivo*). However, this does not rule out the possibility that optimization of pH (Flork et al, 1994) and other factors for *in vitro* conditions may be different from *in vivo* conditions.

Hsp70 (kindly provided by Dr. John Glover, Department of Biochemistry, University of Toronto) was employed as a positive control for the ATP binding assay, since it has been long recognized that hsp70 binds to ATP through its ATP binding domain. ATP is also required for the chaperoning function of hsp70. It has also been shown (Oh et al., 1999), that hsp70 binds well to ATP-agarose binding protein. For this control assay, 2 nM of hsp70 was incubated with 100 µL packed ATP- agarose beads (1-5µM/mL packed resin) for 3 hours at 4°C with rotation. The procedure for the binding assay of hsp70 was the same as used for the GST-1959 fusion protein binding to ATP-agarose beads. The pattern of binding of hsp70 to the ATP-agarose beads was not similar to the GST-1959 fusion protein (Figure 2.10).

Figure 2.8. Binding of GST-1959 to ATP-agarose beads in the presence of $MgCl_2$. 12 % SDSP-PAGE gel stained with coomassie brilliant blue.

A: Specific binding. Lane B (bound protein), GST-1959 protein which remained bound to ATP-agarose beads after washing and eluting with 20 mM free Mg-ATP; lane UB (unbound) protein did not bind after 3 h incubation of GST-1959 with ATP-agarose beads; lanes W1 and W3, after washing beads with washing buffer (150 mM Tris-HCl + $MgCl_2$); lane E, protein eluted with 20 mM free Mg-ATP as a competitor.

B: Non-specific binding, incubation of GST-1959 with 20 mM Mg-ATP for 2h on ice prior to incubation with ATP-agarose beads. Lane B (bound protein), GST-1959 protein which remained bound to ATP-agarose beads after washing and eluting with 20 mM free Mg-ATP; lane UB (unbound) unbound protein after 3 h incubation of GST-1959 with ATP-agarose beads; lanes W1 and W3, after washing with washing buffer (150 mM Tris-HCl + $MgCl_2$); lane E, protein eluted with 20 mM free Mg-ATP as a competitor.

C: Binding of the GST-1959 to the ATP-agarose beads in the absence of $MgCl_2$. SDS-PAGE, gel stained with coomassie brilliant blue. Lane B (bound protein), GST-1959 protein which remained bound to ATP-agarose beads after washing and eluting with 20 mM free ATP; lane UB (unbound) unbound protein after 3 h incubation of GST-1959 with ATP-agarose beads; lanes W1 and W3, after washing with washing buffer (150 mM Tris-HCl); lane E, protein eluted with 20 mM free ATP as a competitor.

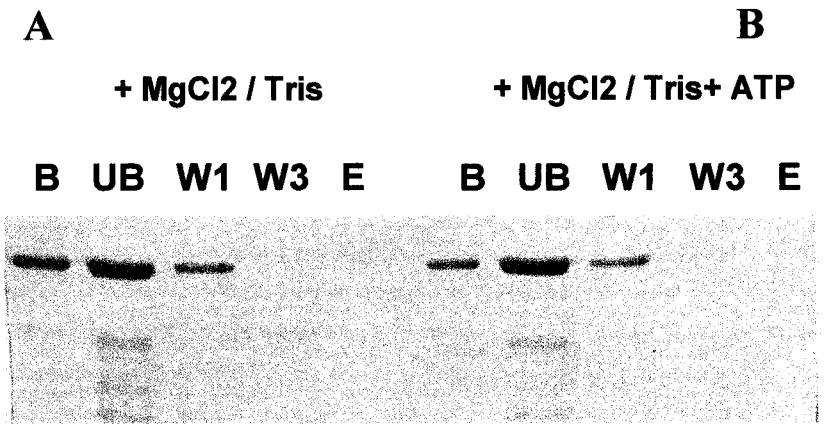
A
B
+ MgCl2 / Tris
+ MgCl2 / Tris+ ATP
B UB W1 W3 E
B UB W1 W3 E

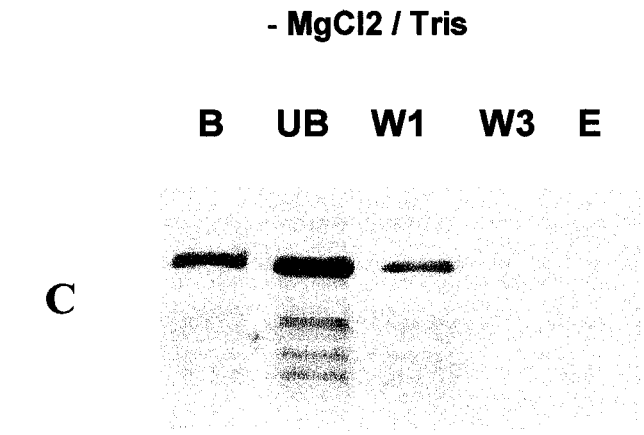
- MgCl2 / Tris
B UB W1 W3 E
C

Figure 2.9. Quantitative analysis of binding of GST-1959 fusion protein to ATP-agarose beads in the presence and absence of MgCl2 and Mg-ATP. Lanes 1-3 represent the protein which remained bound to the ATP-agarose beads after washing and elution. Lane 1, absence of $MgCl_2$. Lane 2, presence of MgCl2. Lane 3, pre-incubation with Mg-ATP. Lanes 4-6 represent the protein that does not bind to the ATP-agarose bead and is recovered in the supernatant. Lane 4, absence of $MgCl_2$; Lane 5, presence of $MgCl_2$; lane 6 pre-incubation with Mg-ATP. Lanes 7-9 represent the amount of protein that was washed out of the beads with washing buffer. Lane 7, in the absence of Mg^{2+}; lane 8, in the presence of Mg^{2+}; lane 9, pre-incubation with Mg-ATP. Densiotometric analysis of SDS-PAGE, (n=5).

Quantitative Analysis of GST-1959 Binding to ATP-agarose Beads

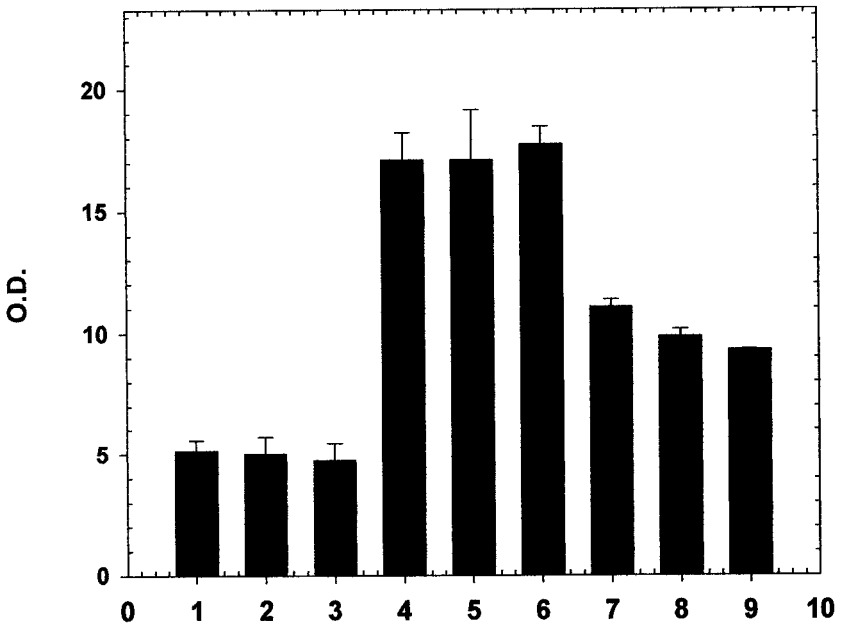

Figure 2. 10. Binding of hsp70 to ATP-agarose beads in the presence of $MgCl_2$. 12 % SDSP-PAGE gel stained with coomassie brilliant blue.

A: Specific binding. Lane B (bound protein), hsp70 protein remained bound to ATP-agarose beads after washing and eluting with 20 mM free Mg-ATP. Lane UB (unbound) unbound protein after 3 h incubation of hsp70 with ATP-agarose beads. Lanes W1 and W3, after washing with washing buffer (150 mM Tris-HCl + $MgCl_2$). Lane E, protein eluted with 20 mM free Mg-ATP as a competitor.

B: Non-specific binding, incubation of hsp70 with 20 mM Mg-ATP for 2h on ice prior to incubation with ATP-agarose beads. Lane B (bound protein), hsp70 protein which remained bound to ATP-agarose beads after washing and eluting with 20 mM free Mg-ATP. Lane UB (unbound) unbound protein after 3 h incubation of hsp70 with ATP-agarose beads. Lanes W1 and W3, after washing with washing buffer (150 mM Tris-HCl + $MgCl_2$); lane E, protein eluted with 20 mM free Mg-ATP as a competitor.

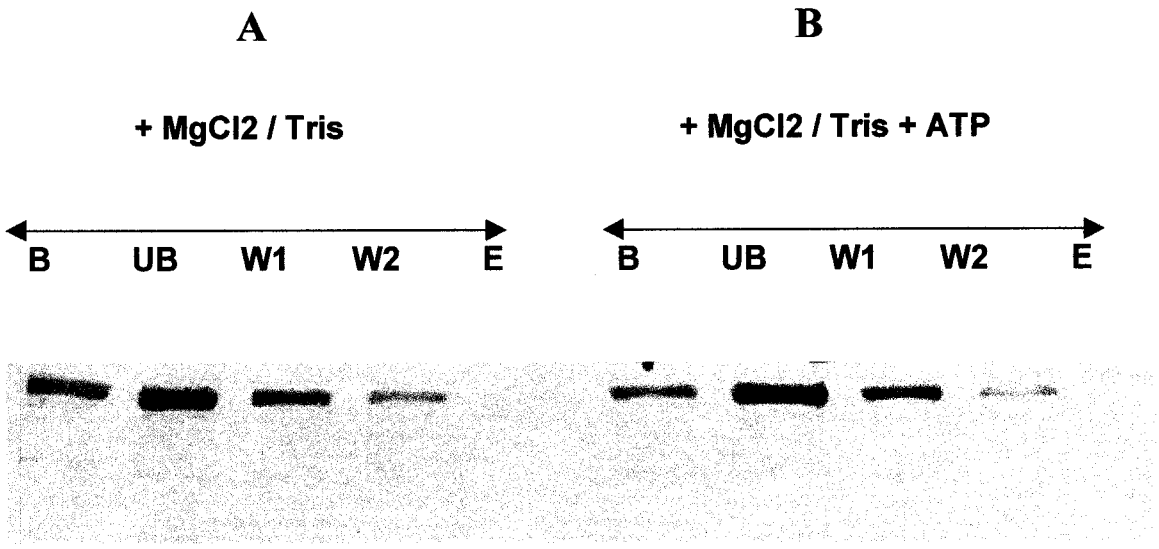

B = Bound UB = UnBound W1, W2, W3 = Wash E = Eluted

2.3.3 Photoaffinity Labelling of GST-1959 by 8-azido-[α-^{32}P]ATP

To further determine whether the recombinant protein GST-1959 possessed the ability to bind ATP, isolated protein was incubated with a photo-active ATP analogue (8-azido-[α-^{32}P]ATP). This radioactive compound has been shown previously to specifically label various ATP binding proteins (Booth et al., 2000). Those experiments suggest that it is capable of binding in a manner similar to ATP

The autoradiogram results of photoaffinity labelling of GST-1959 with 8-azido-[α-^{32}P]ATP (as shown in Figure 2.11) indicates that the GST-1959 fusion protein was photoaffinity-labelled with ATP and that 30 seconds of irradiation was sufficient for labelling. A competition assay (non-specific binding) was then carried out to determine the specificity of photoactivity labelling as follows. The GST-1959 fusion protein was pre-incubated in increasing concentrations of cold ATP (1, 3, 5 mM) with or without $MgCl_2$, prior to incubation with 8-azido-[α-^{32}P]ATP. Photoaffinity labeling of GST-1959 was not inhibited by cold ATP added to the reaction mixture prior to incubation with radioligand (Figure 2.12). Even when the highest concentration of cold ATP (5 mM) was used, ATP labelling was not inhibited. These results suggest that the labelling of GST-1959 by 8-azido-[α-^{32}P]ATP is due to non-specific binding of radiolabelled ATP to the GST tag or the C-terminal protein or both. It has been shown elsewhere (Randak et al., 1995) that the glutathione-S-transferase (GST) protein (Sigma) (lane 1) that was used as a negative control does not bind ATP. However, despite this lack of binding, it showed high degree of labelling with 8-azido-[α-^{32}P] ATP under our experimental conditions. Thus it is possible that any inhibition of specific labelling of the C-terminal protein by cold ATP may be hidden by non-specific radiolabelling of the GST protein. Photoaffinity

labelling of GST-1959 fusion protein was not also affected by the presence or absence of $MgCl_2$ (Figure 2.12, lane, - $MgCl_2$). To determine the level of background, 8-azido-[α-^{32}P]ATP was added to the incubation buffer, as observed in the Figure 2.12 (lane, buffer). There was no reaction between the buffer and radiolabelled azido ATP.

Figure 2.11. Photoaffinity labelling of the GST1959 fusion protein in the presence of 25 pmoles photoactive 8-azido-[α-^{32}P]ATP. Lanes 1-3 were exposed to the UV irradiation for 2 min, lanes 4-6 for 1min and lanes 7-9 for 30 seconds. SDS-PAGE gel, overnight exposure to Kodak XAR film at –70 °C.

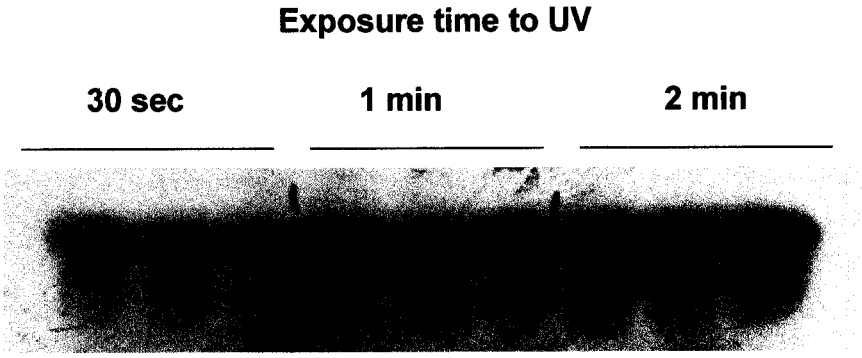
Exposure time to UV
30 sec
1 min
2 min

Figure 2.12. The specificity of photoaffinity labelling of GST 1959 by 8-azido-[α-^{32}P]ATP was determined by pre-incubation of the GST-1959 fusion protein with increasing concentrations of cold ATP with or without $MgCl_2$, prior to incubation with 25 pmole 8-azido-[α-^{32}P]ATP and 2 min exposure to UV. Lane 1, GST protein alone used as a control for non-specific binding. Lane 2, GST-1959 fusion protein plus 25 pmole 8-azido-[α-^{32}P]ATP in the absence $MgCl_2$. Lanes 3,4,5, pre-incubation of GST-1959 fusion protein with 5mM cold ATP. Lanes 6,7,8, pre-incubation with 3 mM cold ATP. Lanes 9,10,11, pre-incubation with 1mM cold ATP. Lane 12 GST-1959 fusion protein plus 25 pmole 8-azido-[α-^{32}P]ATP and Mg^{2+} (no cold ATP). Lane 12, incubation buffer plus 25 pmole 8-azido-[α-^{32}P]ATP. Film exposed to 12% SDS-PAGE gel, overnight exposure at –70 °C.

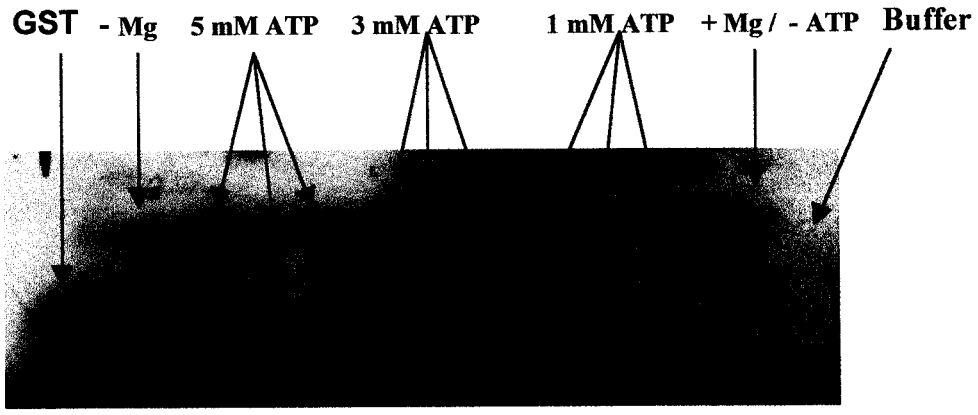
GST
- Mg
5 mM ATP
3 mM ATP
1 mM ATP
+ Mg / - ATP
Buffer

2.3.4 Binding Assay using TNT-ATP

The GST-1959 protein was incubated with TNT-ATP (a fluorescent form of ATP). The intensity of fluorescence of any protein bound to TNT-ATP was detected by scanning spectrofluorometry.

The compound TNT-ATP shows very weak or no fluorescence prior to binding to proteins. Upon addition of 0.3 mM TNT-ATP to GST-1959 and incubation buffer or to incubation buffer alone, an increase in the amount of fluorescence was observed in both protein and buffer samples (Figure 2.13). Increasing the concentration of TNT-ATP from 0.3mM to 0.58 mM caused a quenching effect, therefore the experiment was not continued (Figure 2.13).

Additionally, fluorescence of TNT-ATP is quenched by the presence of various cations, including magnesium (Moutin et al., 1994; Cheng and Koland, 1996) therefore, the existence of Mg^{2+} in these experiments may create or exacerbate the quenching effect by ATP.

Figure 2.13. Binding of TNT-ATP to GST-1959 fusion protein examined by scanning spectrofluorometry. 1) buffer only; 2) buffer plus 0.35 mM TNT-ATP; 3) protein only; 4) protein plus 0.35 mM TNT-ATP; 5) buffer plus 0.58 mM TNT-ATP; 6) protein plus 0.5 mM TNT-ATP.

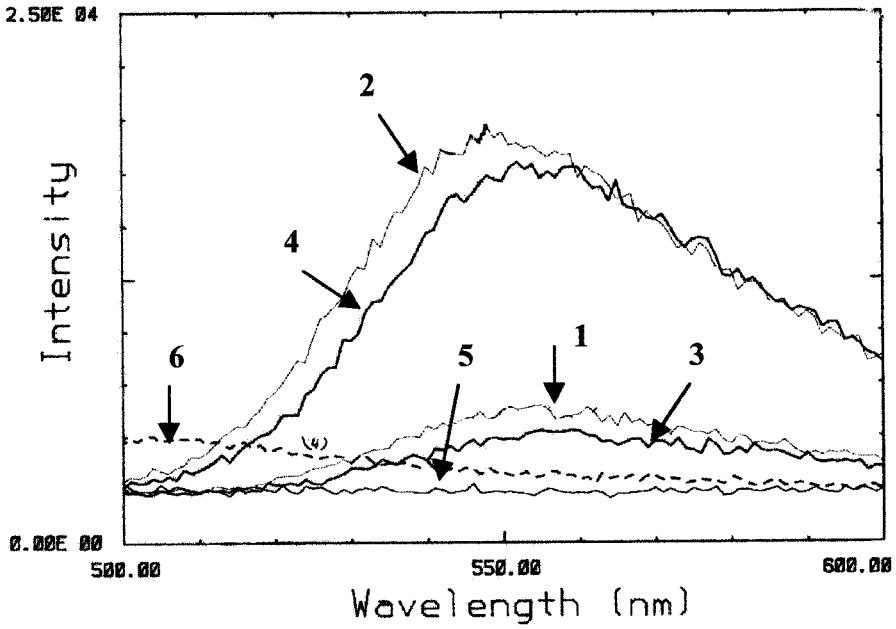
2.50E 04
0.00E 00
Intensity
500.00
550.00
600.00
Wavelength (nm)
1
2
3
4
5
6

2.3.5 Circular Dichroism Analysis

To study the secondary structure composition of the GST-1959 fusion protein and also the effect of Mg-ATP binding on structural elements of this protein, circular dichroism (CD) analysis was performed in the presence and absence of 0.5 mM Mg-ATP. The results are shown in Figure 2.14 and Table 1.

The predicted percentage of the protein containing various secondary structural components of these proteins is shown in Table 1. The predicted secondary structural elements of GST-1959 in the presence of 5mM Mg-ATP were not significantly different than in the absence of Mg-ATP. However, there is about 20% difference in random structure of the protein when Mg-ATP is removed.

Table 2.1. Values represent % of protein with indicated structure.

Secondary Structure	α-helix	β-helix	β-turn	Random
Protein + Mg-ATP	26.1	39.6	23.6	10.7
Protein + buffer	27.1	40.4	23.7	8.8

Figure 2.14. Far-UV circular dichroism spectra of GST-1959 fusion protein in the presence and absence of Mg-ATP.

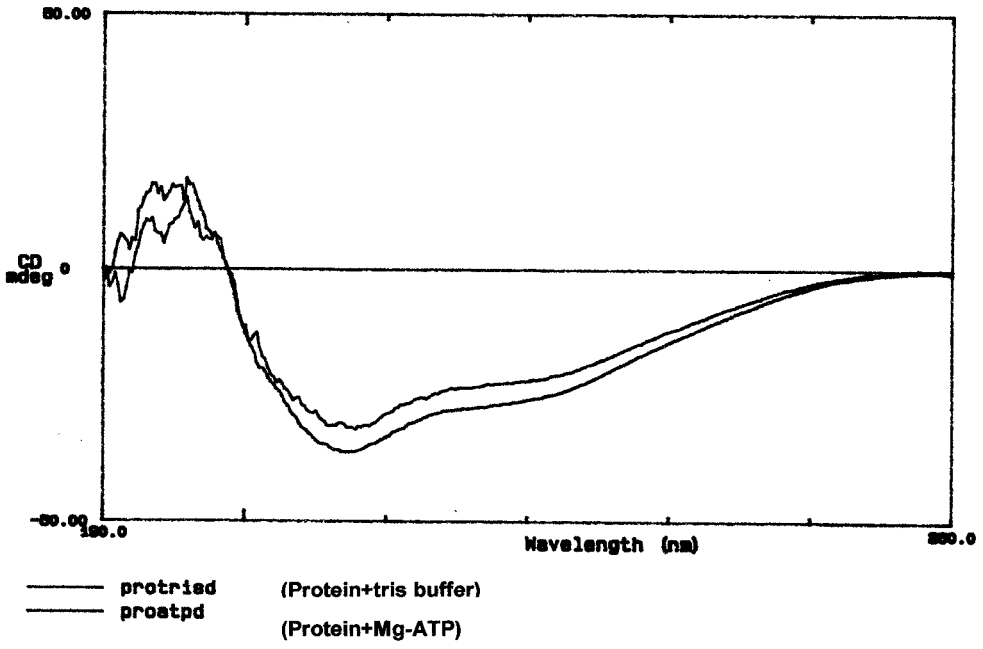
80.00
CD
mdeg 0
-80.00
190.0
Wavelength (nm)
800.0
protried
proatpd
(Protein+tris buffer)
(Protein+Mg-ATP)

2.4 Discussion

2.4.1 Rationale for using α1C Subunit

VDCCS are ubiquitous proteins that play a critical role in the regulation of cellular functions including muscle contraction, enzyme activity, neurotransmitter release, gene transcription, axonal outgrowth, hormonal secretion, and bone formation. Given the important role of L-type calcium channels in cardiac cells, examination of the underlying mechanisms involved in the regulation of these channels and the exact sites of regulation are critical.

The L-type calcium channels of myocardial cells from various species are regulated by intracellular ATP levels controlled via the cAMP dependent protein kinase A (PKA) pathway. This pathway stimulates calcium currents ($I_{Ca,L}$) through L-type calcium channels. The L-type calcium channel current in cardiac cells is inhibited when intracellular ATP is reduced (Irisawa, 1983). Cardiac VDCCs are heteroligomeric proteins comprised of 4 subunits α1C, α2, δ, and β. The pore forming α1C subunit is able to function autonomously as a voltage gated channel when expressed alone in various heterologous expression systems (Perez-Reyes, 1989). This subunit also binds DHP, which classifies it as a L-type channel. The α1C subunits and β subunits are phosphorylated by multiple kinases including PKA, PKC, and CaCMA, which modulate channel activity (Curtis and Catteral, 1985). The C-terminal portion of the full length cardiac α1C subunit is phosphorylated by PKA *in vitro*, and serine 1928 has been identified as a possible site of cAMP-dependent phosphorylation (De Jong et al., 1996).

In addition to cAMP-dependent regulation, intracellular ATP modulates the Ca^{2+} current of L-type channels via an allosteric pathway. This type of regulation has been

also shown in cardiac muscle (O'Rourke, et al., 1992b), and smooth muscle (Yokoshiki, et al., 1997). In guinea pig cardiomyocytes, this allosteric regulation has been shown to be induced by non-hydrolyzable Mg-ATP, indicating that ATP binding but not phosphorylation may be involved (O'Rourke, et al., 1992b).

2.4.2 Rationale for using the C-terminus in Studies of Allosteric Regulation

The studies presented in this thesis were undertaken using a GST-1959 fusion protein derived from the C-terminal portion of the α1C rabbit cardiac L-type calcium channel to determine if this region is involved in allosteric regulation via ATP binding (section 2.1.1). The C-terminal portion was chosen due to its involvement in a number of regulatory processes, including channel phosphorylation by PKA (Mitterdorfer, et al., 1996), AKAP binding (Gao, et al., 1997), and calmodulin binding (Zuhlke et al., 1999), and channel gating. More importantly, electrophysiological experiments that were conducted in our laboratory (Dr. Backx's laboratory) have indicated the direct involvement of the C-terminus in allosteric regulation of calcium channels via ATP. The rabbit cardiac α1C subunit has been well characterized and is comprised of 2171 amino acids, in which the C-terminus spans 664 residues, starting at residue number 1507. Of particular interest is the existence of a modified Walker ATP binding site in the C-terminal portion at position 2057-2065, with homology to the classical Walker A nucleotide binding site (Traut, 1994), which is commonly involved in ATP binding. The classical Walker motif contains GX4GK (S/T), and was first characterized by Walker et al. (1982) by the examination of several ATP binding proteins. In the Walker-A like motif of the α1C region, the amino acid lysine (K) has been substituted by serine (S)

(GX4GS (S/T). Based on this evidence and the electrophysiological experiments conducted in our laboratory, the C-terminal portion was chosen for ATP binding experiments.

2.4.3 Construction and Purification of the GST-1959 Fusion Protein.

The GST-1959 fusion protein used in these studies was generated by heterologous expression of a cDNA construct carrying the distal portion of the α1C terminus of the rabbit cardiac L-type calcium channel transformed into E.coli. This system of expression facilitated large-scale protein synthesis and purification. This was important for functional studies, which required large amounts of protein. E.coli is the fastest and most cost effective prokaryotic expression system. However, prokarytic systems sometimes do not achieve proper folding and post-translational modification of recombinant eukaryotic proteins.

Expression of a GST protein as a tag in frame with a recombinant protein is a good system for synthesis and rapid purification of that recombinant protein (Smith and Johnson, 1988). The tagged protein product is readily purified and the native protein can then be released by *in vitro* cleavage of the GST tag. Glutathione-S-transferase (GST) is a 26 kDa enzyme isolated from Schistosoma japonicum (26 kDa) that has been utilized as a fusion tail for the isolation of a large number of intracellular target proteins expressed in E.coli (Smith and Johnson, 1988). Soluble GST fusion proteins can be purified on immobilized glutathione and eluted with reduced glutathione under non-denaturing conditions (Ford et al., 1991). Intracellular production (in E.coli) of the GST-1959 fusion protein was employed because the C-terminal is cytoplasmic protein and intracellular

production of GST fusion protein results in much higher yields (Ford et al., 1991). One of the concerns about large protein tails such as a GST tag (26 kDa), is that it may interfere with the biological activity of fused protein. In contrast, an advantage of a large tag over a small tag is that the resulting fusion protein is usually more stable. Also it has been shown by Randak et al (1995) that GST fusion protein does not bind to the ATP-agarose resin. The GST-1959 fusion protein in this study was expressed at high levels under the regulation of the tac promoter of the pGEX-2T expression vector (Pharmacia). The secondary structural composition of the GST-1959 fusion protein product measured by CD spectroscopy showed that the protein consisted of: α-helix 27.1 %, ß-sheet 40.4%, ß-turn 23.7 %, and random coil 8.8 %. This vector also has a thrombin cleavage site (Hake and Dixon, 1992) in the C-terminus of the GST protein for removal of the tail after purification by gutathione affinity column (Smith and Johnson, 1988).

When attempting to cleave the GST tag from the fusion protein by thrombin, it was observed that this enzyme fragmented the recombinant protein as well (Figure 2.7). This non-specific cleavage was verified by Western blotting and SDS-PAGE analysis (Figure 2.7 B). This could be related to the presence of impurities in the commercial enzyme preparation (Ford et al., 1991). However, using of an enzyme purchased from a different source did not solve the problem of non-specific cleavage. The existence of thrombin cleavage sites in the target protein is another possibility for cleavage of the C-terminal protein by the thrombin. Examination of the 1959 protein sequence revealed that this protein does contain potential (near consensus) cleavage sites for thrombin. An alternative method would be to generate the desired C-terminal protein from a purified, non-recombinant full length α1C protein. However, the purification of membrane

proteins with low expression levels (such as calcium channels in cardiac myocytes), can be complicated and give low yields, and thus cannot always be a good alternative to the generation of fusion proteins. In addition, transient transfection of the α1C subunit into eukaryotic systems, such as HEK cells, gives low expression levels compared to prokrayotic systems, such as E.coli. Thus, experiments were continued using the full GST-1959 fusion protein, uncut by thrombin.

2.4.4 Binding of ATP to the C-terminal Protein

Crystallization is the best method for elucidating the structure of a protein before and after ATP binding. However, as with other membrane proteins, purification and crystallization of the α1C subunit, would be very complicated. An alternative method to study the structural and functional characteristics of ATP binding is the cloning and study of soluble recombinant protein domains that include the proposed ATP binding regions of these proteins. Previously, a recombinant C terminal protein containing the site for phosphorylation regulation by ATP (Yoshda et al., 1992) was successfully generated from the C-terminus of a rabbit α1C subunit. This study focuses on the investigation of allosteric regulation by ATP binding to a recombinant C-terminal protein.

The aim of this work was to design a soluble protein from the distal portion of the C-terminus protein that has a secondary structure similar to the native protein structure, and to examine ATP binding to this fragment. A recombinant fusion protein construct designed to express the full C-terminal protein was prepared, but no protein was expressed in the E.coli system. This could have been due to its larger size in comparison to the construct made from the distal portion of the C-terminus. Although a longer protein

is more difficult to express, it likely have a tertiary structure more similar to the native protein (Booth, 2000). However, because the protein from the full C-terminal portion could not be expressed, we chose to express a smaller fusion protein, consisting of the distal C-terminal region, containing the Walker A like ATP binding site. The existence of this site was shown by computer alignment of the protein. Also the electrophysiological experiments conducted in our laboratory showed the direct involvement of this distal portion in allosteric regulation by ATP.

2.4.5 ATP Binding using ATP-agarose

The results of binding assays using ATP-agarose beads showed that there was no affinity between GST-1959 and ATP. There were no significant differences between specific and non-specific binding assays. In both assays, a high percentage of the protein remained either unbound to the ATP-agarose beads or washed off in the absence of competitor (20 mM Mg-ATP) and no protein was observed for eluted fraction samples on the SDS gel. The absence of $MgCl_2$ had no effect on the binding of GST-1959 to the ATP-agarose beads.

The conditions used to assay the binding of the GST-1959 fusion protein to the agarose beads were optimal to maintain their binding ability during purification. The same conditions were also used for hsp70 binding assay so that binding comparisons could be made. The conditions for binding assay were the same as the conditions used for electrophysiological experiments that subsequently could not be duplicated. However, these physiological conditions have also been used repeatedly by other researchers for the

same purposes (Randak et al., 1995). Therefore, the lack of binding cannot be attributed to the non-optimal (physiological) conditions used for binding assay.

The concentration of ATP bound to the agarose beads was chosen to be 50 times higher than the concentration of GST-1959 fusion proteins. Thus, the degree of ATP binding under these conditions should be equal to the amount of GST-protein in the mixture. ATP-agarose beads were prepared at the time that binding assays were performed, and used immediately to prevent ATP hydrolysis. ATP-agrose powder was also kept at –20 °C to reduce spontaneous hydrolysis of ATP. All steps of bead preparation and binding assays were carried out on ice. Thus, the high percentage of unbound protein can not be attributed to a paucity of ligand.

2.4.6 Alternative Methods for Binding

Alternative methods such as photoaffinity ATP radiolabelling of GST-1959 fusion protein and spectrofluorimetry of TNT-ATP and GST-1959 were also used to investigate the binding affinity of the C-terminus with Mg-ATP. The results of using these methods were similar to the ATP-agarose method. The binding studies by photoaffinity radiolabelling indicated that ATP does not bind to GST-1959 fusion protein. Although there was a high background of binding of radioligand to protein, pre-incubation of the GST-1959 fusion protein with cold ATP did not prevent this high background radiolabelling indicating that radiolabelled azido-ATP binds to these protein non-specifically. The finding that the radioligand shows no specific affinity with the fusion protein indicate that the C-terminus has no ATP binding site.

Investigation of the allosteric ATP binding of the GST-1959 fusion protein by spectrofluorimetry using TNT-ATP also indicated that there is no ATP binding site on the C-terminus. There was no significant difference in the enhancement of fluorescent intensity of the protein versus the buffer upon addition of TNT-ATP.

2.4.7 CD Analysis of the C-terminal Protein

The secondary structure of the recombinant protein was detected in the presence and absence of Mg-ATP by CD analysis, as shown in table 1. The change in the percentage of the secondary structural elements was not significant in the presence and absence of ATP, except for the random structural areas of the protein. This result may suggest that 1) there is a lack of binding affinity between protein and ATP and 2) the secondary structure is not close to native structure (does not meet the minimal functional unit requirement necessary for the specific binding of ATP). That minimal functional unit has to be predicted while designing the constructs for functional analysis, to maintain native ability for specific binding (Booth, 2000). Based on the secondary structure of the purified full length α1C protein, the minimal functional unit can be predicted. Also the retention of native secondary structure can be investigated by comparison with the native structure. In practice, a series of vectors with various fragment sizes of the desired protein have to be designed in order to select one that is well expressed and has a structure similar to the native protein.

2.5 Conclusion:

Affinity chromatography using ATP-agarose beads as a reliable method was used to detect the binding affinity of GST-1959 to the C-terminal portion of α1C subunit. In addition to affinity chromatography, other highly reliable methods such as spectrofluorimetry, radiolabelling, and circular dichroism were also employed to investigate the binding of ATP to the C-terminal portion of α1C subunit. However, none of those methods indicated that ATP binds to the C-terminus. Additionally, the hypothesis and all conditions used for performing this work were chosen based on the electrophysiological experiments conducted in our laboratory, which have not yet been duplicated. Therefore, ATP may only be involved in phosphorylation of L-VDCCs via cAMP pathway as the only way of regulation that has been discussed in the introduction of this chapter in detail.

2.6 Summary. The influx of calcium through calcium channels triggers excitation-contraction (E-C) coupling and determines the rate and force of contraction in cardiac cells. ATP regulates the influx of calcium through calcium channels by phosphorylation via cAMP pathway, which requires the hydrolysis of ATP.

In this thesis, the allosteric regulation (binding of ATP in non-hyrolizable manner) of calcium channels as a new way of regulation was investigated using a GST-fusion protein made from the C-terminal portion of the rabbit L-type cardiac calcium channel. Affinity chromatography in conjunction with other techniques such as spectrofluorimetry, radiolabelling, and circular dichroism were used to detect ATP binding and allosteric regulation of the channel. The results indicate that there is no

affinity between the fusion protein and ATP, and that Mg^{2+} does not affect binding. Therefore, the initial hypothesis was shown to be incorrect using this model system.

Chapter Three: Expression of Calcium Channel in Aged Brain

3.1 Introduction

Calcium ions (Ca^{2+}) play a critical role in the normal function of neurons within a physiological range. Ca^{2+} overload is mediated by pathological events in the neurons and creates neurotoxicity (Schanne et al., 1987; Gibson and Peterson 1987; Choi, 1988). The intracellular calcium concentration $[Ca^{2+}]i$ is maintained in the normal range (70-100 nmole), i.e. approximately 10,000 fold lower than the extracellular Ca^{2+} ion concentration (Mills and Kater, 1990), by homeostatic mechanisms which allows signalling through activated voltage and ligand-gated Ca^{2+} channels (Bading et al., 1993; Tank et al., 1988; Llinas et al., 1988; Llinas et al., 1992). The mechanisms, which regulate Ca^{2+} homeostasis are: Ca^{2+} influx, Ca^{2+} efflux, sequestering, and buffering (Busa, 1996; Verkhratsky and Toescu, 1998). The calcium hypothesis suggests that altered mechanisms of Ca^{2+} homeostasis underlie neurodegeneration in brain aging and aged-related diseases such as Alzheimer'disease (AD) (Khachaturian, 1984 and 1994). The reported studies on the perturbation of Ca^{2+} homeostasis in the aging process are very inconsistent (Gibson and Peterson, 1987). Most of these studies indicate increases in $[Ca^{2+}]i$ (Martinez et al., 1988; Villalba et al.,1995), while others show decreases $[Ca^{2+}]i$ (Hartmann et al., 1996a and 1996b). Likewise, the same picture has arisen for the possible mechanisms underlying Ca^{2+} alteration in aging. These discrepancies may rely on differences in the strain, sex and age of animal. Whether the perturbation of the $[Ca^{2+}]i$ is related to aging is unclear and remains to be determined.

Alteration of Ca^{2+} influx, particularly increases in Ca^{2+} entry via VDCCs, is suggested to underlie perturbation of Ca^{2+} homeostasis in aging (Landfield, 1994; Landfield and Pilter, 1984). Such an increase is reported to arise primarily via L-type

channels (L-VDCCs) because they can be blocked by dihyropyridines such as nimodipine (Hofmann et al., 1994). Owing to their slow inactivation kinetics and large conductances (27pS for Ba^{2+} ions), L-VDCCs mediate much larger rises of Ca^{2+} influx than other VDCCs into neurons (Hess, 1990). To define how an increase in L-VDCC currents may arise, Landfield's group examined single channel currents of CA1 neurons in brain slices using patch clamp electrophysiology (Thibault and Landfield, 1996; Campbell et al., 1996). The results from this study show an age-dependent increase in the density of L-VDCCs in CA1 nerve cell surfaces.

How changes in the density of functional VDCCs may arise has not yet been examined. Three general mechanisms are possible, each of which may act alone or in concert. First, an increasing number of functional channels at the cell surface could arise through enhanced transcription, translation, and insertion into the cell membrane or a decrease in the rate of mRNA degradation, and of VDCC internalization. Second, more subtle mechanisms might involve the conversion of silent channels to active channels, for example, through second messenger regulation. A third mechanism for an increase in the density of channels could be a change in the distribution of VDCCs over the nerve cells. Which of these mechanisms underlies an increased density of functional channels is unclear.

The possibility of change in the expression level of mRNA encoding L-VDCCs was assayed through the polymerase chain reaction (PCR), using hippocampal neurons in "long-term" (4 wks) culture as a model of aging (Porter et al., 1997). While these studies suggested an age-dependent increase in L-VDCC mRNA, they have not been confirmed in aged rat brain. There is also doubt as to the count of the elevated

expression level of mRNA as an indicator of increased density of functional channels on the cell surface, since there are differences between steady state of mRNA and expression of functional protein.

Region specific changes of VDCCs expression in rat cerebellum has been examined very recently by immunohistochemistry and Western blot analysis (Chung et al., 2001). Increases in the α1C subunit immunoreactivity were observed in the dendrites as well as in the cell bodies of purkinje cells of the aged cerebellum compared to the adult cerebellum. In contrast, immunoreactivity for α1A and α1D subunits decreased in the molecular or granular layers of aged cerebellum. The exact significance of such channel re-distributions is uncertain. One possibility is that, these alterations in the distribution of VDDCs channel in the aged rat cerebellum may contribute to impairments of Ca^{2+} homeostasis during aging (Chung et al., 2001). The level of expression of α1C, α1A and α1D subunits of VDCCs in the adult and aged rat cerebellum was also examined (Chung et al., 2001). As detected by immunoblotting the α1D subunit expression was significantly decreased in the aged cerebellum, whereas the others remained unchanged (Chung et al., 2001). However, few studies have been focussed on age related alterations in the expression of the VDCCs subunits in the aged brain particularly in the aged hippocampus.

More convincing approaches include determining the expression levels of various subunits of L-VDCCs and measuring the numbers of VDCCs using radioactive ligands through binding assay. These approaches are the focus of this study. In this chapter we examined the expression level of L-VDCCs in general by radioligand binding assay and in detail by measuring the expression of various subunits α_{1C}, β_3, $\alpha_2\delta$

in hippocampus, cerebellum and cortex from aged and young adult Fischer 434 rats brain. L-VDCCs is a major mode of Ca^{2+} influx for signalling, gene expression, enzyme activation, and excitability (Catterall et al., 1988; Campbell et al, 1988). L-VDCC is associated with α_{1C}, β_3, $\alpha_2\delta$ in a 1:1:1 stoichiometry (Catterall et al., 1988; Campbell et al, 1988).

The regions of study, including cortex and particularly the hippocampus, are centres of memory and cognition and are thus affected by aging and aged related diseases such as Alzheimer's disease (Geinisman et al., 1995). The cerebellum was used to detect whether the aging effect is regional specific (Reynolds and Carlen, 1989). These regions express all major classes of VDCCs (Jaffe et al., 1994).

These experiments did not create compelling evidence for changes in the expression level of VDCC subunits except for the $\alpha_2\delta$ subunit and no significant changes were observed in overall expression levels of L-VDCCs in 23 month old rats.

3.2 Materials and Methods

3.2.1 Preparation of Brain Membranes

For aging studies membranes were prepared (Hartshorne and Catterall, 1984; Jones and So, 1993) from four male young adult (2 month) and four male aged (23 month) Fischer 434 rats (Harlan Sprague Dawley, Indiapolis, IN). Young adults or aged rats were decapitated after CO2 asphyxiation, and brains were carefully removed. Rat brains were dissected to obtain the hippocampus, cortex, and cerebellum. The dissected regions were homogenized by 8 strokes of a Potter-Elvejhem tissue grinder in approximately 4.5 mL total volume of buffer A (0.32M sucrose, 5mM Tris HCl, pH 7.4 at 4°C). The homogenized tissue was centrifuged at $70g_{av}$ for 10 minutes at 4°C in

buffer A. The pellet was discarded, and the supernatant was centrifuged again ($27,000g_{av}$). The resulting pellet (prepared membrane) was resuspended in 1-2 mL of sucrose buffer C (5mM HEPES-Na^+, 0.32M sucrose, pH7.4), and stored in 200 microlitre aliquots in liquid nitrogen. All buffers contained protease inhibitor agents and iodoacetamide, to prevent proteolysis and thiol exchanges respectively. All steps were carried out on ice or at 4°C. The concentration of membrane proteins was determined by the Lowry assay (Lowry, 1951) using bovine serum albumin (BSA) as a standard .

3.2.2 Radioligand Binding Studies

For [^{3}H]Isradipine (PN200-110) binding, the method of Lee et al. (1984) with some modification was employed. To assay total binding (specific plus non-specific), 70-100 μg of brain membranes were incubated with [^{3}H] Isradipine ([^{3}H](+) PN 200-110 (83Ci/mmole, Amersham) in tubes containing Tris buffer (50 mM pH7.4, 1.5mM $CaCl_2$) plus fresh protease inhibitor (0.1mM PMSF) at the following concentrations: 4, 8, 16, 32, 64,128, 256, 512 pM. All incubations were carried out in a total volume of 1ml at room temperature for 60 minutes, in the dark.

To determine non-specific binding in a duplicate set of tubes, 100 μl of 10 μM Nifidipine (Amersham, Inc) was added to each reaction tube before incubation with [^{3}H] Isradipine. Reaction mixtures were diluted by adding 4 ml portions of ice cold Tris buffer (pH 7.4), filtered through Whatman GF/B filters using vacuum filtration (Hoefer), and the filters were washed twice with 4 ml portions of ice cold Tris buffer. The radioactivity of the filters [^{3}H]PN 200-110 was determined by using a liquid scintillation counter (Beckman Instruments Inc.Fullerton, CA.) with an efficiency of 35%. The

efficiency was determined by measuring the radioactivity of 10 µl of 1 nM [^{3}H] PN-200-110.

Specific binding was defined by subtracting the radioactivity of non-specific (samples plus 100µl Nifidipine 10 µM) from total bound radioactivity.

3.2.3 Western Immunoblotting

In order to resolve different L-VDCCs subunits, the previously prepared membrane protein was diluted with an electrophoresis sample buffer [0.0625 M Tris-HCl (pH6.8); 10%(v/v) glycerol; 2% (w/v) sodium dodecyl sulfate (SDS); 5% β-mercaptoethanol; and 0.001% (w/v) bromophenol blue], boiled for 4-5 minutes, and loaded on to the 6-7.5% gradient SDS-polyacrylamide gel for electrophoresis (SDS-PAGE) (Lammli, 1970). The separated proteins were transferred electrophoretically to 0.45µm nitrocellulose membranes (Towbin et al., 1979). The blots were checked for even protein loading by Ponceau staining, and then were placed in 5% non-fat dry milk (NFDM) in TBS (Tris buffered saline, pH7.5) overnight in the cold room to block non specific binding. The blots were washed 3X (15min/wash) with TTBS [TBS plus 0.05%(v/v) Tween-20] and TBS respectively, incubated for 2 hr with primary antibodies diluted in 5% NFDM in TBS (anti β_3 1:500; anti $\alpha_2\delta$ 1:2000; α_{1C} 1:300-5000) at room temperature. The blot was then washed again in 3X TTBS and 3XTBS (15min/wash), exposed to horseradish peroxidase (HRP)-conjugated secondary antibodies (donkey anti-rabbit ; goat anti-mouse) diluted in 5% NFDM in TBS (1: 2000-4000) for one hour at room temperature, and finally rewashed in 3X TTBS, 3X TBS (15min/wash) to remove free secondary antibodies. Specificity of the antibodies was controlled by pre-

immune sera or blockade by competing peptide agents. The blots were exposed to the film after chemiluminescence enhancement with ECL detection reagents (ECL; Amersham, Oakville, Ontario, Canada). The images were quantitated by densitometry with a Bio-Rad Model GS-670 imaging densitometer. Molecular weights were determined with prestained markers (Kaleioscope, Bio-Rad, Mississauga, Ontario, Canada).

3.3 Results and Discussion

Expression of L-VDCCs was investigated through a radioligand binding assay and electrophoresis immunoblotting in aged and young adult rat brains.

3.3.1 Wetern Immunoblot Analysis of the Expression of L-VDCC Subunit Proteins in Hippocampus, Cortex and Cerebellum

The expression levels of L-VDCC subunit proteins (α_1, β_3 and $\alpha_2\delta$) in aged and young adults were determined by electrophoresis immunoblotting to detect any changes in aged versus young adults. In these studies the proteins bands visualized on the films were quantitated by densitometry. Various proteins concentrations were loaded per subunit and per region (aged and adults) to generate standard curves for detection in the linear range of densitometer.

3.3.2 Expression of β_3 Subunit Protein

Expression levels of the β_3 subunit protein in the hippocampus, cortex, and cerebellum from aged (23 month) and young adult (2 month) Fischer 434 rats brain were

examined by immunoblot analysis with polyclonal MAPS purified antibodies raised by Dr. Jones. These antibodies were highly specific for the β_3 subunit (Jones et al, 1997).

Modulation of calcium channel activity by ß subunits has been shown previously (reviewed by Catterall, 1995). The ß subunits strongly affect the functional properties of $\alpha 1$ subunits of L-type channeles. As co-expression of this subunit with the $\alpha 1$ subunit results in a 10 fold increase in Ca^{2+} currents and affects the number of DHP receptors, and their activation /inactivation kinetics (reviewed by Catterall, 1995). Surprisingly, our data analysis did not indicate any significant changes in the expression levels of β_3 in the aged hippocampus, cortex, or cerebellum in comparison with young adults (paired t-test, $P>0.05$) (Figures 3.1 and 3.2).

These results are not consistent with some electrophysiological studies that indicated the increased density of L-VDCCs in aged rats hippocampus (Landfield, 1994), although we can not preclude the possibility of differential compensatory changes in discrete cell population. Owing to technical limitations, it was not possible to examine the expression levels of the subunits in the neuronal compartments distinctly.

Furthermore, β_3 subunits are associated with both N and L-VDCCs in a 1:1 ratio (Catterall et al., 1988; Campbell et al., 1988) and therefore our data are indicative of total β_3 subunit measurements, not the fraction which is exclusively complexed with L-VDCCs (α_{1C} or α_{1D}). Thus, an increase in the density of the L-VDCCs in aging (i.e. elevated expression level of α_{1D} (Porter et al., 1996)) can possibly compensate for the decrease in N-VDCCs in aged neurons (Moresco et al., 1989). Alternatively, changes in the degree of coassembly may occur in aging as opposed to elevated levels of expression of β_3 subunit. Thus immunoprecipitation analysis might be carried out to investigate any

changes in the degree of coassembly of the β_3 subunit with main pore (α_{1C}) in aged rat brain.

Figure 3.1. Expression levels of β3 subunits in hippocampus, cerebellum and cortical membranes of aged and adult male rats in representative experiments as determined by immunoblotting. Immunoblots were probed with MAPS purified β3 antibody.

A) Lanes correspond to the following amounts of aged and adult hippocampal membrane protein loaded on the gel respectively: 2.5, 5, 10, and 20 μg.

B) Lanes correspond to the aged and adult cortical membrane protein (2.5, 5, 10, 20 μg).

C) Lanes correspond to aged and adult cerebellar membrane protein (2.5, 5, 10, 20μg). Arrowheads at left denote positions of molecular weight markers. **Ad**=Adult and **Ag**=Aged

D) Densitometric analysis of visualized protein bands on the gel related to the β3 subunits expression in cortex, cerebellum and hippocapus. X ordinate represents ratio of data from aged /adult, data normalized to the value seen at 20 μg, data obtained from four separate sets of animals.

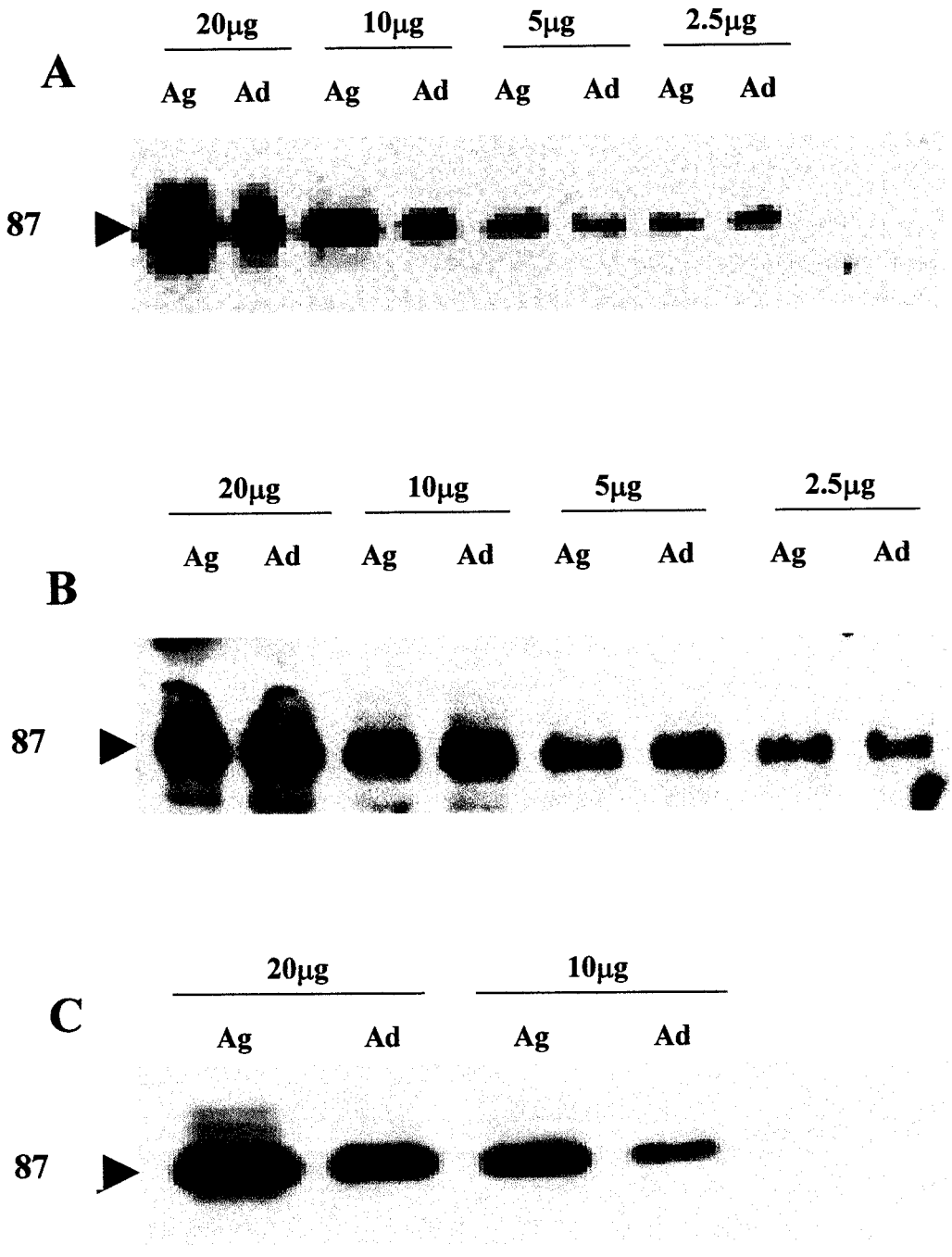
A
20μg
10μg
5μg
2.5μg
Ag Ad Ag Ad Ag Ad Ag Ad
87
B
20μg
10μg
5μg
2.5μg
Ag Ad Ag Ad Ag Ad Ag Ad
87
C
20μg
10μg
Ag Ad Ag Ad
87

D

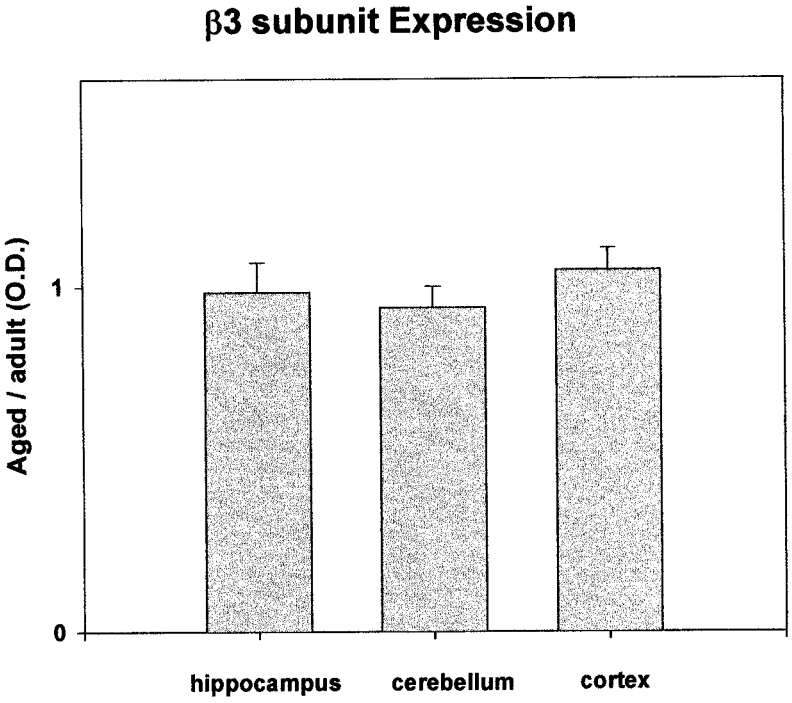
β3 subunit Expression
Aged / adult (O.D.)
1
0
hippocampus
cerebellum
cortex

3.3.3 Expression of $\alpha_2\delta$ Subunit Protein

The $\alpha_2\delta$ subunit protein expression in the cortex, hippocampus, and cerebellum was examined by commercial monoclonal antibody to skeletal muscle protein which also cross reacts with $\alpha_2\delta$ proteins from brain tissues (Upstate Biotechnology, Lake Placid, NY) (Figure 3.2A and B). Expression levels of $\alpha_2\delta$ increased in the aged hippocampus in comparison with the adult hippocampus. Paired T-test analysis indicated that the differences are significant ($P<0.05$). However, the differences in the expression levels of $\alpha_2\delta$ in the aged cortex and cerebellum were not significant ($P>0.05$).

In contrast to the β_3 subunit expression, an elevated expression level of $\alpha_2\delta$ in aged hippocampus coincide with electrophysiological studies in the aged hippocampus (Landfield, 1994). The $\alpha_2\delta$ subunit is common in all VDCCs; therefore, this increase may also reflect coassembly of $\alpha_2\delta$ with other channels rather than L-VDCCs (Jones et al., 1997). To examine the change in the degree of coassambly with α_{1C} or α_{1D}, immunoprecipitation analysis should be carried out.

Figure 3.2. Expression levels of $\alpha_2\delta$ subunits in hippocampus, cerebellubm and cortical membranes of aged and adult male rats as determined by immunoblotting. Immunoblots were probed with $\alpha_2\delta$ antibody. Representative experiments are shown.

A) Lanes corresponds to aged and adult hippocampal membranes protein (2.5, 5, 10, 20 μg). Arrowheads at left denote positions of molecular weight markers.

B) Lanes correspond to the following amounts of adult and aged cortical membranes

C) Lanes correspond to the adult and aged cereberal membranes protein (2.5, 5, 10, 20μg). **Ad** = Adult and **Ag** = Aged

D) Densitometric analysis of visualized protein bands related to the $\alpha_2\delta$ subunits expression in cortex, cerebellum and hippocapus. X ordinate represents ratio of data from aged /adult, data normalized to the value seen at 20μg, data obtained from four separate sets of animals. Paired t-test analysis indicated that the differences are significant ($P<0.05$).

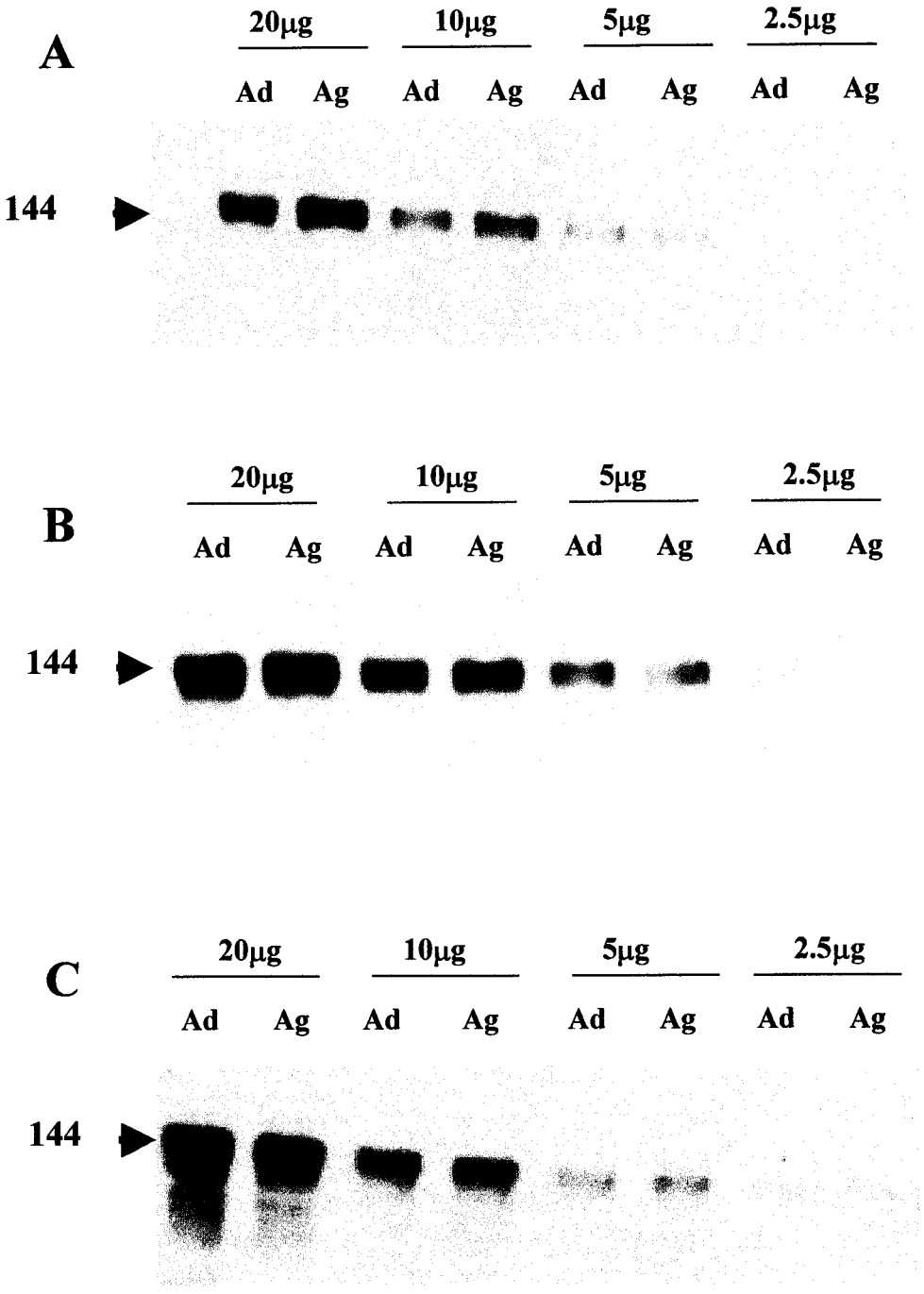
A
20μg
10μg
5μg
2.5μg
Ad Ag Ad Ag Ad Ag Ad Ag
144
B
20μg
10μg
5μg
2.5μg
Ad Ag Ad Ag Ad Ag Ad Ag
144
C
20μg
10μg
5μg
2.5μg
Ad Ag Ad Ag Ad Ag Ad Ag
144

D **α2δ Expression**

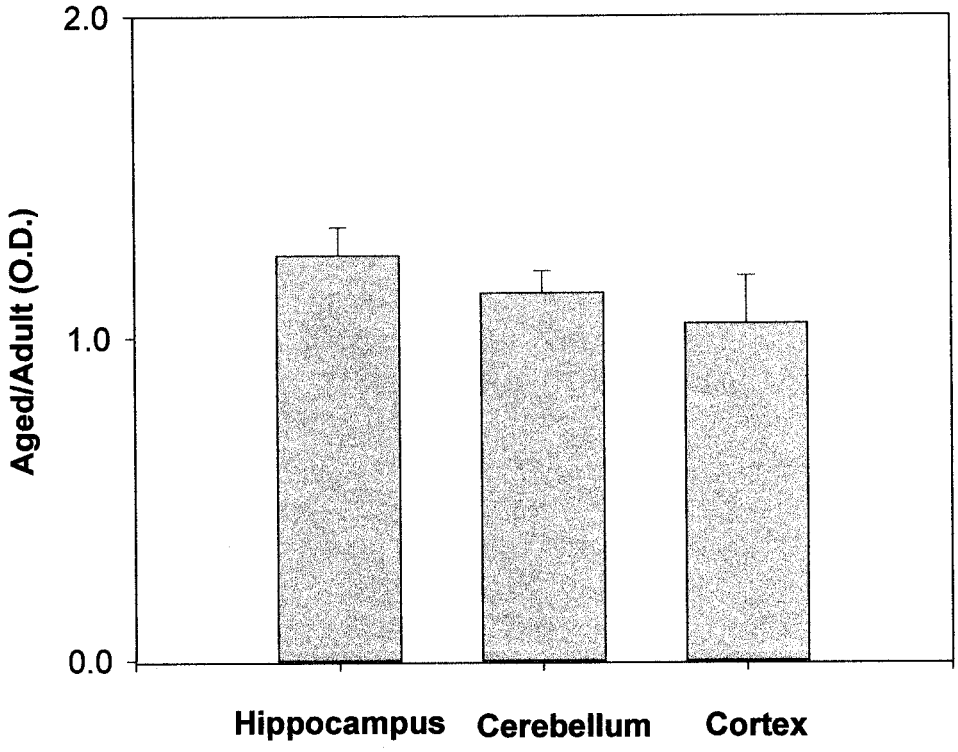

3.3.4 Expression of α_{1C} Subunit Protein

Expression of α_{1C} was examined with antibodies from different sources (Almone Co., Streissnig Lab.), however there were no resolved bands or the visualized bands were degraded.

3.3.5 Expression of L-VDCCs examined by Radioligand Binding

Expression of L-VDCCs in the hippocampus from aged and young adult rat brain was investigated by using ^{3}H-Isradipine. [^{3}H]-Isradipine is a selective ligand from 1,4-dihyropyridine family of calcium channel antagonists that binds saturably and reversibly with high affinity to specific sites that appear to mediate the blockade of calcium ion flux through VDCCs (Lee et al., 1984; Striessnig et al., 1998).

Equilibrium binding was analyzed by linear regression of Scatchard plots (Weiland and Oswald, 1985) and the equilibrium dissociation constant (K_d) and concentration of binding sites (B_{max}) were determined (Figure 3.3 and 3.4). The membrane density of binding sites (fmole/mg of protein) was calculated by dividing the B_{max} by the concentration of protein.

The effect of age on the K_d and B_{max} values of PN200-110 binding to the hippocampus of the male rat brain is depicted in table (3.1). No significant changes in the K_d and B_{max} (fmole/mg) for PN200-110 binding were observed with age in the hippocampus (Figures 3.3 and 3.4).

Our results are not in agreement with an increase in binding sites of PN-200-110 (Battaini et al., 1985), or a decrease in binding of this ligand to the hippocampus in aging studies (Govoni et al., 1985; Bangalore and Triggle, 1995; Yamada et al., 1996).

However, they are confirmed by other studies that indicated no changes in binding of PN200-110 to the L-VDCCs from aged hippocampus (Dooley et al., 1988; Golik et al., 1992; Araki et al., 1997;). These results may reflect the age of rats that were used in these experiments (2 and 23 months). Binding of PN200-110 decreases in the 30 month old rat hippocampus as compared to the 6 month old (Bangalore and Triggle, 1995) but there are no changes in the 18 month rat hippocampus or 24 month old (Araki et al, 1997), which is the age range we studied. The selection of age is also region-dependent; for example, significant changes in the binding density of the L-channel occur in the cortex at the age of 12 months, which is earlier than the changes observed in the hippocampus (Bangalore and Triggle, 1995).

Throughout the literature, the effect of aging on L-VDCC binding characteristics is inconsistent and controversial. These discrepancies may rely on differences in the strain and age of animal, and /or in the protocol adopted for membrane preparation and incubation time.

Table 3.1. [^{3}H]PN200-110 binding to the aged and young adult hippocampus from 4 male Fisher 344 rats.

	K_d (pM)	**B_{max} (fmol / mg prot)**
Aged hippocampus	63	80
Young adult hippocampus	55	78

Figure 3.3. Scatchard plots of [^{3}H]PN200-110 binding to rat membrane from aged (panel A) and young adult (panel B) hippocampus. Each point represents the average of six determinations.

A

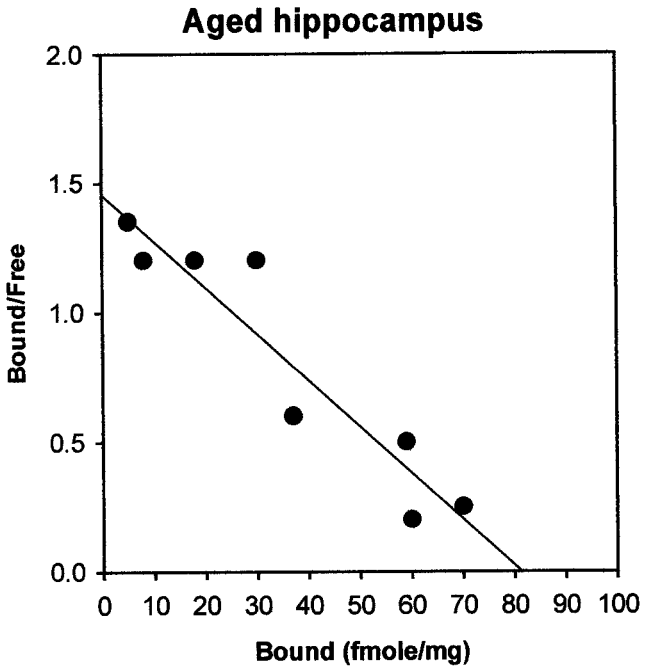
Aged hippocampus
2.0
1.5
1.0
0.5
0.0
Bound/Free
0 10 20 30 40 50 60 70 80 90 100
Bound (fmole/mg)

B

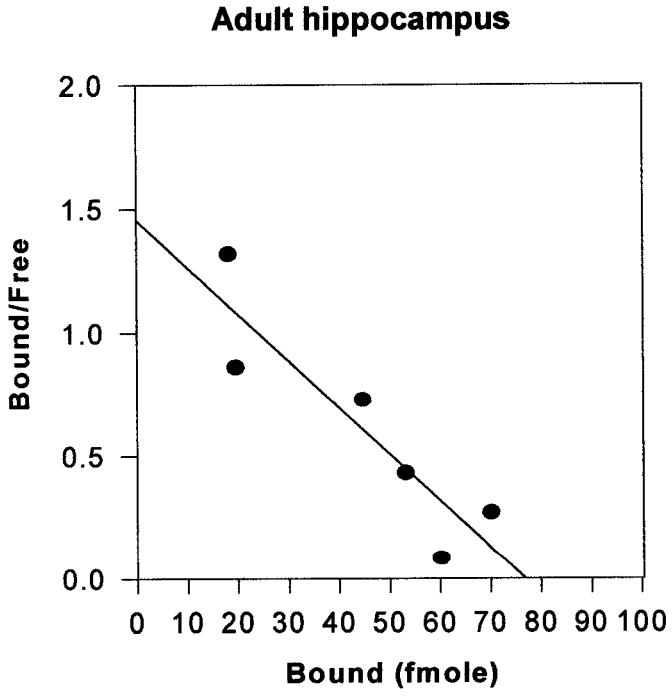
Adult hippocampus
2.0
1.5
1.0
0.5
0.0
Bound/Free
0 10 20 30 40 50 60 70 80 90 100
Bound (fmole)

Figure 3.4. Saturation binding of [^{3}H]PN200-110 to the aged hippocampus (panel A) and young adult (panel B) hippocampus. Each point represents the average of six determinations. CPM= Counts per minute.

Saturation Binding in Aged Hippocampus

A

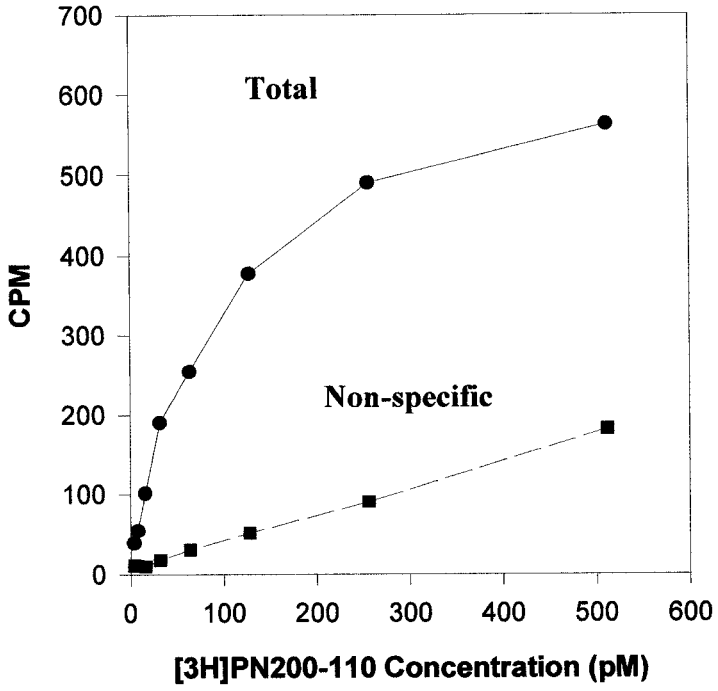

Saturation Binding in Adult Hippocampus

B

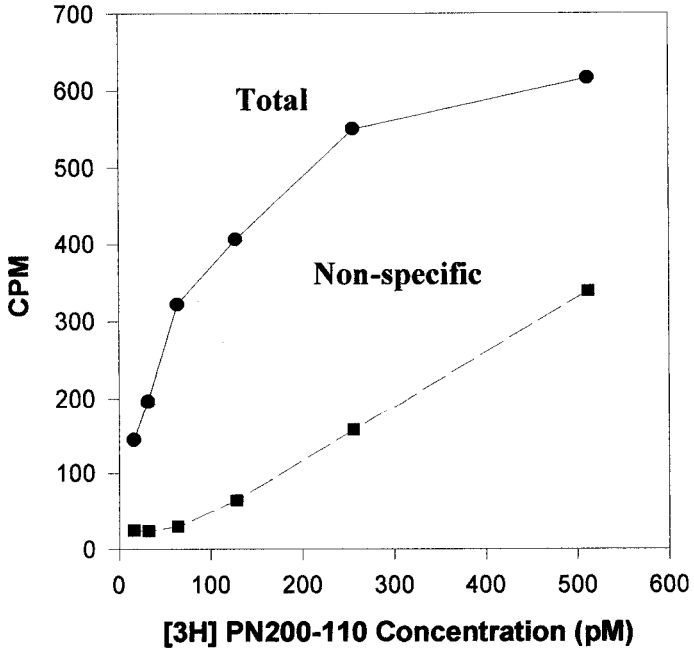

3.4 Conclusion

As discussed in this chapter, the expression level of the $\alpha_2\delta$ was increased in the aged hippocampus. However, the expression levels of β_3 did not change significantly in the studied regions. No significant changes were observed in the expression levels of $\alpha_2\delta$ in the cortex and cerebellum. Radioligand binding assay with PN200-110 did not indicate any changes in the density of L-VDCCs in aged rat brains compared to the young adults. These results suggest that expression levels of L-type Ca^{2+} channels in the aging brain is both subunit- and region-specific.

Although both α_{1C} and α_{1D} subunits participate in the formation of L-type Ca^{2+} channels in mammalian brain, the differential expression of α_{1D} and α_{1C} subunits have not been detected in this study. Thus, in the aging brain, it would be interesting to determine if differences exist between the two L-type channels with respect to their subunit composition. Moreover, all known β and $\alpha_2\delta$ subunit isoforms also participate in the formation of L-VDCCs. Therefore, diverse isoforms of α_{1C}, β and $\alpha_2\delta$ subunits can potentially lead to formation of various L-type Ca^{2+} channels with different subunits composition. This may also lead to the diversity of calcium channels activity in the brain. Further studies must focus on the effect of aging on this channel diversity. Thus, it is of particular interest to determine if the expression levels of other isoforms of ß and α_1 and α_2 subunits change in the aged brain. Also, It is important to determine if these changes affect the coassembly of these subunits in the aging brain by co-immunoprecipitation.

Chapter Four: Adult Neurogenesis in Ulip-1 Knockout Mice

4.1 Introduction

4.1.1 Importance of the Study

The hippocampus is an area of the brain, which plays a role in memory and learning. This involvement has been shown physiologically, it has also been demonstrated in cases of brain pathology. Lesions in the hippocampus have led to the dysfunction of learning ability (Morris, 1984 and 1987). The hippocampus is the most seriously affected part of brain in the patients with Alzheimer disease (AD), which is associated with loss of memory and cognition (Roses, 1996). Memory decline in aging is also attributed to the changes in hippocampal function (reviewed in Squire, 1992). In contrast, an enriched environment creates positive changes in the hippocampus, both structurally and metabolically (Kempermann et al., 1997).

Both the plasticity of hippocampus (shown by LTP) and the occurrence of adult neurogenesis provide a unique role for hippocampus in memory, learning and also pathology of brain. Thus, the investigation of the mechanisms underlying neurogenesis in the adult hippocampus may lead to the establishment of therapeutic strategies for aging, memory and cognitive diseases. To understand the role of the neurogenesis in the adult hippocampus, we have to understand the signalling pathways involved in regulation of neurogenesis. One approach to study the regulation is to use an *in vivo* knockout mouse model. Specifically we used Ulip-1 knockout mice blocking one of the key protein markers (Ulip-1) specifically expressed during neurogenesis.

4.1.2 Anatomy of the Hippocampus (hippocampal formation)

The hippocampus is a cortical structure located bilaterally in the brain. The hippocampal formation appears as an elongated C-shaped structure. The term "hippocampal formation" refers to cytoarchitecturally distinct regions, including the dentate gyrus and the hippocampus proper, the subiculum complex (SC) and the entorhinal cortex (EC). The hippocampus proper is subdivided into three fields: CA3, CA2, and CA1. These distinct regions are linked one to another by unique unidirectional projections. The main unidirectional pathways within hippocampus are: (1) the perforant pathway, which originates in the entorhinal cortex; (2) the mossy fibers, which connect dentate gyrus cells to CA3 pyramidal neurons; (3) the Schaffer collaterals of the CA3 pyramidal axons, which make synaptic connections to the CA1. The axons of CA1 neurons then complete the circuit by relaying signals from the CA1 back to the EC via SC (Figure 4.1) (Amaral and Witter, 1995).

4.1.3 Dentate Gyrus

The dentate gyrus (DG) is formed of 3 layers: the molecular layer or noncellular layer, the granular cell layer and the polymorphic layer or hilus. The molecular layer (ML) does not contain neuronal cell bodies and consists of dendrites extending from granular cells and axonal inputs (Amaral and Witter, 1995).

The granular cell layer (GCL) is comprised of tightly packed columns of round granule cells (10 μm in diameter). The dendrites of these cells extend into the molecular layer where they connect with axonal projections from the EC via the perforant pathway. The dendritic morphology of granule cells varies depending on their localization in the

GCL and the degree of cell maturation (Wang et al., 2000). The axons of granule cells, which were called "mossy fibers'' by Ramon y Cajal, pass through the hilus and make connections with CA3 neurons. In the CA3, some mossy fibers travel deep to the pyramidal cell layer and are called infrapyramidal bundle. Mossy fibers travelling within pyramidal cells are known as intrapyramidal bundle and those that travel superficially to the pyramidal layer are suprapyramidal projection (Amaral and Witter, 1995).

The hilus or polymorphic layer which is surrounded by GCL and ML contains many different type of cells, the most common of which are large mossy cells (23-35 μm in diameter) which receive collateral input from mossy fibers projecting to the CA3, axons of mossy cells project into the molecular layer (Amaral and Witter, 1995).

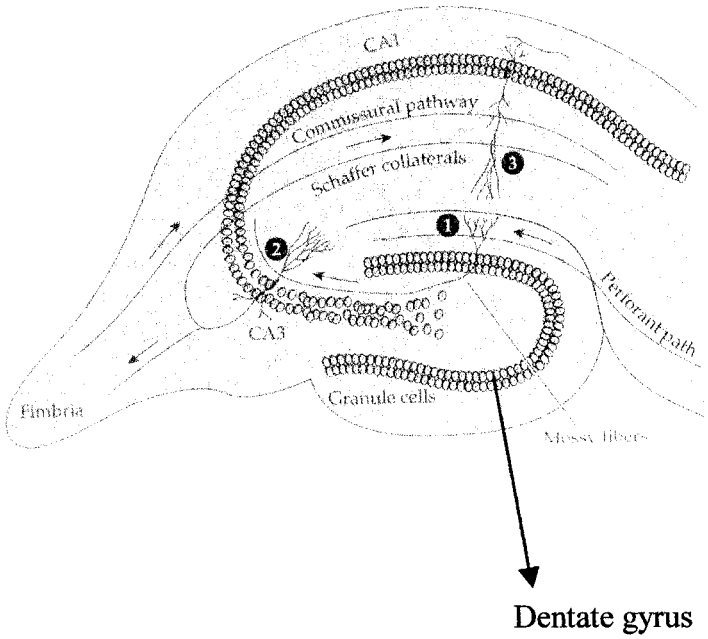

Figure 4.1. Structure of the hippocampus. Schematic diagram of the anatomical components of the hippocampus, in particular the elements of trisynaptic pathway. (Adapted from Bliss, TV. and Dolphin, AC. (1982), Trends in Neuro Science 9:289)

4.1.4 Neurogenesis in the Adult Brain

New neurons are generated throughout adulthood in the dentate gyrus of the hippocampus in mammals, including mice (Kempermann et al. 1997), rats (Cameron et al. 1993), tree shrews (Gould et al., 1997), meadow voles (Galea and McEwen 1999), monkeys (Gould et al. 1998) and humans (Eriksson et al. 1998). The olfactory bulbs (OB) are also well known to display adult neurogenesis (Peretto et al., 1999). New cells in the olfactory bulbs first proliferate in the sub ventricular zone (SVZ) and migrate along the rostral migrating stream (RMS). From the olfactory bulbs they disperse and differentiate into new neurons (Lois and Alvarez, 1993). Recently, newly generated neurons have been observed in other regions of brain including the neocortex, preoptic area, central gray, thalamus and hypothalamus (Huang et al., 1998; Gould et al., 1999; Pencea et al., 2001). The site of origin of these newly generated cells in the adult brain still has not been identified. In the neocortex they may be generated in the SVZ and then migrate into the neocortex (Gould et al., 2002).

Adult neurogenesis was first shown by using radiolabelled thymidine (^{3}H-thymidine) autoradiography technique. In this technique ^{3}H-thymidine is incorporated into DNA during cell division. Therefore newly born cells can be identified and traced through radioactive labelling. This technique was first used by Altman and was followed up by many other researchers (Altman and Das, 1967; Kaplan and Hinds, 1977; Kaplan and Bell, 1984; Cameron et al., 1993). Altman's elegant works, with the help of ^{3}H-thymidine (mitotic indicator), showed that new cells proliferate in the SGZ of the adult DG.

The concept of adult neurogenesis was not generally accepted until recently. The controversy remained over the identity of newborn cells: it was not shown that the newborn cells were indeed neurons rather than glia. Kaplan and Hinds (1977) used ^{3}H-thymidine in conjunction with electron microscopy to study the identity of newborn cells during neurogenesis in the adult rat. Using electron microscopy, they showed that ^{3}H-thymidine labelled cells in the DG of adult rats have morphological characteristic of neurons such as dendrites and synaptic contact on cell bodies (Kaplan and Hinds, 1977). Synapses on the cell body and proximal processes of the ^{3}H-thymidine labelled cells 20 days after injection have been demonstrated (Kaplan and Bell, 1984). Double labelling of ^{3}H-thymidine cells with dyes injected into the mossy fibers has also shown that these cells have projections characteristic for DG granule cells (Stanfield and Trice, 1988).

The identification of newborn cells was further proved by using mitotic marker in conjunction with neuronal marker. Cameron (1993) used ^{3}H-thymidine in combination with neuronal specific enolase (NSE). Three weeks after injection, 80% of the cells labelled with ^{3}H-thymidine were NES positive. This evidence shows that new cells are generated in the adult DG and most of these newly generated cells are differentiating into neurons. The occurrence of adult neurogenesis in the DG was further established with the development of new techniques, such as the use of mitotic marker BrdU (5-bromo-3-deoxyuridine) in conjunction with neuronal marker for mature and immature neurons to detect the fate and identity of labelled cells. Like ^{3}H-thymidine, BrdU is incorporated into cells during the S phase of the cell cycle. In contrast, BrdU is a non-isotopic substance that can be visualized by immunohistochemical method. Using BrdU in combination with neuronal marker such as neuronal nuclei (NeuN) and calcium binding protein (CaBP) has

also demonstrated that majority of adult-generated cells in the dentate gyrus of rats and mice differentiate into neurons (Kuhn et al., 1996; Gould et al., 1997; Kempermann et al., 1997). Interestingly, Adult neurogenesis has also been shown in humans with the help of BrdU marker. For example, postmortem tissue from the hippocampus and the subventricular zone of cancer patients were immunolabelled for BrdU and neuronal markers to investigate the cell proliferation in adult human brain. These tissues were obtained from cancer patients who received BrdU administration for diagnostic purposes. (Eriksson et al., 1998).

4.1.5 Modulation of Neurogenesis in the Adult DG

The dentate gyrus is a plastic organ. Its structure constantly undergoes dynamic changes by continual proliferation and addition of new cells to the GCL. The hippocampus is unique in that most of the cells in this brain structure are generated postnatally (Schlessinger et al., 1975). In the rat, neurogenesis is very high in the first two weeks after birth and most (85%) of granule cells are produced during this period of time. New cells are continuously added to the SGZ of the DG in the rat; however, the rate of neurogenesis in rats diminishes two weeks after birth. These newly born cells are packed into the GCL, which results in an increase in overall size of the DG by increasing the number of granule cells (Bayer et al., 1982). New cells migrate into the GCL and are located deeper with time (45-450 days old) (Crespo et al., 1986). In mice studies have demonstrated that the total number of granule cells increases for the first 6 months and then it remains constant (Kempermann et al., 1998).

The rate of neurogenesis in adulthood varies among species and changes with aging. The total number of neurons in the GCL of the adult mouse falls in the range of 300,000-640,000, (O'Kusky et al., 2000). In the adult rat, it has recently been estimated that 9,000 new cells per day are added into the GCL compared to 50,000 per day during developmental period (Cameron and Mckay, 2001). On the other hand, a proportion of the new cells dies by apoptosis. Thus, the subtle balance between cell production and cell death determines the number of cells and also the volume of GCL and ML.

Exogenous and endogenous factors can affect the rate of cell proliferation and/or survival of granule cells in the dentate gyrus Some of the factors (exogenous and endogenous factors) that influence adult neurogenesis in the dentate gyrus include stress, (Gould and Tanapat, 1999; McEwen, 1999), exercise (van Praag et al. 1999), learning (Gould et al. 1999), enriched environments (Kempermann et al., 1997; Nilsson et al. 1999), and aging (Kuhn et al., 1996).

With aging, a selective decrease in the generation of granule cells has been found to occur due to the decreased proliferative activity of granule cell precursors (Kuhn et al., 1996). Suppression of neurogenesis in the DG by glucocorticoide hormones seems to be responsible for the reduction of neurogenesis in aged animals. As shown by Cameron and McKay (1999), adrenalectomy stimulates the generation of new cells in aging, the death of dentate gyrus granule neurons is also greatly increased by this treatment (Nichols et al., 2001). A recent study showed age-related resistance to induced apoptosis and neurogenesis 6 months after removal of the adrenal gland, which was associated with increased expression of growth factor-beta1 (Bye et al., 2001). Although the high level of glucocorticoid hormones may be involved in the process of decreased neurogenesis with

aging, this involvement of glucocorticoids to brain aging depends on the physiological and cellular state of aged brain (Nichols et al., 2001)

Several studies have shown that an enriched environment such as larger cages equipped with several devices and a wild environment, learning a task, or exercising, promote the survival of newly proliferated cells in the DG of mice and rats (Kempermann et al., 1997; Nilsson et al., 1999). In contrast, the rate of cell proliferation in the DG decreases in stressful environments such as exposure to the odor of a predator, exposure to unfamiliar males, or social isolation (presumably through the actions of glucocorticoid stress hormones) (Tanapat et al., 2001; 1998).

In addition to acting through glucocortocoid hormone, stressful environments can also decrease the rate of neurogenesis through excitatory neuronal input via NMDA receptors (Cameron et al. 1995).

In contrast to adrenal steroid hormones, the sexual steroid hormones have stimulatory effects on neurogenesis in the DG. Estrogen secreted from ovaries increases the proliferation of granule cells in the DG in rat (Tanapat et al., 1999). The rate of cell production increases during the estrous cycle.

4.1.6 Expression of Young Neuronal Marker Proteins

4.1.6.1 Axonal Guidance and Pathfinding

In the rat DG, new neurons develop in the subgranular zone (SGZ), migrate into the granule cell layer (GCL), then differentiate and extend axons, called mossy fibers, to the CA3 region (Gage et al., 1998). The complexity and precision of neuronal circuity underlies the function of the nervous system. Axonal guidance and pathfinding are the

mechanisms by which the vast number of neurons that make up the nervous system are correctly connected together. Axonal guidance and pathfinding are important processes in development of nervous system and in few region of the adult brain where neurogenesis persist. During development, elongating axons are guided to their targets by a complex series of events involving the transduction of multiple extracellular guidance cues into specific growth cone behaviour (Winberg et al., 1998). Furthermore, the morphology of axonal arbors is regulated by both positive and negative signals. Axonal growth cones are directed by guidance molecules to follow specific pathways, to turn at particular guidepost, and to identify appropriate synaptic target cells at selected embryonic stages. Guidance molecules combine with high affinity receptors on the cell surface of axonal growth cones. Combination of guidance molecules and receptors stimulate intracellular signaling pathways and modulate axonal outgrowth. Guidance molecules can have multiple effects (e.g. repulsion or attraction) on the growing axons, depending on the type receptor / signalling pathway activated. Semaphorins make up one of several classes of guidance molecules involved in axon guidance. Collapsin, one member of this family, has been shown to cause growth cone collapse in several types of neurons (Nakamura et al., 2000).

Proteins such as doublecortin (DCX), neuronal cell adhesion molecule (PSA-NCAM), Unc-33-like phosphoproteins (Ulips) and the Collapsin response mediator proteins (CRMPs) are expressed concomitantly with neuronal migration/differentiation. Due to the complexity of this process, many other proteins may also be involved. Nevertheless, DCX, PSA-NCAM, and Ulips serve as useful marker of young neurons within the adult brain.

The highly polysialylated form of neuronal cell adhesion molecule (PSA-NCAM) has been shown to be transiently expressed by cells with features characteristic of granule neurons in the SGZ labelled with a thymidine analog (Seki and Arai, 1993). The presence of thymidine analog indicates that the cells have recently divided. PSA-NCAM expression in neurons is mainly confined to the developmental period (Sunshine et al., 1987), and is thought to be involved in neuronal migration, neurite extension (Doherty et al., 1990), axon pathfinding (Tang et al., 1992) and synaptic remodelling (Jorgensen, 1995). PSA-NCAM might therefore be involved in the development of young granule neurons as they migrate and/or extend processes forming synaptic connections (Seki and Arai, 1996).

4.1.6.2 Doublecortin

Doublecortin (DCX) is a Microtubule-Associated Protein (MAP) and like PSA-NCAM is expressed in migrating / differentiating neurons in the CNS and PNS (Nacher et al., 2001). This phosphoprotein is ubiquitously expressed in the developing brain of mammals including mice and rats. DCX protein expression in mice begins at day E10 and continues until postnatal day 5 (Francis et al., 1999). This expression profile of DCX is very similar to the expression of CRMPs (see below) in embryonic rat (Byk et al., 1998). Also, Nacher et al (2001) found that the cells expressing DCX in the adult rat brain have a similar expression pattern as CRMP-4. In adulthood DCX expression is limited to the areas of neurogenesis such as the SGZ of DG (Nacher et al., 2001; Gleesen et al., 1999).

DCX has been found to be associated with stable microtubules *in vivo*. The importance of microtubules in neurite ougrowth and pathfinding has been demonstrated by their presence in growth cones of growing axons and by studies that have shown the importance of microtubules and their remodelling in growth cones in response to guidance cues (Tanaka and Kirschner, 1991; Challacombe et al., 1997). Therefore, DCX might be involved in axonal outgrowth and guidance by interacting with microtubules and like CRMP-2 (see below) regulating their dynamics (Tanaka and Krischner, 1991; Challacombe et al., 1997; Gu and Ihara, 2000). In general, the DCX protein like the other members of MAP family may help to stabilize microtubules and stimulate tubulin polymerization which has been shown in neuronal cell cultures (Gleesen et al., 1999).

Clinical evidence for the involvement of DCX in axonal outgrowth and guidance comes from patients (female heterozygotes) with mutations in the DCX gene. These patients present with a "double cortex" feature (Gleeson et al., 1998), which is an indication of defects in axonal outgrowth and the involvement of this protein in axonal maturation and elongation.

Therefore, the role of DCX in cortical development may be limited to primates. In mice, for example DCX plays a role in hippocampal development but not in the cortex (Nacher et al., 2001)

4.1.6.3 Ulip Family

Ulip-1 is an intracellular phosphoprotein that has been identified from mouse brain (Byk et al., 1996; Quinn et al., 1999; Gaetano et al., 1997). This protein shares 98% homology with CRMP-4. The CRMP-4 is a member of a family of proteins that are

involved in axonal growth in rat. It is found transiently in post-mitotic neurons, such as granule cells from the DG of the hippocampus (Quinn et al., 1999). Other members of Ulip/CRMP family are Ulip3/CRMP-1, Ulip2/CRMP-2 and Ulip4 /CRMP-3 (Byk et al., 1998). The Ulip-1/CRMP-4 gene is highly expressed in developing brain. The expression of this protein is regulated during development, reaching a peak at approximately 5 days after the birth (during maturation of neurons) when there is a high rate of development of synaptic connections (Wang and Srittmatter, 1996).

The Ulip/CRMP protein is expressed in the dentate gyrus of adult rats in the early stages of differentiation and is therefore used as a marker for immature neurons (Parent et al., 1997; Scott et al., 1998; Quinn et al., 1999). Immunocytochemistry analysis of this protein has revealed that Ulip-1/CRMP-4 is expressed in neuronal cell bodies, neurites, and growth cones of postmitotic neurons (Minturn et al., 1995). Nacher (2000) showed that CRMP-4 expression in the CNS is associated with migrating cells and axonal outgrowth. *In vivo* and *in vitro* experiments support the involvement of these proteins in axonal guidance and pathfinding. For example, mutation in Unc-33, a CRMP-2 homolog in C-elegans, causes errors in pathfinding and neurite growth leading to abnormal movement and egg laying (Siddiqui, 1990; Siddiqui et al., 1991). Recently, it has been shown that CRMP-2 promotes the assembly of microtubules *in vitro* which suggests the involvement of this protein in axonal growth and branching. CRMP-2 binds tubulin heterodimers with affinity higher than it binds to the preassembled microtubules. It seems that CRMP-2 copolymerizes with tubulin dimers into microtubules. Like CRMP-2 other isoforms of CRMP (1,3,4) also interact with tubulin heterodimers (Fukata, 2002).

In vitro evidence in support of the involvement of CRMPs in the intracellular signaling cascade of collapsins is shown in studies where an anti-CRMP-62 antibody was introduced into chick dorsal root ganglion (DRG) neurons, inhibiting axonal collapse in response to Sema3A (collapsin-1) (Nakamura et al., 2000; Goshima et al., 1995). It has also been shown that CRMP-4 is strongly expressed and phosphorylated in response to nerve growth factor (NGF) treatment in PC12 cells (Byk et al., 1996 ; 1998).

In this study I have analyzed cell proliferation and neuronal morphology in the adult hippocampus in Ulip-1 knockout mice, in comparison with wild type and heterozygous animals, using immunohistochemistry.

4.1.7 Goals of this Chapter

A central hypothesis of this chapter is that Ulip/CRMP expression modulates (suppresses or enhances) neurogenesis in the adult. Thus, deletion of this gene will change neuronal proliferation. To address this hypothesis, we used an *in vivo* Ulip-1 knockout mouse model. Neurogenesis in the adult hippocampus is an especially important process, since its plasticity is thought to underlie learning, memory, and pathologies such as ischemic cell death, epilepsy and Alzheimer disease (Roses, 1996; Lobner and Lipton, 1993; McNamara, 1994; Gould et al., 1997). Thus, understanding of the regulation of the neurogenesis will help in understanding of the physiology and pathology of the brain.

My experimental plan:

A) To detect the genotype of each mouse by PCR analysis. B) To define neurogenesis in the dentate gyrus of the adult -/-, -/+ and +/+ mice using the proliferative marker

Ki67. C) To investigate the state of neuronal differentiation/migration in the dentate gyrus of the adult -/-, -/+ and +/+ mice, using the immature neuronal marker DCX. D) To define the morphology of mature neurons and gross anatomy of hippocampus in adult -/-, -/+ and +/+ mice using NeuN, Calbindin.

The results of these studies demonstrate that the rate of cell proliferation increases significantly in the dentate gyrus of the adult -/- mice compared to wild type and heterozygous animals. There was also a parallel enhancement in the presence of immature neurons, which indicates that Ulip-1 plays an inhibitory role in neurogenesis. The defasciculated appearance of the interpyramidal mossy fibers indicates that the Ulip-1 protein may also play some role in hippocampal cytoarchitecture.

4.2 Materials and Methods

In this study, a total of 12 littermate male and female mice (C57BL/6 strain) were used, five of which were homozygous knockout for Ulip-1/CRMP-4 (-/-), 4 were homozygous wild type (+/+) and three were heterozygous (-/+). The knockout mice were generated at the laboratory of Dr. C. Thiele (NIH, Bethesda, USA) as described below (4.2.1). The mice were bred and raised in the University of Toronto facility, to the age of 3-5 months before they were sacrificed and their hippocampi were dissected out for immunohistochemical analyses.

4.2.1 Generation of Ulip Knockout Mice

4.2.1.1 Targeting Vector, Electroporation, and Selection of Positive ES Cells

The replacement type targeting vector was made by sequentially inserting DNA fragments into a pBSII vector. A SalI PGK-TK fragment containing the thymidine kinase gene for negative selection was inserted into the XhoI site; a 5 kb XhoI/SmaI of the 5' region of Ulip containing a small portion of exon I was inserted into the XhoI/SmaI site: a 2.5kb SmaI/SpeI fragment 3' to exon 1 of Ulip was inserted into the SmaI/SpeI site. The lacZ gene was inserted into the SmaI/SalI site of PSA ßgal and finally a SmaII fragment containing both the LacZ-neomycin genes was inserted into the SmaII site in the recombinant pBSII and renamed MG#5 (Fig. 4.2). This construct knocks out most of Ulip exon I and knocks in the ß-galactosidase gene into the region 3' of the Ulip preserving the Ulip promoter. MG#5 was introduced into embryonic stem (ES) cells by electroporation. A Southern blot analysis of candidate ES cell clones revealed that the Ulip gene recombines with the targeting vector at a frequency of approximately 1 in 10. Positive ES cell clones were microinjected into recipient blastocysts to generate chimeric mice containing cells with the Ulip-targeted allele. Chimeric mice have been bred to the SJ129 and C57B6 strains of mice. Only C57B6 was used in the present study. All this work was done in the laboratory of Dr.C. Thiele (Bethesda, NIH, USA)

4.2.2 Genotyping

To detect the genotype of mice used in this study PCR amplification of DNA extracted from tail tips was performed.

4.2.2.1 DNA Extraction

Mice tail tips were incubated in 500 µl proteinase K buffer (50 mM Tris-HCl, pH 8, 100mM EDTA, 100 mM NaCl, 1 % SDS) plus 35 µl proteinase K (10mg / ml) at 65°C with shaking overnight to extract DNA. Followed by incubation with 20 µl RNAse A (10 mg/ml) for 2 hrs at 37°C. Choloroform extraction was performed by adding 200 µl 5 M NaCl plus 700 µl choloroform to above reaction mixture, shaking and centrifuging for 15 min at 14,000 rpm. The aqueous layer was transferred to the pre-labelled tube, filled with equal volume of 100% ethanol, to precipitate the DNA. The precipitated DNA was then isolated by centrifugation at 14,000rpm for 15 min. Precipitated DNA was washed in 70 % ethanol, centrifuged again for another 15 min at room temperature. The DNA was dissolved in 50 µl of dd H2O overnight. Isolated DNA from mouse tail was quantified by spectrophotometry and used for genotyping by PCR.

4.2.2.2 PCR

DNA prepared as described above was used as a template to amplify a 203 bp fragment from wild type and a 513 bp fragment from the ß-galactosidase gene inserted into the exon-1 of Ulip-1 gene in knockout mice. Reactions were performed in 50 µl volumes, each containing 100 ng of DNA extracted from tail, 5µl of 10 X PCR buffer, 25 mM MgCl2 (5µl), 1 µl of each primer (50 pM) 5'ggggactggggagatttact 3' (WTF), 5' taggacatggtggcgattct 3' (WTR), 5' aatgggataggtcacgttgg 3', (MR), 4 µl of 10 mM dNTP (dATP, dTTP, dGTP, dCTP), and 0.25 µl of Ampli Tag Gold DNA polymerase (PE Biosystems Inc.)

The cycling reactions were performed in a thermal cycler (MWG-BIOTECH PRIMUS 96 plus). The first cycle was at 95° C for 10 min, 95° C for 0.2 min, 55° C for 0.4 min, 72° C for 1 min, followed by 34 cycles of 95° C for 0.2 min. 20μl of each sample was diluted with 10 μl gel loading buffer and electrophoresed on a 1.5 % agarose gel at 70 mV for about 2hours. DNA molecular weight marker was loaded in one of the gel lanes to determine the molecular weight of each band. The gel was photographed under UV light.

4.2.3 Tissue Preparation for Immunohistochemistry

Animals were anaesthetized with halothane or by intraperitoneal (IP) injections of Somnotol (60 mg/kg; MTC Pharmaceuticals, Ontario). They were then perfused transcardially with ice-cold phosphate buffered saline (PBS; 8.5 mM Na_2HPO_4, 1.9 mM $NaH_2PO_4 \cdot H_2O$,137 mM NaCl, 2.7 mM KCl) , followed by ice-cold 8% paraformaldehyde in 0.1 M phosphate buffer (PB, pH 7.4), after which the brains were removed. The hippocampus was isolated and post-fixed overnight in 8% paraformaldehyde fixative. It was then mounted and sectioned transversally on a vibratome at 40 μm and the slices were stored in PBS containing 0.1 % sodium azide at 4°C until use (Kee et al., 2001).

4.2.4 Microscopy and Quantitation

Representative images were taken using a Nikon Optiphot-2 epifluorescence microscope with either 10X and 20X dry lens or 100X oil immersion lens. The signal for Alexa 488 labeling (green) was detected using an Omega XF22 filter, and the Alexa 568

labelling (red) was detected using a Nikon BA590 filter. Images were digitized by a SensiCam CCD black and white camera attached to the microscope.

A profile counting method using fluorescence microscopy was used to quantify the total number of Ki-67 positively labelled cells within the SGZ of the DG. Cells were counted at 100X magnification under oil immersion lens. Only the labelled cells within a narrow band separating the GCL and the hilus (i.e. SGZ) were counted. Approximately ten sections from each hippocampus were quantified for each animal. Some sections were omitted from counting due to tissue destruction during storage. Cell counts were averaged for each animal, and then averaged over each group of animals. The rates of neuronal proliferation within the DG of -/-, -/+ and +/+ mice were assumed to be proportional to the total number of dividing cells (Ki67+) within the subgranular zone of dentate gyrus. Statistical analysis was done using SigmaStat (Jandel Scientific) analysis software. 1-way ANOVA analysis was employed to detect the significancy of differences between groups of animals.

The DCX immunoreactivity was also quantified by counting the DCX+ cells in the inner edge of granular cell layer using profile counting method. DCX+ cells were only counted within upper blade of the DG. In this procedure the sections were selected randomly from all parts of the DG and examined at high magnification (40X objective, and 100X oil immersion) by fluorescence microscopy. The cell numbers were expressed as the number of positively labelled cells (DCX+) in the upper blade of the DG.

Statistical analysis was done using SigmaStat (Jandel Scientific) analysis software. 1-way ANOVA analysis was employed to detect the significancy of differences between groups.

4.2.5 NeuN, Immunohistochemistry

48-well multidishes (Nunc) were used for incubations and washes. Free-floating sections were washed with PBS to remove any sodium azide and then incubated with NeuN antibody. The NeuN antibody (mouse anti NeuN, MsX NeuN; Chemicon) was diluted at ratio of 1:500 in 0.3% Triton-X in PBS solution. Five hippocampal sections were placed in each well and 500 µl of diluted antibody solution was added to each well. Sections were allowed to incubate for 24 hours with gentle shaking at 4°C. The sections were then washed three times in PBS for 5 minutes each and the secondary incubation was carried out. The fluorochrome-conjugated secondary antibody (Alexa 488 goat anti-mouse; Chemicon) was diluted at 1:200 in 0.3% Triton-X solution and added to each well. Sections were incubated with the secondary antibody for 2 hours in the dark at room temperature. After the 2 hours incubation, sections were washed again 3 times with PBS and rinsed with double distilled water. The labelled sections were then mounted onto slides using the anti-fade mounting medium (Permafluor, Molec. Probes). The slides were left in the dark at room temperature to air dry and later assessed for positive labelling.

4.2.6 Calbindin Immunohistochemistry

Sections were washed with PBS to remove any sodium azide and then incubated with Calbindin antibody. The calbindin antibody (rabbit anti-Calbindin D-28K, Chemicon International, Inc.) was diluted at a ratio of 1:500 in 0.3% Triton-X in PBS solution and sections to be labelled were allowed to incubate for 24 hours at 4°C with gentle shaking. The sections were then washed 3 times at 5 minutes each in PBS,

followed by a 2 hour incubation with fluorescent-conjugated secondary antibody (Alexa 568/488 goat anti-rabbit, 1:200 in 0.3% Triton-X solution; Chemicon) at room temperature. Sections were then rinsed and mounted as described above.

4.2.7 Ki-67 Immunohistochemistry

Sections were washed with PBS to remove any sodium azide and then incubated with Ki-67 antibody. The Ki-67 antibody (rabbit anti-Ki67, Novo Castra Labs Ltd.) was diluted at a ratio of 1:1000 in 0.3% Triton-X in PBS solution and sections to be labelled were allowed to incubate for 72 hours at 4°C with gentle shaking. The sections were then washed 3 times at 5 minutes each in PBS, followed by a 2 hour incubation with fluorescent-conjugated secondary antibody (Alexa 488 goat anti-rabbit, 1:200 in 0.3% Triton-X solution; Chemicon) at room temperature. Sections were then rinsed and mounted as described above.

4.2.8 Doublecortin (DCX) Immunohistochemistry

Sections were washed with PBS to remove any sodium azide and then incubated with DCX antibody. 48-well multidishes (Nunc) were used for incubations and washes. The DCX antibody (goat anti-Doublecortin (C-8), Santa Cruz Biotechnology, Inc.) was diluted at ratios of 1:100 in 0.3% Triton-X in PBS solution. Five hippocampal sections were placed in each well and 500 µl of the diluted antibody solution were added to each. Sections were allowed to incubate for 48 hours with gentle shaking at 4°C. The sections were then washed three times in PBS for 5 minutes each and the secondary incubation was carried out. The fluorochrome-conjugated secondary antibody (Alexa 488, chicken

anti-goat, Chemicon) was diluted at 1:200 in 0.3% Triton-X solution and added to each well. Sections were incubated with the secondary antibody for 2 hours in the dark at room temperature. After the 2 hour incubation, sections were washed again 3 times with PBS and rinsed with double distilled water. The labelled sections were then mounted onto slides using the anti-fade mounting medium (Permafluor, Molec. Probes). The slides were left in the dark at room temperature to air dry and later assessed for positive labelling.

4.3 Results

4.3.1 Genotyping

Mutant mice were generated (Thiele et al, NIH, Bethesda, USA, unpublished data) by replacement of the first coding exon of the Ulip-1 gene with a ß-galactosidase gene cassette (Figure 4.2). DNA from tail samples of each animal used in this study was examined by PCR to determine each genotype (Figure 4.3). The expected size of the Ulip-1/CRMP-4 DNA fragment produced using our PCR primers in wild type alleles is about 203 bp, and 513 bp in the ß-galactosidase substituted fragment. Ulip-1 knockout mice (-/-) show only the presence of the ß-gal fragment, the heterozygous mice (+/-) show both fragments and wild type mice (+/+) show only the Ulip-1 fragment (Figure 4.3).

wild type allele

Exon1 construct (mg#5)

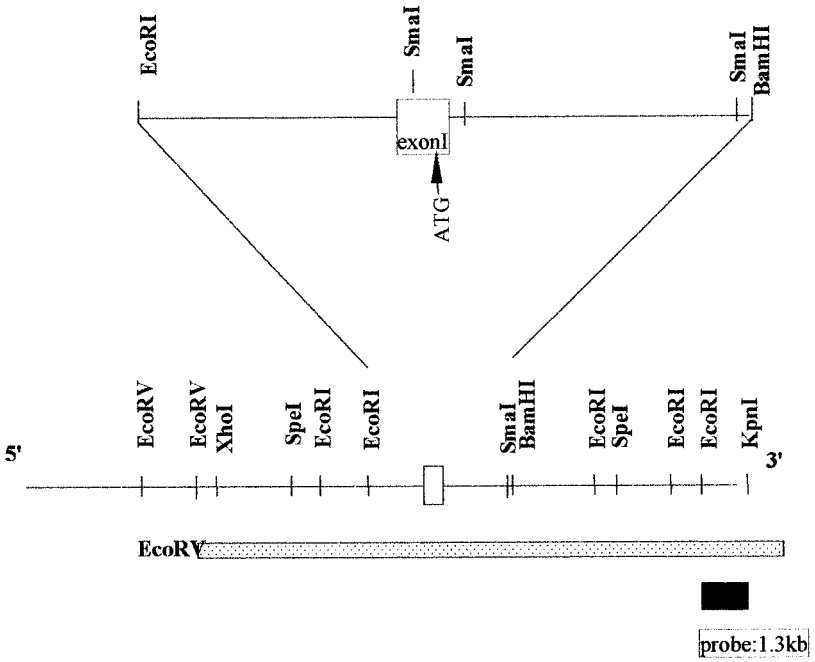

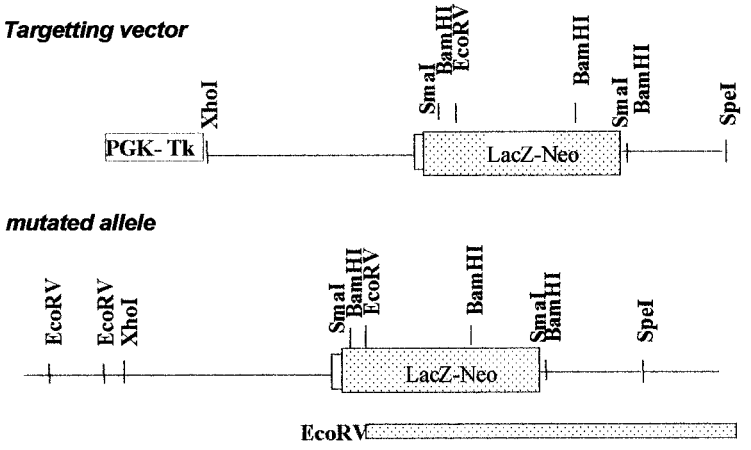

Figure 4.2. Ulip-1 KO construction

Figure 4.3. Genotyping of newly born mice using PCR method. Example of PCR analysis of each phenotype on 1.5 % electophoretic agarose gel. The 530 bp bands belong to -/- mouse and 230 bp bands belong to +/+ mice, M= standard molecular weight marker.


513 bp
203 bp

4.3.2 Immunohistochemical Analysis of Neurogenesis in Ulip-1 Knockout Mice

To investigate the mechanisms that underlie adult neurogenesis, The Ulip-1 knockout mouse was used as an *in vivo* model. The effect of a Ulip-1 null mutation on neurogenesis in subgranular zone (SGZ) of the DG of the adult -/-, -/+ and +/+ mice was investigated by neurogenesis markers using selective antibodies including Ki67, doublecortin (DCX), calbindin (CaBP), neuronal nucleic protein (NeuN) and Ulip-1/CRMP-4.

4.3.3 Cell Proliferation Determined by Ki67 Immunohistochemistry

Ki67 was used as a marker for neuronal proliferation in the adult dentate gyrus of -/-, -/+ and +/+ mice.

This marker was expressed in the nuclei of the labelled cells (Scholzen and Gerdes, 2000) in the proliferative zone including border of the hilus and the surrounding granule cell layer (GCL) of all groups of mice (-/-, -/+, +/+), as expected (Figure 4.4). A few cells labelled with Ki-67 were also found in the hilus of the DG.

The rates of progenitor cell proliferation within the DG of -/-, -/+ and +/+ mice were also detected as the total numbers of dividing cells (Ki67+) within the subgranular zone of dentate gyrus. Our results show a dramatic effect on neuronal proliferation as a consequence of Ulip-1 deletion. The mean of total Ki67 counts in the knockout mice was 21.2 ± 2.7 cells /section (n =5 animals) and that in the heterozygous was 15 ± 1.1 cells section (n=4 animals), in the wild type 8.9 ± 1.9 cells/section (n=3 animals). These differences between groups are statistically significant (1 way ANOVA test ($P<0.05$)).

These results clearly suggest the enhancement of cell proliferation in the subgranular zone of the -/- and -/+ mice in comparison with +/+ mice as demonstrated in Figure 4.5

In rats, these newly born cells give rise primarily to neurons and not glia (Cameron et al., 1993; Cameron and McKay, 2001). The location of Ki67+ cells was similar to those labelled with BrdU as shown by our laboratory and elsewhere (Kempermann et al., 1997).

Figure 4.4. Ki67 labelling of representative tissue sections of adult mice hippocampus.

A) Transverse slices of dentate gyrus from -/- animals immunolabelled for Ki67. Arrows indicate nuclei of Ki67+ cells on the border of hilus and granular cell layer(proliferatingzone)

B) Representative sections of DG of the -/+ mice labelled with Ki67 antibodies. Arrows indicate the nuclei of Ki67+ cells in the proliferating zone.

C) Representative sections of transverse slices of DG of +/+ mice labelled with Ki67 antibodies. Arrows indicate the nuclei of Ki67+ cells in the proliferatingzone. Photography was done at 100X magnification.

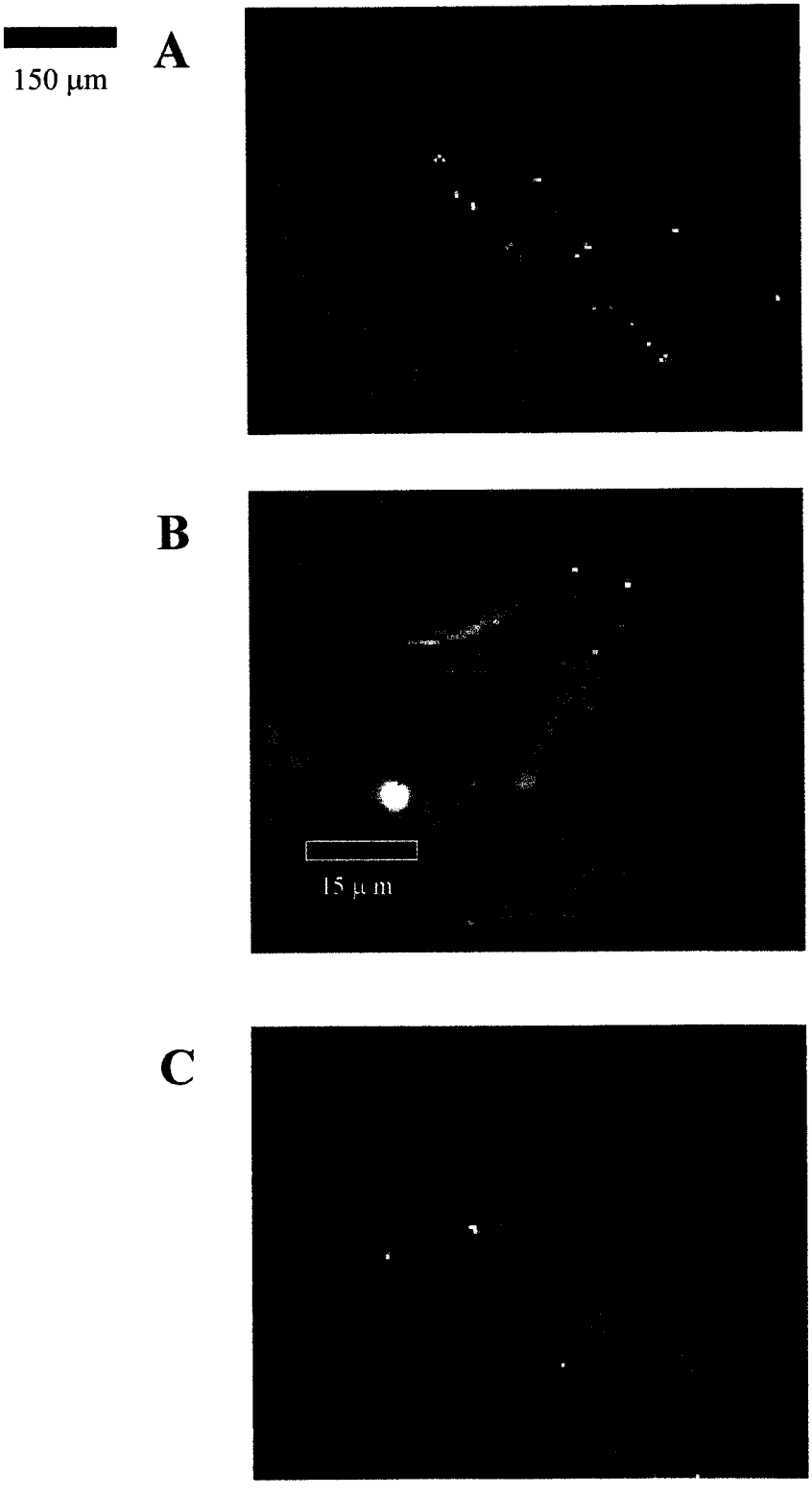
150 µm
A
B
15 µm
C

Figure 4.5. Comparison of Ki67 immunoreactivity in the hippocampus from-/-, -/+ and +/+ mice. The rates of progenitor cell proliferation were detected as the total number of Ki67+ cells within the subgranular zone of dentate gyrus. The Y ordinate denotes the mean of total Ki67+ cells counts in the knockout mice (21.2 ± 2.7 cells/section) (5 animals and 25 sections), in the heterozygous mice (15 ± 1.1 cells/section) (4 animals and 22 sections), and in the wild type mice (8.9 ± 1.9 cells/section) (3 animals and 20 sections), (1 way ANOVA test ($P<0.05$)).

The increase in the number of Ki67+ cells (residing in the proliferating zone) in -/- and -/+ mice relative to +/+ mice is interpreted as an enhancement of progenitor cell proliferation.

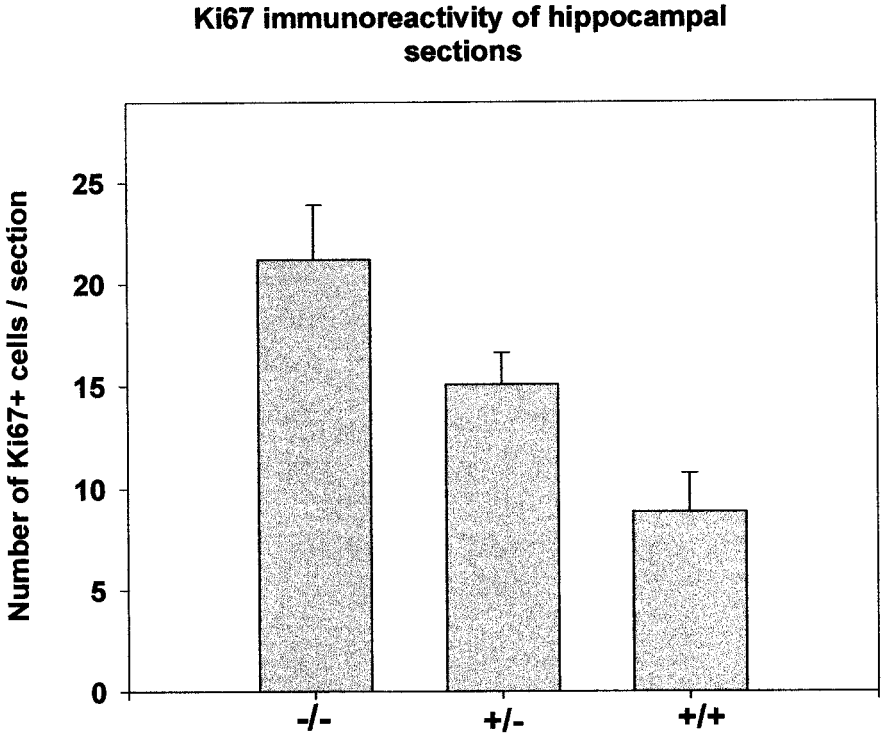
Ki67 immunoreactivity of hippocampal sections
Number of Ki67+ cells / section
25
20
15
10
5
0
-/-
+/-
+/+

4.3.4 Increase of DCX Immunohistochemistry in Ulip-1 Knockout Mice

Doublecortin (DCX) marker was used to investigate the state of differentiation of granule neurons three groups of mice. DCX and CRMP-4 (homologous of Ulip-1) are both immature neuronal markers with similar expression pattern in adult dentate gyrus. It is likely that in +/+ animals both proteins are expressed in the same neurons.

Hippocampal sections from 3 groups of littermate mice, Ulip-1 knockout (-/-), heterozygous (+/-) and wild type (+/+) mice, were immunostained with DCX antibody. The wild type group was used as a probe (control) for detection of the DCX expression and for morphological analysis of DCX+ neurons. The number of neurons expressing this protein and the morphology of neurons were compared among three groups.

As shown in Figure 4.6 (A, B, C), in all three groups of mice, DCX+ cells were present within the subgranular zone and the inner granule cell layer of the dentate gyrus. Most of the labelled cells appeared in the inner layer of GCL, with dendrites extending into the molecular layer and the axons projecting into the hilar region (Figure 4.7). As expected, DCX was expressed in the periphery of somata, dendrites and in axons of young granule cells throughout the dentate gyrus. These cells had characteristics of immature neurons, including fusiform cell bodies, single primary dendrites and sometimes abnormal dendritic orientations, similar to those that have been described with CRMP-4 immunoreactivity (Nacher et al., 2001). Some cells appeared in clusters within the SGZ with characteristic of newly born neurons (4.7 B).

Upon quantitative comparison of knockout and wild type mice, prominent differences were observed in expression levels of DCX between groups. DCX was overexpressed in knockout mice compared to wild type littermates (Figure 4.6, A, B, C).

Visual assessment of cells labelled with DCX antibody indicated that there was a striking increase in the number of the cells which express DCX in the granule cell layer and SGZ of the dentate gyrus of Ulip-1 knockout mice in comparison with wild type mice. The expression profile of DCX in the SGZ of heterozygous mice resembled that of mutant mice (Figure 4.6). This pattern of expression was similar in all parts of the DG (ventral and dorsal).

The DCX immunoreactivity was quantified by counting the DCX+ cells in the inner edge of the granular cell layer. DCX+ cells were only counted in the upper blade. Quantitative analysis of DCX immunoreactivity indicated that the number of immature neurons identified by DCX labelling within the upper blade of the DG was significantly higher in -/- and -/+ in comparison to +/+ mice ($P<0.05$, ANOVA one way) (Figure 4.8).

Figure 4.6. DCX labelling in representative tissue sections from adult mouse hippocampus. Transverse slices of DG immunolabelled for DCX from Ulip-1 knockout (-/-) mice (A) from heterozygous -/+ mice (B), and wild type mice +/+ (C). Note that all DCX+ immature neurons are located near the sugranular zone of DG with dendrites extending into the granular cell layer (GCL) in all animals. Greater numbers of DCX+ immature neurons in the representative sections of the DG of -/- and -/+ mice appear to be present. Similar results were apparent from analysis of tissue sections from all available animals; refer to text for detail. Photography was done at 100X total magnification

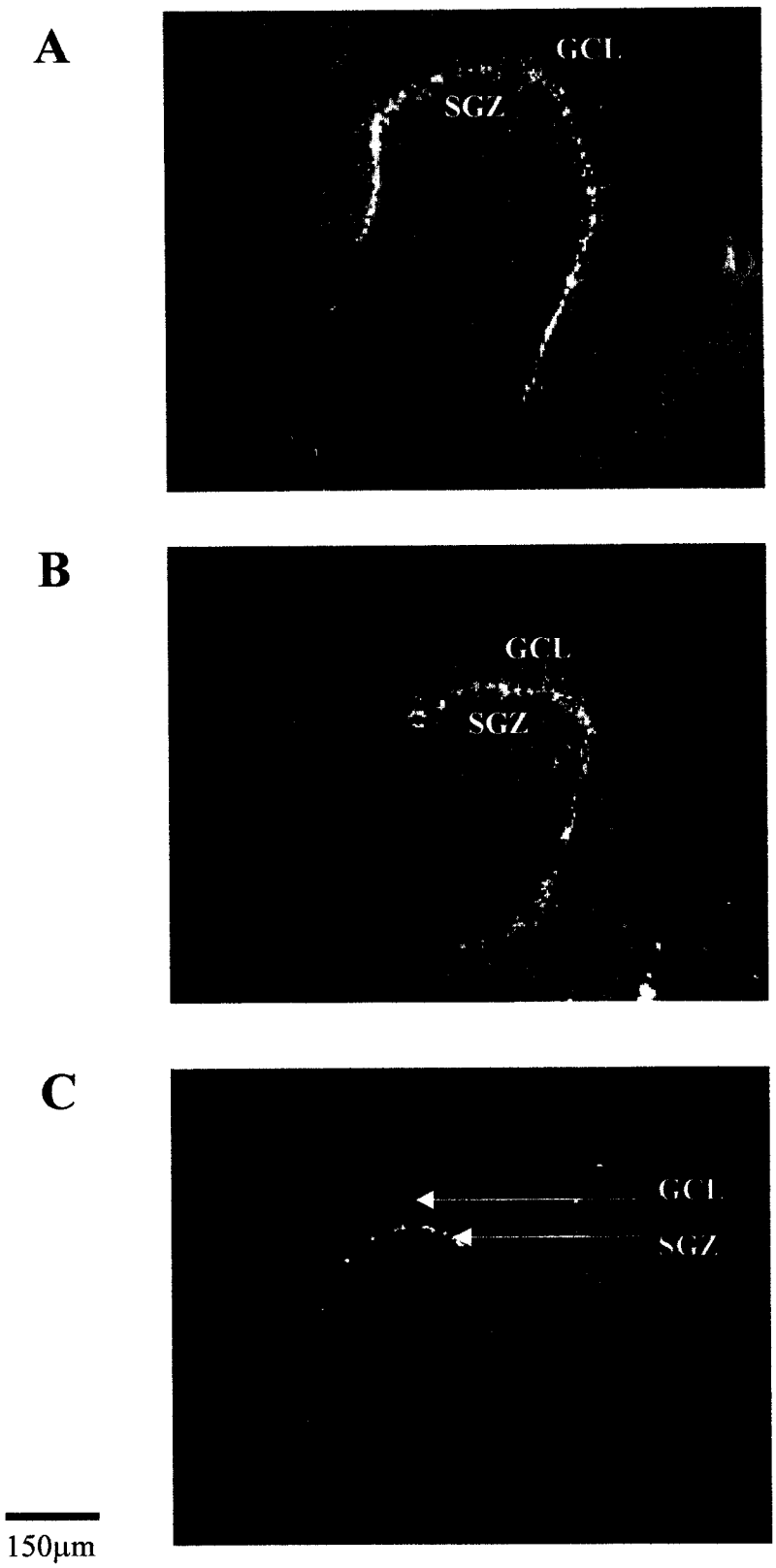
A
GCL
SGZ
B
GCL
SGZ
C
GCL
SGZ
150μm

Figure 4.7. A) Higher magnification of DCX+ immature neurons. Arrows point out DCX+ immature neurons residing in the subgranular zone of the DG with immature dendrites extending into the granular layer. DCX was expressed in cell body, dendrite and axon of neuron. B) A cluster of DCX+ cell bodies near SGZ. Photography was done at 1000X total magnification.

A

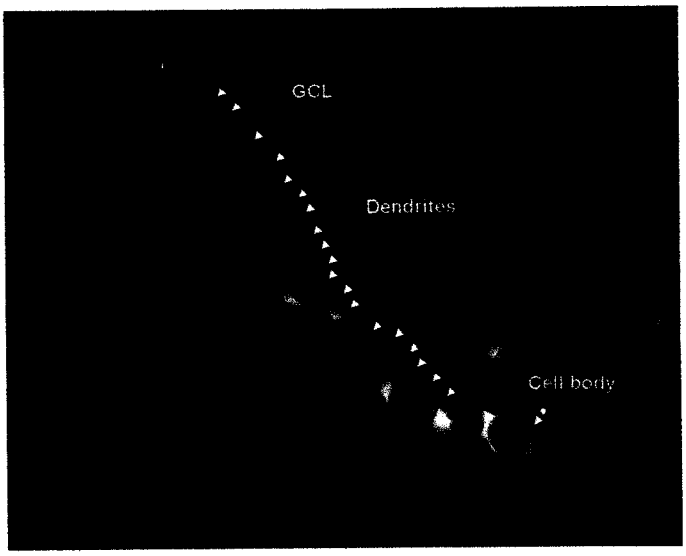

B

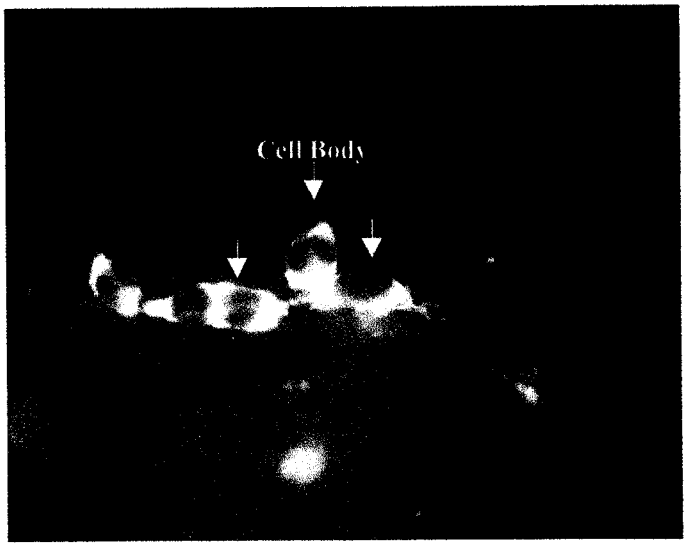

15μm

Figure 4.8. Comparison of DCX immunoreactivity in the hippocampal sections from -/-, -/+ and +/+ mice. Y ordinate denotes the mean of DCX+ cells count/upper blade/section ± SEM in the subgranular zone of the dentate gyrus from 5 -/- (38 ections) and 4 -/+ (26 sections) and 3 +/+ mice (16 sections). Increase in the number of DCX+ cells in -/- and -/+ mice is interpreted as an enhancement of neurogenesis (1 way ANOVA test ($P<0.05$)).

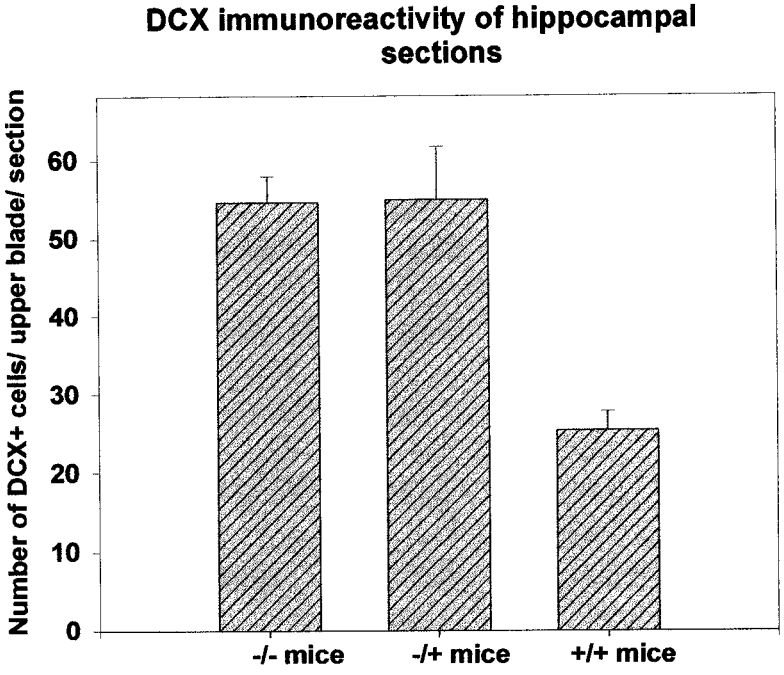
DCX immunoreactivity of hippocampal sections
Number of DCX+ cells/ upper blade/ section
60
50
40
30
20
10
0
-/- mice
-/+ mice
+/+ mice

4.3.5 NeuN Immunoreactivity in Dentate Gyrus

The anti-NeuN antibody was used to determine gross changes in the neuronal cell number in the dentate gyrus and CA1, CA2 and CA3 of the hippocampus in mutant and heterozygous animals compared to wild type mice. This antibody labelled the cell bodies of granular cells of the dentate gyrus, as well as the pyramidal neurons of the CA1, CA2 and CA3 regions. No differences in the labelling of cells between wild type and Ulip knockout mice were observed by visual assessment as shown in Figure 4.9 (only the dentate gyrus is illustrated).

Figure 4.9. NeuN labelling in representative tissue sections from adult mouse hippocampus. A) -/-, B) -/+, and C) +/+. Nuclear neuron (NeuN) is a marker for mature neurons. No significant differences were observed with this marker in the DG of -/-, -/+ and +/+ mice. Different shapes of DG can be accounted for dorso-ventral variability in DG morphology. Photography was done at 100X total magnification.

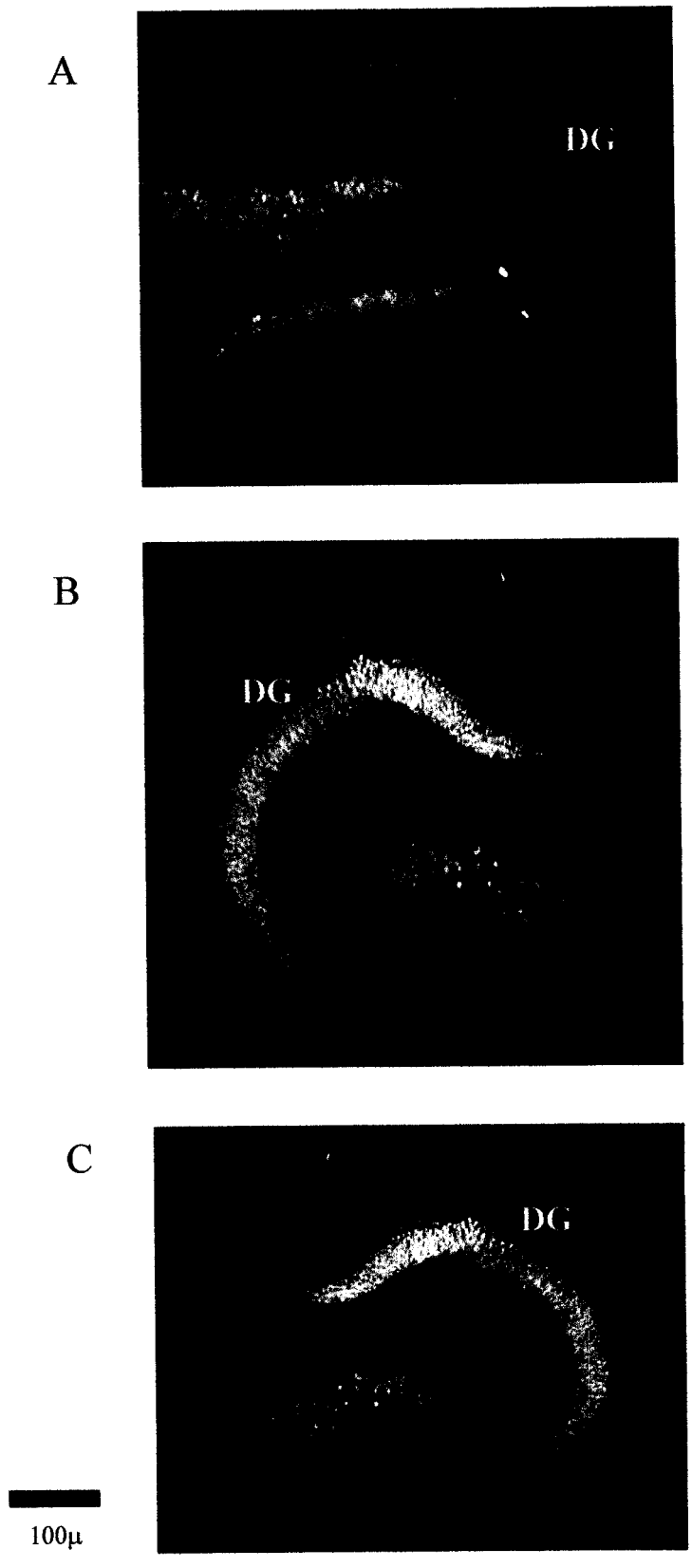
A
DG
B
DG
C
DG
100μ

4.3.6 Calbindin Immunoreactivity in the Hippocampus

The morphology of mature neurons was examined by immunoreactivity for the expression of calbindin (CaBP or calcium binding protein) in cell bodies, dendrites and axons of mature neurons. The expression of this protein was observed in the cell bodies as well as in the axons (mossy fibers) of the granule cells. As expected, immature cells in SGZ are not labelled with this marker (see dark gap at the inner edge of GCL).

The appearance of mossy fibers in both Ulip-1 knockout and wild type labelled with the CaBP marker is shown in Figure 4.10. In wild type mice, the hippocampal mossy fibers leave the hilus in two distinct branches; the main long branch known as the suprapyramidal projection, and the shorter branch known as the infrapyramidal projections. These two projections are connected by intrapyramidal projections. There are a few intrapyramidal projections between these two bundles of mossy fibers and the two branches are clearly distinct (Figure 4.10 C). In some knockout mice, however, we observed many intrapyramidal projections between infra and supra pyramidal mossy fibers, making them less distinct and giving them a fibrous appearance and a pattern of defasciculation (Figure 4.10 A). The pattern of mossy fibers in the -/+ mouse stands between -/- and +/+ mice (less fasiculation) (Figure 4.10 B).

Figure 4.10. Effect of Ulip-1 gene knockout on mossy fiber development (morphology) using Calbindin as a marker for mature neurons. Representative sections of hippocampus from -/- (A), -/+ (B) and +/+ (C) mice and sections labelled for calbindin are shown. In total, 15 sections from 3 mice in each of the three categories were examined. Note that in all representative sections calbindin protein was expressed in the cell bodies as well as in the axons of the granule cells (mossy fibers).

In the +/+ type mouse (C) hippocampal section, infrapyramidal and suprapyramidal projection are distinct and fewer intrapyramidal projections were observed. Also note the defasiculation pattern of mossy fibers in -/- (A). In the -/+ mouse (B), the pattern of mossy fibers stands between -/- and +/+ mice (less fasiculation). IPP: Infrapyramidal Projection; SPP: Suprapyramidal Projection. Photography was done at 100X total magnification.

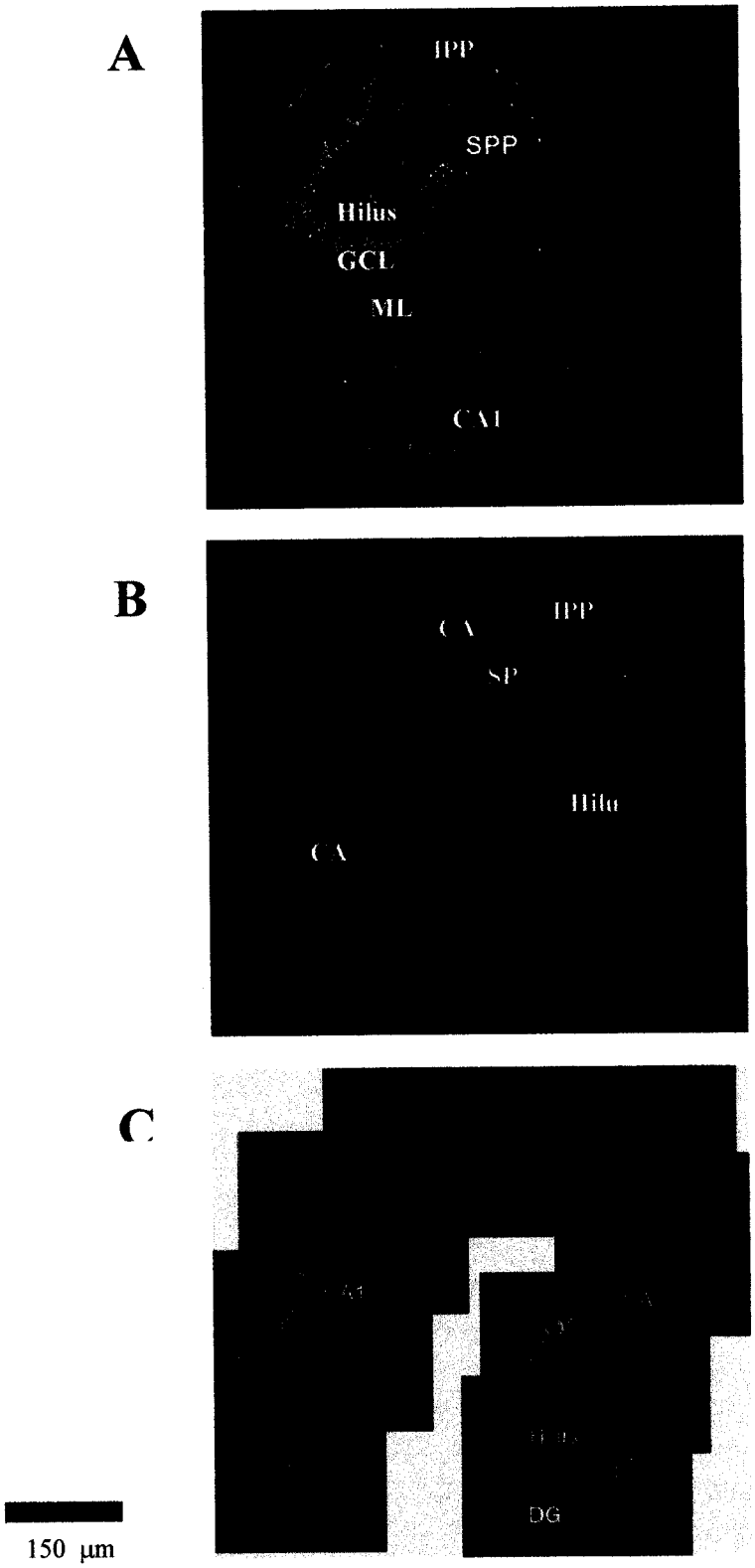
A
IPP
SPP
Hilus
GCL
ML
CA1
B
IPP
CA
SP
Hilu
CA
C
DG
150 µm

4.4 Discussion

4.4.1 Rationale for using Ulip-1 Knockout Mice

In this study, the *in vivo* Ulip-1 knockout mouse model was used to examine the mechanisms underlying adult neurogenesis in the hippocampus. This mouse was produced in the laboratory of Dr. C. Thiele (NIH, Bethesda).

The rationale for making these knockout mice primarily comes from experiments which screened for genes involved in development of peripheral nervous system tumors. These experiments found that Ulip-1 expression was downregulated in these tumors. On the basis of this finding, Ulip-1knockout mice were produced to investigate tumorigenesis in the peripheral nervous system..

We chose to use the Ulip-1 knockout model to investigate the mechanisms underlying adult neurogenesis for two reasons. First, this protein is downregulated in peripheral nervous system tumors, which indicates its possible involvement in cell proliferation. Secondly, the Ulip-1 protein is almost exclusively expressed in the nervous system and its expression is strongly upregulated during development. In the adult brain, Ulip-1 expression is confined to regions with neurogenesis such as DG (Quinn et al., 1999; Byk et al., 1996).

4.4.2 Identity of Ki67+ Cells in the Wild Type Mice used as Controls

The Ki67+ nuclei within the granular cell layer showed morphological characteristics similar to the precursor of DG granule cells in the SGZ, and were located almost entirely within a strip bordering the GCL and hilus which is known as a proliferative zone. This is where new dentate granule cells are normally produced, and thus the Ki67+ nuclei most likely represent newly generated granule cells. The presence

of Ki-67+ cells in the proliferative zone is consistent with previous observations of newly born cells in this region (Kempermann et al., 1997). However, cells expressing Ki-67 do not co-express the young neuronal marker CRMP-4 or DCX. This suggests that CRMP-4/DCX expression occurs later in cell development (differentiating/migrating stage) compared to the expression of Ki67 protein in the cell cycle (Kee et al., 2002).

It has also been reported that low numbers of adult-born glial cells are present in the DG, particularly in the hilus and molecular layer of the DG (Cameron et al., 1993; Kuhn et al., 1996). These glial cells are generated in the proliferative zone, the border of the GCL and the hilus. However, most of the precursor cells labelled with Ki67 are differentiated into neurons (up to 80% depending on the environment), and they can be distinguished from glial precursor cells by their larger nuclear size (Cameron et al., 1993; Gould et al., 1997). We also found a few Ki67+ cells in hilus, ML and GCL throughout the hippocampus.

4.4.3 Identity of Ki67+ Cells in Knockout and Heterozygous Mice.

As in the wild type mice (control animal), the Ki67+ nuclei within the DG of -/- and -/+ mice are located in the proliferative zone, the region between inner edge of the GCL and the hilus.

4.4.4 Cell Proliferation in Knockout vs Heterozyous and Wild Type Mice

In this study the proliferative marker Ki67 (Scholzen and Gerdes, 2000) was used to investigate the effect of Ulip-1 deletion on precursor cell proliferation in the adult knockout, heterozygous and wild type littermates. Ki67 is an endogenous protein, which

is expressed during the mitotic cycle. Using Ki67 as a proliferative marker allows us to examine the effect of Ulip-1 knockout on the actual proliferation levels of precursor cells, since Ki67 protein is expressed in all stages of mitosis. (Kee et al., 2002). However, the fate of Ki67+ cells cannot be determined by this marker, due to its lack of expression in immature and mature neurons. Therefore, I could continue with BrdU marker, which incorporates into DNA molecule during S-phase; therefore, the cells carrying BrdU could be traced and their identity could be estimated by using other markers.

Deletion of the Ulip-1 gene in the Ulip-1 knockout mouse model led to enhancement of cell proliferation in the SGZ of the DG as was shown by Ki-67 immunostaining. This enhancement for heterozygous mice stands between -/- and +/+ mice. It is possible that deletion of Ulip-1 gene has affected the length of cell cycle i.e. by increasing the duration of cell division rather than increasing neurogensis per se. However, deletion of the Ulip-1 gene also led to overexpression of doublecortin (DCX) protein, which is a specific marker for neurons in the migration/differentiation stage (Gleeson et al., 1999; Francis et al., 1999). Thus, it is likely that this gene is involved in neurogenesis.

4.4.5 Identity and Proliferation of Cells Labelled with DCX

In this study we used the differentiating/migrating marker DCX to investigate the effect of Ulip-1 deletion on the proliferation of immature neurons in adult knockout, heterozygous and wild type littermates. Also, we aimed to detect whether the enhancement of cell proliferation observed by Ki67 in knockout mice coincides with neuronal differentiation.

DCX + cells reside within the subgranular zone of the dentate gyrus where the newly proliferated cells differentiate into neurons. DCX was expressed in the cell body, periphery, dendrites, and in the axons of the SGZ cells throughout the dentate gyrus of all groups of mice (-/-, -/+, +/+). DCX+ cells in those mice had the morphology characteristic of immature neurons, including fusiform cell bodies, single primary dendrites, and in some instances abnormal dendritic orientations, similar to those that have been described for immunoreactivity with CRMP-4 in subgranule cells of the dentate gyrus in the rat (Nacher et al., 2001). The distribution of young neurons in the mouse dentate gyrus appeared to be similar to that of young neurons in the rat dentate gyrus (Figure 4.6). Most, if not all, of the labelled cells appeared in the inner layer of granular cell layer, with dendrites extending into the molecular layer of the axons projecting into the hilar region.

In this study, the number of immature neurons, as detected by DCX+ cells, was drastically increased in the DG of knockout mice when compared to wild type. This increase in DCX+ cells may be a result of increased neurogenesis in the DG of knockout mice, as previously indicated by Ki67, a marker of cellular proliferation. These parallel increases in the density of Ki67+ and DCX+ cells may suggest that enhanced proliferation leads to upregulation of neurogenesis in the DG of Ulip-1 knockout mice.

4.4.6 Possible Mechanisms Involved in Enhanced Expression of DCX in Ulip-1 Knockout Mice

Upregulation of neurogenesis in Ulip-1 knockout suggests that Ulip-1 seems to be involved in inhibiting neurogenesis, as demonstrated by the results seen with the Ki67

and DCX markers in Ulip-1 knockout mice. This finding is unexpected because the strong up-regulation of Ulip-1/CRMP-4 has been reported in regions of the brain with adult neurogenesis such as the DG. It is also unexpected, because of studies showing an up-regulation of the CRMP-4 protein at the peak of neurogenesis during development (Quinn et al., 1999). This increase in DCX+ and Ki67+ cells also does not seem to be in agreement with previous studies showing that the expression of CRMP-4 in PC12 cells is strongly upregulated in response to NGF (Nerve growth factor) treatment, a factor that influences neuronal proliferation and differentiation (Minturn et al., 1995; Byk et al., 1996 and 1998). However, the following suggested mechanisms may explain this discrepancy.

The Ulip-1 protein may be involved in the processes of axonal guidance and pathfinding. Once axons have developed and reached their destination, the process of axonal collapse occurs, which may then establish a negative feedback signal to down regulate neurogenesis. Lack of Ulip-1 may abolish this functional link in the knockout mice, resulting in enhancement of neurogenesis. In fact, it has been shown in brain grafts that if the differentiation of neurons can not be completed, the graft proliferates and becomes a tumor (Temple, 2001). This suggests that there might be a link between the generation of new cells and neuronal differentiation. On the other hand, the possible effect of Ulip-1/CRMP-4 on the expression of other isoforms of this protein (CRMP-1, CRMP-2, and CRMP-4) has not been investigated. The balance between expression and function of different isoforms may lead to regulation of newly born cells in the DG.

Alternatively, the increase in immature neurons shown by the DCX marker could be to due to a reduction in cell death and an increased level of cell survival. Recently, it

has been shown that impairment of cell proliferation led to the reduction of cell death and an increased survival rate of progeny cells in rats that had been treated with an agent that blocks proliferation (Ciaroni et al., 2002). It is possible that a similar mechanism is involved in the Ulip-1 knockout mice during development. That is, in the developmental period, Ulip-1knockout mice may experience a decrease in neurogenesis and therefore establish a compensatory mechanism that leads to the enhancement of neurogenesis and an increased survival rate of new neurons in the adult knockout mice. Complementary experiments are necessary to prove the above explanation. Such experiments could include detecting the rate of cell death and cell survival by TUNEL and BrdU labelling in conjunction with mature markers such as CalB and NeuN during development and adulthood.

The higher level of expression of DCX judged by immunoreactivity in knockout mice could be due to an increase in proliferation of the newly born cells in the SGZ of the DG, as shown by Ki67 marker. Alternatively, individual mutant cells may make more DCX per cell. Another possible explanation for the enhancement of DCX+ in knockout mice is that the cells which express DCX are defective and do not migrate out of the SGZ as they do normally. Two possible reasons could account for the overexpression of DCX in knockout mice. First, an increase in the expression of DCX might compensate for the lack of Ulip-1 protein. Compensation mechanisms of this type often occur in knockout mice (Catalano et al., 1998). Alternatively, overexpression of DCX might be a secondary effect, due to the expression of other proteins, such as isoforms of Ulip-1. Both DCX and Ulip-1 seem to be involved in axonal guidance and pathfinding and have a similar developmental profile, thus this compensation by DXC seemed reasonable.

It has also been shown that one member of the CRMP-4 family of proteins is involved in axonal collapsing through the Semaphorin signaling pathway (Nakamura et al., 2000) (Figure 4.1). It is possible that expression of Ulip-1, down-regulates the expression of DCX, which might be located downstream of Ulip-1, as one of the components in the signal transduction pathway for axonal repulsion. Therefore, lack of Ulip-1 may remove tonic inhibition from the expression or function of DCX, leading to a striking expression of DCX. It is also possible that these proteins control expression of each other at transcriptional/translational levels. It has been shown that DCX is involved in axonal elongation and CRMP-2 in axonal collapse; therefore, the balance between expression of both proteins is important to lead to the proper targeting of axons to their correct location. Overexpression of DCX suggests that there is a functional relationship between the DCX protein and Ulip-1. As a result, they might belong to the same signalling pathway or different pathways with functional dependency. However this protein was used as a marker for immature neurons, and could simply show the effect of Ulip-1 gene deletion on the processes of neurogenesis, and not the direct effect of this mutation on DCX expression. Finally, proliferation and increased numbers of DCX+ cells could occur independently of each other.

4.4.7 Identity and Morphology of Mature Neurons in the Knockout, Heterozygous and Wild Type Mice using the Marker Calbindin

To investigate the effect of Ulip-1 knockout on the morphology of mature neurons in the hippocampus calbindin protein was immunolabelled. This protein is expressed in

the cell body, axons and dendrites of mature neurons in the granular cell layer (Kee et al., 2001). As expected, immature cells in SGZ are not labelled with this marker.

The defasciculation and abnormal intrapyramidal mossy fibers observed in the hippocampal CA3 region of Ulip-1 knockout and heterozygous mice are compatible with the findings in the unc-33 (gene homologous of Ulip-1) knockout in C. elegans, where many neurons exhibit errors in pathfinding and/or premature termination of their axons. Similar structural changes (defasiculation) have also been observed in NCAM mutant mice or PSA deficient mice (Seki and Rutishauser, 1998). PSA-NCAM is selectively expressed in developing neurons as discussed in introduction of this chapter (4.1.6.1) (Seki and Rutishauser, 1998).

The involvement of the Ulip/CRMP family in the signalling pathway of axonal guidance and axonal collapse has been shown elsewhere (Goshima et al., 1995). CRMP is one of intracellular components of a signalling pathway that mediates the Sema3A cue for axonal collapse (Nakamura et al., 2000). Sema2a guidance molecule (member of semaphorine family of guidance molecules in invertebrates) in grasshoppers not only plays a role in axonal guidance, it also stimulates axons to fasiculate with each other (Isbister et al., 2000). In E8 chick retinal ganglion cells, the growth cones exhibit a spread morphology in the absence of Sema3A stimulation as opposed to a needle-like normal collapsed appearance in the presence of Sema3A (Nakamura et al, 2000). Therefore it is possible that lack of the Ulip-1 gene as a component of signalling cascade interrupts the signal transduction in response to semaphorin guidance cue molecules and leads to defasiculation of intrapyramidal mossy fiber projections, as was observed in the Ulip-1 knockout mice. However, the defasciculation and abnormal intrapyramidal mossy fibers

in Ulip-1 knockout mice may be established as a result of an increase in the number of newly born cells in the SGZ, which interrupts the normal fasiculation process. These structural changes may also be a secondary effect due to the overexpression of DCX.

These findings may suggest that Ulip-1 plays an important role in the axonal projections of granular cells into fasciculated bundles. However, more comprehensive analyses are needed to detect the cause of the morphological changes in the mossy fiber projections, by using suitable techniques.

4.4.8 Neuronal Phenotype as Determined by NeuN Expression

The expression of NeuN has been observed in most neuronal cell types throughout the adult nervous system. NeuN is expressed at the end of the cell cycle, and/or with the initiation of terminal differentiation of the neuron (Mullen et al. 1992). This protein is useful and important in the determination of neuronal phenotypes within brain tissue.

The morphological analysis of NeuN+ cells in the hippocampus of +/+, +/- and -/- mice indicated that these cells had characteristics of mature neurons. No differences in the volume or total number of cells in the granule cell layer were observed by visual inspection in a comparison of the dentate gyrus -/-, -/+ and +/+ mice. The question which now arises is what is the fate of the new cells generated in the SGZ of adult knockout mice. And what is the effect of neuronal enhancement on the volume and the number of cells in the granule cell layer. What does enhancement do if not lead to the increasing of the volume of the GCL? It is possible that the new cells die off. If not, whether the volume remains unchanged at the expense of old cell death. If it is not the fact, what is

the contribution of these extra new born cells to the overall volume and the number of cells in the granular cell layer. This contribution may be so small that it cannot be detected by visual inspection. The contribution of these cells to the function of hippocampus is also not known. However, to determine this, a detailed analysis of granule cell layer, including the volume and the numbers of cells, should be conducted.

4.5 Summary and Conclusions

Immunolabelling with Ki67 revealed differences in hippocampal cellular proliferation between -/-, -/+ and +/+ mice. An increased number of Ki67+ cells were found within the proliferative zone (SGZ) of the DG of Ulip-1 knockout mice. Using DCX, a marker of immature neurons, it was shown that the number of the cells labelled with DCX in the SGZ of -/- and -/+ mice was markedly increased compared to the +/+ mice. Calbindin a marker for mature neurons, showed that intrapyramidal mossy fibers have a defasiculated appearance in CA3 region in -/- mice.

These results suggest the involvement of Ulip-1 gene expression in cell proliferation within hippocampus. Surprisingly, this involvement seems inhibitory. Thus, removal of inhibition by deletion of the Ulip-1 gene may lead to an increase in the rate of neurogenesis. These enhancements are not likely due to an increase in the glial cell production, because there is a parallel increase in the number of DCX+ cells, which is expressed exclusively in immature neurons. Whether or not the increase in cell production is due to changes in cell survival rate is not known. Whether these enhancements lead to an increase in the volumes of the GCL and the ML it is not known, and should be investigated by quantitative methods. The rate of cell death should be

detected by measurements of apoptosis. Further questions that are raised here are what is the fate of these cells and what is the rate of survival? What are the physiological consequences of neurogenesis enhancement?

Although our results demonstrate an increased rate of cell division in the Ulip-1 knockout mice, we have not proven that newly generated cells are functional and we do not know the physiological significance of this enhancement. Also, we have not demonstrated how this protein affects neurogenesis. However, these findings provide a basis to investigate the physiological consequences of increased this neurogenesis by performing tests such as the spatial memory test (water maze test) or electrophysiological test (LTP). These data also provide a basis to investigate how brain neurogenesis is regulated.

4.6 Future Directions

In order to examine the fate of the newly generated cells another proliferative marker, such as BrdU (which incorporate into the DNA during S-phase) can be used in conjunction with immature and mature neuronal markers such as DCX and NeuN or calbindin. The rate of cell proliferation can be detected by quantification of the BrdU+ cells after the last BrdU administration. The rate of cell survival can be determined at least one-month after the last BrdU injection. Cell death can be also determined by measuring numbers of cells undergoing apoptosis.

The physiological consequences of an enhanced neurogenesis in Ulip-1 knockout mouse model can be examined by electrophysiological experiments (LTP) and/or by water maze memory test (spatial memory test) in the -/-, -/+ and +/+ mice.

Chapter Five: General Discussion

Allosteric Regulation of L-VDCCs: In chapter two of this study, I have addressed the following hypothesis: Mg-ATP binds directly to the C-terminal portion of the α1C subunit of the rabbit L-type calcium channel in non-hyrolyzable manner (i.e., allosterically) and this regulation is independent of phosphorylation.

In an attempt to understand the above mechanisms of ATP dependent regulation of L-VDCC channel activity, logical questions to ask are a) does ATP bind directly to the channel, b) which subunit is involved, and c) which part of subunit contains an ATP binding motif. Some of these questions were answered by electrophysiological experiments in conjunction with molecular biology. The electrophysiological experiments conducted simultaneously in the laboratory indicated that the site of allosteric regulation by Mg-ATP is located on the α1C subunit, and more specifically, on the distal portion of the C-terminus of this subunit. Furthermore, bio-computational analyses using computer assisted protein alignments revealed that the C-terminus of the rabbit cardiac a1C subunit contains a Walker A-like sequence that is critical for this allosteric regulation by Mg-ATP observed in cardiomyocytes. In addition, the C-terminus of the α1C subunit is cytoplasmic and thus is a good target for ATP binding. Moreover, the C-terminus is involved in a number of regulatory processes including channel gating, phosphorylation by PKA, and docking of AKAP and calmodulin. Therefore, the C-terminal portion was a good candidate to carry a motif involved in direct allosteric regulation of L-VDCCs. However, it remained to be answered whether the ATP molecule binds to the distal portion of C-terminus directly, and whether Mg2+ is necessary for binding, as was originally suggested by electrophysiological experiments.

To test the direct binding of ATP molecule to the C-terminus (allosteric regulation) a recombinant protein (GST-1959 fusion protein) was generated from the distal portion of the C-terminus in a heterologous system using E. coli. This expression system facilitated large-scale protein synthesis and purification, which was important for functional studies. However, prokaryotic systems, like E.coli, sometimes do not achieve proper folding and post-translational modifications of recombinant eukaryotic proteins.

Binding assays were performed by various techniques. However, binding of Mg-ATP to the GST-fusion protein generated from the C-terminus was not demonstrated by these studies. Although all possible and reliable techniques were employed, including affinity chromatography, azido-ATP radiolabelling, circular dichroism (CD), and fluorescent ATP labelling, none of these methods were able to detect any affinity between the fusion protein and Mg-ATP. However, the ATP molecule has previously been shown to regulate L-type calcium channels by phosphorylation of α1C subunits and ß subunits through the cAMP pathway (De Jong et al., 1996; Curtis and Catteral, 1985).

Expression of L-VDCCs in Aged Brain: The hypothesis for this chapter was based on Landfield's study that demonstrated an age-dependent increase in the density of functional L-VDCCs in CA1 nerve cell surfaces. The results of Landfield's study could be explained by three general mechanisms. First, an increasing number of functional channels at the cell surface could arise through enhanced transcription, translation, and insertion into the cell membrane or a decrease in the rate of mRNA degradation, and of VDCC internalization. Second, more subtle mechanisms might involve the conversion of silent channels to active channels, for example, through second messenger regulation, or

change in the auxiliary subunit composition or degree of co-assembly. A third mechanism for an increase in the density of channels could be the change in the distribution of VDCCs over the nerve cells. Which of these mechanisms underlies an increased density of functional channels is unclear.

In this chapter we examined the expression levels of L-VDCCs in general by radioligand binding assay and in detail by measuring the expression of various subunits β_3, $\alpha_2\delta$ in hippocampus, cerebellum and cortex from aged and young adult Fischer 434 rats brain by Western blotting analysis. Although, the involvement of L-type channels as a key factor in aging has been reported in the literature (Tollefson, 1990; Yamada et al., 1996), the expression levels of β_3, $\alpha_2\delta$ subuints which play an essential role in modulation and expression of functional channels at the cell surface has not been studied in the aged brain. Therefore, I examined whether or not the expression of the constituents subunits of L-VDCCs (β_3 and $\alpha2\delta$) are altered in the aged brain and whether or not their expression are region- and subunit specific.

My data showed that the expression levels of the $\alpha_2\delta$ increased in the aged hippocampus. However, no significant changes were observed in the expression levels of $\alpha_2\delta$ in the aged cortex and cerebellum compared to the young adults. The expression levels of β_3 did not change significantly in the studied regions. Radioligand binding assay with PN200-110 did not indicate any changes in the density of L-VDCCs in aged rat brains compared to the young adults.

It is likely that the increased levels of expression of the $\alpha_2\delta$ subunit in the aged hippocampus observed in this study, contribute to an age-dependent increase in the density of functional L-VDCCs in the hippocampus. It is believed that "auxiliary subunits

modulate channels properties by assisting the α_1 subunit in establishing a proper conformation suitable for a functional calcium channel, rather than affecting expression, trafficking, or stability of α_1 subunit" (reviewed by Catterall, 1995). As shown, the co-expression of α_1 subunit with $\alpha_2\delta$ subunit results in an increase in the functional expression and changes in the gating properties of L-VDCCs (Randall and Benham, 1999). On the other hand, the overall expression of L-type VDCCs showed no changes in binding of the radiolabelled ligand to hippocampal L-VDCCs in the aged brain. These results may suggest the increase in the density of functional L-VDCCs that has been observed in the aged brain (Thibaut and Landfield, 1996) might be as a result of the conversion of silent channels to active ones through changing the subunit composition and not changing the overall expression of this channel.

It is also likely that changes in the degree of co-assembly of the channel occur in aging, as opposed to elevated levels of expression of the β_3 subunit. An immuno-precipitation analysis could be carried out to investigate any changes in the degree of co-assembly of the ß3 subunit with the main pore (α_{1C}) in aged rat brain. The β_3 subunit also co-assembled with other α_1 subunits (i.e. α_{1B}, α_{1D}) and in this study only the total expression of this subunit has been detected not the fraction coassembled with α_{1C} subunit. Therefore, we cannot rule out the possibility of the compensation effect related to the altered expression of other α_1 subunits in aging for example decrease in α_{1B} (N-VDCCs) or increase in α_{1D} (L-VDCCs) have ben shown elsewhere (Moresco et al., 1989; Porter et al., 1996). Owing to different isoforms of β_3 subunit and heterogeneity of ß subunit in general, it is of particular interest to invetigate the expression levels of other

isoforms of ß subunit in aged brain. These results suggest that the expression level of L-type Ca^{2+} channels in aging is subunit- and region-specific.

Ulip-1 and Neurogenesis/Neurodegeneration: In the chapter four of this thesis, the mechanism underlying adult neurogenesis was examined in the hippocampus of the Ulip-1 knockout mouse. In this study, it has been demonstrated that the deletion of the Ulip-1 gene in this mouse model results in enhancement of cell proliferation in the SGZ of the adult mice, as indicated by the proliferative maker Ki67. These enhancements are not likely due to an increase in glial cell production. A parallel increase has also been shown in differentiating/migrating cells with the immature neuronal marker (DCX) in the Ulip-1 knockout compared to wild type animals. The involvement of Ulip-1 in neurogenesis seems to be inhibitory, which is not in agreement with upregulation of this protein during development and with the region showing neurogenesis in adulthood. However, this increase in immature neurons, as shown by the DCX marker, could be due to a reduction in cell death and an increased level of cell survival, rather than an increase in neurogenesis (Caironi et al., 2002). Therefore, the rate of cell death and cell survival should be investigated to clarify the cause of this enhancement. Furthermore, the fate and functionality of these newborn cells, the physiological consequences of this enhancement, and how this protein affects neurogenesis remain to be investigated.

The involvement of the Ulip family of proteins in the processes of axonal guidance and pathfinding through Sema-3 signalling pathway has been previously reported (Nacher et al., 2000). The effect of the deletion of this protein on the morphology of mature neurons was also investigated using NeuN and CaBP (neuronal

markers for mature neurons). The defasciculation of mossy fibers, which is indicative of morphological alterations, observed in the knockout mice is in agreement with the role of this protein family in axonal growth and pathfinding.

One member of the family of Ulip proteins is a component of the Sema-3 signalling pathway for axonal collapse (Nakamura et al., 2000). It has also been shown that the Sema-3 signalling cue molecule is involved in epithelial cell proliferation in the lung (Kagoshima et al., 2001). In addition, the Ulip family of proteins is also involved in neuronal migration and differentiation, and contributes to the cytoarchitecture of the brain. For example, the deletion of *unc 33* gene (the homologue of Ulip-1 gene in C. elegans) has led to the defects in axonal targeting, egg laying and abnormal movement (Siddiqui, 1990; Siddiqui et al., 1991). The involvement of this protein family like calcium channels has also been demonstrated in brain neurodegenerative diseases such as AD. In the AD brain, increased levels of highly phosphorylated Ulip/CRMP2 are accompanied with neurofibrillary tangles (a hallmark of AD) (Yoshida et al., 1998; Gu et al., 2000). This suggests a possible role of the Ulip family of proteins in AD via abnormal regulation of microtubule assembly in neurons (Fukata et al., 2002).

Is there any link between Ulip-1 and calcium channel in the processes of neurodegeneration/ neurogenesis? These studies have provided new information on the involvement of calcium channels and Ulip-1 on the regulation of the processes of neurodegeneration and neurogenesis.

The allosteric regulation of L-VDCCs by ATP was one the focus of this thesis. The effect of aging on the expression of L-VDCCs in rat brain, with an emphasis on the

expression of this channel in the aged hippocampus, was another focus of this thesis. Additionally, the mechanisms underlying adult neurogenesis have also been studied, in the hippocampus of knockout mouse model. Now the question is raised as to how these studies are correlated. The regulation and expression of L-VDCCs was studied to address the question of whether the changes observed in the aged hippocampus are due to altered protein expression or regulation. Studying the expression of L-VDCCs in aging and in adult neurogenesis are indeed two sides of the same coin, in that both of them attempt to explain why the numbers of neurons are altered (neurogenesis and neurodegeneration) in the adult hippocampus. Knowledge of all aspects of VDCCs may reveal how the rate of expression and regulation of L-VDCCs affects neurogenesis or neurodegeneration in the aged hippocampus, as discussed below.

The role of calcium channels in pre- and postnatal development of the hippocampus has previously been studied. It has been shown that calcium influx is necessary for all aspects of neurogenesis, such as cell division, neuronal outgrowth, pruning, and cell polarity (Purves et al., 1986; Johnson and Dekwerth, 1993). However, how calcium channels and influx of calcium through these channels contributes to neurogenesis is not well understood. It is known that mitogenic factors activate calcium channels and cause selective elevation of cytosolic calcium (Munaron et al., 1997). The involvement of calcium in the differentiation process of neurons has also been demonstrated in cultured embryonic spinal cord neurons (Holliday et al., 1991; Spitzer, 1995). Regions of the brain with active neuronal proliferation and migration are associated with expression of VDCCs mRNA both pre and postnatally (Tanaka et al., 1995;). The expression of N-VDCCs, sub-type of calcium channels, in the developing rat

hippocampus is concomitant with their proposed role in the hippocampal development (Jones et al., 1997).

How calcium influx and calcium channels expression correlate functionally with Ulip-1 gene expression in the process of neurogenesis is not known, but both have been implicated in the important processes of neurogeneis and neurodegeneration. The involvement of the Ulip-1 protein in neuronal cell proliferation seems to be inhibitory. This inhibitory involvement of Ulip-1 gene in cell proliferation has not only been demonstrated by their down-regulation in peripheral nervous system tumor (Dr. Thiele, personal communication), but also by cell proliferation enhancement in the hippocampus of Ulip-1 knockout mice. It seems the Ulip-1 protein has an opposite function (inhibitory) compared to calcium channels, which have a positive effect on neurogenesis. Now the question is raised as to how these proteins (VDCCs and Ulip-1) are related. It will be interesting to examine whether there is any direct correlation between their function (for example, does Ulip-1 have any inhibitory effects on the VDCCs). It will also be interesting to consider for future studies whether there is a common link between calcium channels and the molecular machinery involved in neurogenesis, for example, to investigate the expression levels of N-and L-VDDCs in the Ulip-1 knockout, in comparison with wild type mice.

It seems that a homozygous deletion of the mouse Ulip-1 gene has created a microenvironment that might be beneficial for neurogenesis. Thus, recognition and examination of the factors that are involved in neurogenesis and neurodegeneration, and the possible changes in these factors during aging and in neuropathology, may be useful

in answering the above questions and finding strategies to prevent or treat neurodegenerative diseases.

References

Allshire, A., Piper H.M., Cuthbertson, K.S., Cobbold, P.H (1987) Cytosolic free Ca2+ in single rat heart cells during anoxia and reoxygenation. Biochem. J. 244 (2): 381-385.

Altman, J., Das, G.D (1967) Postnatal neurogenesis in the guinea pig. Nature 214: 1089-1101.

Alvarez-Buylla, A., Garcia-Verdugo J.M., Tramontin A.D (2001) A unified hypothesis on the lineage of neural stem cells. Nat Rev Neurosci (4): 287-93

Amaral, D.G. and Witter, M.P (1995) Hippocampal Formation. In: The Rat Nervous System, G. Paxinos, ed., Academic Press: San Diego pp. 443-493.

Ansari, K.A., Kaplan, E., Shoeman, D (1989) Age-related changes in lipid peroxidation and prtective enzymes in the central nervous system. Growth Dev aging 53: 117-121.

Araki, T., Kato H., Nagaki S., Shuto K., Fujiwara T., Itoyama Y (1997) Effects of viconate on age-related alterations in [^{3}H]MK-801,[^{3}H]glycine, sodium-dependent D-[^{3}H]aspartate, ^{3}H]FK-506 and [^{3}H]PN200-110 binding in rats. Mech Aging Dev, 95:13-29.

Backx, P.H., O'Rourke B. and Marban E (1991) Flash photolysis of magnesium-DM-nitrophen in heart cells. A novel approach to probe magnesium- and ATP-dependent regulation of calcium currents. Am. J. Hypertens. 4: 416S-421S.

Bading , H., Ginty, D.D. and Greenberg, M.E (1993) Regulation of gene expression in hippocampal neurons by distinct calcium signalling pathways. Science, 260: 181-186.

Baimbridge, K.G., Celio, M.R. and Rogers, J.H (1992) Calcium-binding proteins in the nervous system. Trends in Neurosci. 15: 303-308.

Bangalore, R. and Triggle, D.J (1995) Age-dependent change in voltage-gated calcium channels and ATP-dependent potassium channels in Fisher 344 rats. Gen. Pharmac. 26(6): 1237-1242.

Barry, E.L (2000) Expression of mRNAs for the alpha 1 subunit of voltage-gated calcium channels in human osteoblast-like cell lines and in normal human osteoblasts. Calcif. Tissue Int. 66(2): 145-50.

Battaini, F., Govoni S., Riu R.A. and Trabucchi M (1985) Age dependent increase in Verapamil binding to rat cortical membranes. Neurosci. Lett. 61: 67-71.

Bayer, S.A., Yackel J.W., Puri P.S (1982) Neurons in the rat dentate gyrus granular layer substantially increase during juvenile and adult life. Science, 21:216(4548): 890-2

Bean, B.P (1990) Calcium channels: gating for the physiologist. Nature 348: 192-193.

Bean, B.P (1989) Classes of calcium channels in vertebrate cells. Annu Rev. Physiol. 51: 367-384.

Berridge, M.J., and Irvine, R.F (1989) Inositol phosphates and cell signalling. Nature 341: 197-205.

Berridge, M.J (1993) Inositol phosphates and calcium signalling. Nature 361: 315-325.

Bers, D.M (1991) Excitation – contraction coupling and cardiac contractile force, Kluwer Academic Press, Dordrecht, pp. 254.

Biel, M., Ruth, P., hullin, R., Stuhmer, W., Flockerzi, V. and Hofmann, R (1990) Primary

structure and functional expression of a high voltage activated calcium channel from rabbit lung. FEBS Lett 269: 409-412.

Blaustein, M.P (1988) Calcium transport and buffering in neurons. Trends in Neurosci 11: 438-443.

Blinks, J.R. Wier, W.G., Hess, P. and Prendergast, F.G (1982) Measurement of Ca2+ concentrations in living cells. Prog Biophys Biochem Mol Biol 40: 1-114.

Booth, C.L., Pulaski, L., Gottesman, M. M., and Pastan, I (2000) Analysis of the properties of the N-terminal nucleotide-binding domain of human P-glycoprotein. Biochemistry 39: 5518-5526.

Bunemann, M., Gerhardstein B.L., Gao, T. and Hosey, M. M (1999) Functional regulation of L-type calcium channels via protein kinase A-mediated phosphorylation of the ß2 subunit. J Biolo Chem 274 (48): 33851-54.

Busa, W.B (1996) Regulation of intracellular free calcium transport In: Molecular Biology of Membrane Transport Disorders, edited by S.G. Schultz et al. pp. 427-446. Plenum Press, New York.

Bye, N., Zieba, M., Wreford N.G., Nichols N.R (2001) Resistance of the dentate gyrus to induced apoptosis during ageing is associated with increases in transforming growth factor-beta1 messenger RNA. Neuroscience 105(4): 853-62

Byk, T., Dbransky T., Cifuentes-Diaz C., Sobel, A (1996) Identification and molecular characterization of unc-33-like phosphoprotein (Ulip), a putative mammalian homolog of the axonal guidance-associated unc-33 gene product. J Neurosci 16: 688-701.

Byk, T., Ozon, S., Sobel A (1998) The Ulip family phosphoproteins: common and specific properties. Eur J Biochem 254:14-24.

Cachelin, A.B., DePeyer, J.E., Kokubun, S., Reuter, H (1983) Ca^{2+} channel modulation by 8-bromocyclic AMP in cultured heart cells. Nature 304: 462-464.

Callewaert, G., Cleemann, L., Morad, M (1988) Epinepherine enhances Ca^{2+}current-regulated Ca^{2+}release and Ca^{2+} re-uptake in rat ventricular myocytes. Proc Natl Acad Sci USA. 85: 2009-2013.

Cameron, H.A., McEwen B.S. and Gould E (1995) Regulation of adult neurogenesis by excitatory input and NMDA receptor activation in the dentate gyrus. J Neurosci 15: 4687-4692.

Cameron, H.A. and McKay R.D (2001) Adult neurogenesis produces a large pool of new granule cells in the dentate gyrus. J Comp Neurol 435: 406-417.

Cameron, H.A., Woolley C.S., McEwen B.S. and Gould E (1993) Differentiation of newly born neurons and glia in the dentate gyrus of the adult rat. Neuroscience 56: 337-344.

Campbell, K.P., Leung, A.T., Sharp, A.H (1988) The biochemistry and molecular biology of the dihydropyridine-sensitive calcium channel. Trends Neurosci. 11: 425-30.

Campbell, L.W., Hao, S.Y., Thibault, O., Blalock, E.M., Landfield, P.W (1996) Aging changes in voltage-gated calcium currents in hippocampal CA1 neurons. J Neurosci. 16: 6286-6295.

Carafoli, E (1992) the Ca^{2+} pump of the plasma membrane. J Biol Chem 267: 2115-2118.

Carafoli, E (1987) Intracellular calcium homeostasis. Annu Rev Biochem 56: 395-433.

Castellano, A., Wei, X., Bimbaumer, V., and Perez-Reycs, E (1993) Cloning and expression of a third calcium channel ß subunit. J Biol Chem 268:3450-3455.

Catalano, S.M, Messersmith E.K., Goodman, C.S., Shatz, C.J., Chedotal, A (1998) Many major CNS axon projections develop normally in the absence of semaphorin III. Mol Cell Neurosci 11(4): 173-82.

Catterall, W.A., Seagar, M.J., and Takahashi, M (1988) Molecular properties of the dihydropyridine-sensitive calcium channel. J Biol Chem 263: 3535-3538.

Catterall W.A (1995) Structure and function of voltage-gated ion channels. Annu Rev Biochem 64: 493-531.

Celio, M.R (1990) Calbindin-D_{28k} and parvalbumin in the rat nervous system. Neuroscience 35: 375-475.

Challacombe, J.F., Snow D.M., Letourneau P.C (1997) Dynamic microtubule ends are required for growth cone turning to avoid an inhibitory guidance cue. J Neurosci 17(9): 3085-95

Charnet, P., Richard, S., Gurney, A.M., Ouadid, H., Tiaho, F., and Nargeot, J (1991) Modulation of Ca^{2+} currents in isolated frog heart atrial cells studied with phosphosensitive probes. Regulation by cAMP and Ca^{2+}: a common pathway. J Mol Cell Cardiol 23(3): 343-356.

Chang, C.T., Wu, C.S. and Yang, J.T (1978) Circular dichroic analysis of protein concentration: Inclusion of the ß-turn. Anal Biochem 91: 13-31.

Cheng, K., and Koland, J.G (1996) Nucleotide binding by the epidermal growth factor receptor protein-tyrosine kinase. J Biol Chem 271: 311-318.

Choi, D.W (1988) Glutamate toxicity and diseases of the nervous system. Neuron 1: 623-634.

Chung, Y.H., Shin, C.M., Kim, M.J., Shin, D.H., Yoo, Y.B., Cha, C.I. (2001) Differential alterations in the distribution of voltage-gated calcium channels in aged rat cerebellum. Brain Res 903(1-2):247-252

Ciapa, B., Pesando, D., Wilding, M., Whitaker, M (1994) Cell-cycle calcium transients driven by cyclic changes in inositol trisphosphate levels. Nature 368(6474): 875-878

Ciaroni, S., Cecchini, T., Ferri, P., Ambrogini, P., Cuppini, R., Riccio, M., Lombardelli G., Papa, S., Del Grande P (2002) Impairment of neural precursor proliferation increases survival of cell progeny in the adult rat dentate gyrus. Mech Ageing Dev 123(10):1341

Clapper, D.L., Walseth, T.F., Dargie, P.J., et al (1987) Pyridine nucleotide metabolites stimulate calcium release from sea urchin egg microsomes desensitized to inositol triphosphate. J Biol Chem 267: 15475-15484.

Clark, R.F., Goate A.M (1993) Molecular genetics of Alzheimer's disease. Arch Neurol 50: 1164-1172.

Cobbold, P.H., and Bourne, P.K (1984) Aequorin measurements of free calcium in single heart cells. Nature (Lond.). 312: 444-446.

Collin, T., Wang, J-J., Nargeot, J., Schwartz, A (1993) Molecular cloning of three isoforms of the L-type voltage-dependent calcium channel ß subunit from human heart. Circ. Res. 72: 1337-1344.

Creighton, T.E (1984) Proteins, sructure and molecular biology properties. W.H. Freeman and Company New York.

Crespo, D., Stanfield B.B., Cowan W.M (1986) Evidence that late-generated granule cells do not simply replace earlier formed neurons in the rat dentate gyrus. Exp Brain Res 62(3): 541-8

Curtis, B.M., and Catteral, W.A (1987) Reconstitution of the voltage-sensitive calcium channel purified from skeletal muscle transverse tubules. Biochemistry 25(11): 3077-3083.

De Jong, K.S., Murphy, B.J., Colvin, A. A., Hell, W.J., Takahashi, M. aand Catterall, W.A (1996) Specific phosphorylation of a site in the full-length form of the alpha 1 subunit of the cardiac L-type calciumchannel by adenosine 3', 5'-cyclic monophosphate-dependent protein kinase. Biochemistry 35:10392-10402.

Demaurex, N., Romanek R., Orlowski J., and Grinstein, S (1997) ATP dependent of Na+ / H+ exchange: nucleotide specificity and assessment of the role of phospholipids. J Gen Physiol 109: 117-128.

Deutsch, N., Klitzner, T.S., Lamp S.T., Weiss J. N (1991) Activation of cardiac ATP-sensitive K+ current during hypoxia: correlation with tissue ATP levels. Am J Physiol 261: H671-676

Diebold, R.J., W.J. Koch, P. T. Ellinor, J-J. Wang, M. Muthuchamy, D.I & A. Schwartz (1992) Mutually exclusive exon splicing of the cardiac calcium channel α1, subunit gene generates developmentally regulated isoforms in the rat heart. Pro Sci USA 89: 1497-1501.

Di Lisa, F., Gambassi, G., Spurgeon, H., and Hansford, R.G (1993) Intramitochondrial free calcium in cardiac myocytes in relation to dehydrogenase activation. Cardiovasc Res 27:1840-1844.

DiPolo, R., Beauge, L (1993) In squid axons the Ca2+i regulatory site of the Na+/Ca2+ exchanger idrastically modified by sulfhydryl blocking agents. Evidences that intracellular Ca2+i regulatory and transport sites are different. Biochim Biophys Acta 1145(1): 75-84

Doetsch, F., Garcia-Verdugo, J.M, Alvarez-Buylla A (1999) Regeneration of a germinal layer in the adult mammalian brain. Proc Natl Acad Sci U S A 96(20): 11619-24

Doherty, P., Cohen J., Walsh F.S (1990) Neurite outgrowth in response to transfected N-CAM changes during development and is modulated by polysialic acid. Neuron 5(2): 209-19

Dooley, D.J., Licker, M. Lupp A., and Osswald H (1988) Distribution of [125I]ω-conotoxin GVIA and [^{3}H]isradipine binding sites in the central nervous system of rats of different ages. Neurosci Letters,**93**: 318-323.

Drain, P., Li, L., and Wang, J (1998) K_{ATP} channel inhibition by ATP requires distinct functional domains of the cytoplasmic C terminus of the pore-forming subunit. Proc Natl Acad Sci USA. 95: 13953-13958.

Dunlop, K., Luebke, J.I., Turner, T.J (1995) Exocytosis Ca^{2+} channels in mammalian central neurons. Trends Neurosci 18: 89-98.

Ellinor, P.T., Zhang, J.F., Randall, A.D., Zhou, M., Schwartz, T.L., Tsien, R.W. and Horne, W.A (1995) Functional expression of a rapidly inactivating neuronal calcium channel. Nature 363: 455-458.

Eriksson, P.S., Perfilieva, E., Bjork-Eriksson, T., Alborn, A.M., Nordborg, C., Peterson, D.A. and Gage F.H (1998) Neurogenesis in the adult human hippocampus. Nat Med **4,** 1313-1317.

Fabiato, A (1985) Time and calcium dependence of activation and inactivation of calcium –induced release of calcium from the sarcoplasmic reticulum of a skinned canine cardiac Purkinje cell. J Gen Physiol 85: 247-2489.

Fabiato, A (1989) Appraisal of the physiological relevance of two hypotheses for the mechanism of calcium release from the mammalian cardiac sarcoplasmic reticulum: Calcium-induced release versus charge-coupled release. Mol Cell Biochem 89:135-140.

Fischer, A.J, Reh, T.A (2001) Muller glia are a potential source of neural regeneration in the postnatal chicken retina. Nat Neurosci 4(3): 247-52

Florke, H., Thinnes, F.M., Winkelbach, H., Stadtmuller, U., Paetzold, G., and et al (1994) Channl active mammalian porin, purified from crude membrane fractions of human B lymphocytes and bovine skeletal muscle, reversibly binds adenosine triphosphate (ATP). Biol Chem Hoppe-Seyler 375: 513-520.

Ford, C.F., Ilari, S. and Glatz, C. E (1991) Fusion tails for the recovery and purification of recombinant proteins. Protein Expression and Purification 2: 95-107.

Fosset, M., Jaimovich, E., Delpont, E.m Lazdunski, M (1983) [^{3}H] nitrendipine receptors in skeletal muscle. J Biol Chem 258: 6086-92.

Fox, A.P., Nowycky, M.C. and Tsien, R.W (1987a) Kinetic and pharmacological properties distinguishing three types of calcium currents in chick sensory neurones. J Physiol (Lond) 394: 149-172.

Fox, A.P., Nowycky, M.C. and Tsien, R.W. (1987b) Single channel recordings of three

types of calcium channels in chick sensory neurones. J Physiol (Lond) 394: 173-200.

Francis, S.H. and Corbin, J.D (1994) Structure and function of cyclic nucleotide-dependent protein kinases. Annu Rev Physiol 56:237-272

Francis, F, Koulakoff, A, Boucher, D, Chafey, P, Schaar, B, Vinet, MC,Friocourt, G,McDonnell, N, Reiner O, Kahn ,A, McConnell, SK, Berwald-Netter,Y, Denoulet, P, Chelly, J (1999) Doublecortin is a developmentally regulated, microtubule-associated protein expressed in migrating and differentiating neurons. Neuron 23(2): 247-56

Fukata, Y, Itoh, T.J., Kimura, T., Menager, C., Nishimura T, Shiromizu, T., Watanabe H., Inagaki, N., Iwamatsu, A., Hotani, H., Kaibuchi, K (2002) CRMP-2 binds to tubulin heterodimers to promote microtubule assembly. Nat Cell Biol 4(8):583-91.

Gage F.H., Kempermann, G., Palmer, T.D., Pherson, D.A., Ray, J (1998) Multipotent progenitor cells in the adult dentate gyrus. J Neurobiol 36(2): 249-66.

Gaetano, C., Matsuo, T., Thiele C.J (1997) Identification and characterization of a retinoic acid-regulated human homologue of the unc-33-like phosphoprotein (h Ulip) from neuroblastoma cells. J Boil Chem 272: 12195-12201.

Galione, A., Lee, H.C., Busa, W.B (1991) Ca - induced Ca release in sea urchin egg homogenates: Modulation by cyclic ADP- ribose. Science 253:1143-1146.

Gao, T., Yatani, A., Dell'Acqua, M.L., Sako, H., Green, S.A., Dascal, N., ScottJ.D., and Hosey, M.M (1997) cAMP- dependent regulation of cardiac L-type Ca^{2+} channels require membrane targetting of PKA and phosphorylation of channel subunits. Neuron19: 185-196.

Geinisman, Y., de Toledo-Morrell L., Morrell, F. and Heller, R.E (1995) Hippocampal markers of age-related memory dysfunction: behavioral, electrophysiological and morphological perspectives. Prog Neurobiol. 45: 223-252.

Gibson, G.E., Peterson, C (1987) Calcium and the aging nervous system. Neurobiol. Aging 8: 329-343.

Ghosh, A., Greenberg M.E (1995) Calcium signaling in neurons: molecular mechanisms and cellular consequences. Science 268(5208): 239-47

Ghosh, A., Ginty, D.D., Bading, H., Greenberg, M.E (1994) Calcium regulation of gene expression in neuronal cells. J Neurobiol 25(3): 294-303

Gleeson, J.G., Allen, K.M., Fox, J.W., Lamperti, E.D., Berkovic, S., Scheffer, I., Cooper E,C., Dobyns, W.B., Minnerath, S.R., Ross, M.E., Walsh, CA (1998) Doublecortin, an brain-specific gene mutated in human X-linked lissencephaly and double cortex syndrome, encodes a putative signaling protein. Cell 92:63-72.

Gleeson, J.G., Lin, P.T., Flanagan, L.A., Walsh, C.A (1999) Doublecortin is a microtubule-associated protein and is expressed widely by migrating neurons. Neuron 23: 257-271.

Goldhaber, J.I., Parker, J.M. and Weiss, J. N (1991) Mechnaisms of excitation-contraction coupling failure during metabolic inhibition in guinea-pig ventricular myocytes. J Physiol (Lond) 443: 371-386.

Golik, A. Kadar, T., Raveh, L., Modai, D., Weissman, B.A (1992) Aging does not alter the binding characterstics to voltage dependent calcium channels in the brain of CW1 mice. J Basic Clin Physiol Pharmacol 3(2): 109-118.

Goshima, Y., Nakamura, F., Strittmatter, P., Strittmatter, S.M (1995) Collapsin-induced growth cone collapse mediated by an intracellular protein related to UNC-33. Nature 376(6540): 509-14.

Gould, E., McEwen, B.S., Tanapat, P., Galea, L.A. and Fuchs, E (1997) Neurogenesis in the dentate gyrus of the adult tree shrew is regulated by psychosocial stress and NMDA receptor activation. J Neurosci 17: 2492-2498.

Gould, E., Tanapat, P., McEwen B.S., Flugge, G. and Fuchs E (1998) Proliferation of granule cell precursors in the dentate gyrus of adult monkeys is diminished by stress. Proc Natl Acad Sci U.S.A 95: 3168-3171.

Gould, E. and Tanapat P (1999) Stress and hippocampal neurogenesis. Biol Psychiatry 46: 1472-1479.

Gould, E., Beylin, A., Tanapat, P., Reeves, A. and Shors T.J (1999) Learning enhances adult neurogenesis in the hippocampal formation. Nat Neurosci 2: 260-265.

Gould, E., Gross, CG. (2002) Neurogenesis in adult mammals: some progress and problems. J Neurosci 22(3): 619-23

Govoni, S., Rius, R.A., Battaini F., Bianchi A.and Trabucchi M (1985) Age-Related reduced affinity in [^{3}H]nitrendipine labeling of brain voltage dependent calcium channels. Brain Res 333: 374-377.

Gu, Y, Hamajima, N., Ihara, Y (2000) Neurofibrillary tangle-associated collapsin response mediator protein-2 (CRMP-2) is highly phosphorylated on Thr-509, Ser-518, and Ser-522. Biochemistry 39(15): 4267-75

Gu, Y., Ihara, Y (2000) Evidence that collapsing response mediator protein-2 is involved in the dynamics of microtubules. J Biol Chem 275(24): 17917-20.

Gurnett, C.A., DeWaard, M., Campbell, K.P (1996) Dual function of the voltage-dependent Ca^{2+} $\alpha_2\delta$ subunit in current stimulation and subunit interation. Neuron 16: 431-440.

Hake, D.J. and Dixon, J.E (1992) New vectors for High level expression of recombinant proteins in bacteia. Analytical Biochem 202: 293-298.

Hamada, k, Yamazaki, J., Nagao, T (1998) Shortening of monophasic action potential duration during hyperkalemia and myocardial ischemia in anesthetized dogs. Jpn J Pharmacol 76(2): 149-154.

Hansford, R.G (1991) Dehydrogenase activation by Ca^{2+} in cells and tissues. J Bioenerg Biomem 23: 823-854.

Hartmann, H. et al (1996a) Down-regulation of free intracellular calcium in dissociated brain cells of aged mice and rats. Life Sci 59: 435-449.

Hartmann, H. et al (1996b) Region-specific down regulation of free intracellular calcium in the aged rat brain. Neurobiol Aging 17: 557-563.

Hartshorne, R,P. and Catterall, W.A (1984) The sodium channel from rat brain. Purification and subunit composition. J Biol Chem 259: 1667-1765.

Hartzell, H. C. and Fischmeister, R (1987) Effect of forsklin and acetylcholine on calcium current in single isolated cardiac myocytes. Molec Pharm 32: 639-645.

Heilbrunn, L.V (1965) The action of calcium on muscle protoplasm. Physiol Zool 13: 88-94

Hennesseg, J.P.Jr. and Johnson, W.C.Jr (1981) Information content in the circular dichroism of proteins. Biochemistry 20: 1085-1094.

Henzi, V., McDermott, A.B (1992) Characreristics and function of Ca2+ and inositol 1,4,5-triphosphate-releasable stores of Ca2+ in neurones. Neuroscience 46: 251-274.

Hescheler, J., Kameyama, M., Trautwein, W., Mieskes, G. and Soling, H.D (1987) regulation of the cardiac calcium channel by protein phosphatases. Eur J Biochem 165: 261-266.

Hescheler, J., Mieskes, G., Ruegg, J. C., Takai, A. and Trautwein, W (1988) Effects of a protein phosphatase inhibitor, okadaic acid, on membrane currents of isolated guinea-pig cardiac myocytes. Pflugers Arch 412: 248-252.

Hess, P (1990) Calcium channels in vertebrate cells. Annu Rev Neurosci 13: 1337-1356.

Hillman, D., Chen, S., Aung, T.T., Cherksey, B., Sugimori, M.and Llinas, R.R (1991) Localization of P-type calcium channels in the central nervous system. Proc Natl Acad Sci U.S.A. 88: 7076-7080.

Hofmann, F., Biel, M., and Flockerzi, V (1994) Molecular basis for Ca^{2+} channel diversity. Ann Rev Neurosci 17: 399-418.

Holliday, J., Adams R.J., Sejnowski, T.J., Spitzer, N.C (1991) Calcium-induced release of calcium regulates differentiation of cultured spinal neurons. Neuron 7(5): 787-96

Huang, L, DeVries G.J., Bittman, E.L (1998) Photoperiod regulates neuronal bromodeoxyuridine labeling in the brain of a seasonally breeding mammal. J Neurobiol 36(3): 410-20

Hullin, R., Singer-Lahat, D., Freichel, M., Dascal, N., Hofmann, F., and Flockerzi, V (1992). Calcium channel ß subunit heterogeneity: functional expression of cloned cDNA from heart, aorta and brain. EMBO J 11: 885-890.

Hymel, L., Schindler, H., Inui, M., et al (1988) Reconstitution of purified cardiac muscle calcium release channel (ryanodine receptor) in planar bilayers. Biochem Biophys Res Commun 152: 308-314.

Irisawa, H., Kokubun, S (1983) Modulation by intracellular ATP of the slow inward current in isolated single ventricular cells of the guinea pig. J Physiol (Lond) 333: 321-337.

Isbister, C.M., O'Connor T.P (2000) Mechanisms of growth cone guidance and motility in the developing grasshopper embryo. J Neurobiol 44(2):271-80

Jaffe, D.B., Fisher, S.A.,and Brown, T.H (1994) Confocal laser scanning microscopy reveals voltage-gated signals within hippocampal dendritic spines. J Neurobiol 25: 220-233.

Johnson, E.M Jr., Deckwerth, T.L (1993) Molecular mechanisms of developmental neuronal death. Annu Rev Neurosci 16: 31-46

Jones, O.T. and So, A.P (1993) preparation and characterization of biotinylated analogs of ω-conotoxin. Anal Biochem 214: 227-232.

Jones, O.T., Bernstein, G.M., Jones, E.J., Jugloff, D.G.M., Law, M., Wong, W., Mills, L.R (1997) N-type calcium channels in the developing rat hippocampus: subunit, complex, and regional expression. J Neurosci 17: 6152-6164.

Jorgensen, O.S (1995) Neural cell adhesion molecule (NCAM) as a quantitative marker in synaptic remodeling. Neurochem Res 20(5):533-547.

Kagoshima, M., Ito, T (2001) Diverse gene expression and function of semaphorins in developing lung: positive and negative regulatory roles of semaphorins in lung branching morphogenesis. Genes Cells 6(6): 559-71.

Kameyama, M., Hofmann, F., Trautwein, W (1985) On the mechanism of beta-adrenergic regulation of the Ca channel in guinea-pig heart. Pflugers Arch 405(3): 285-93.

Kaplan, M.S., Bell, D.H (1984) Mitotic neuroblasts in the 9-day-old and 11-month-old rodent hippocampus. J Neurosci 4(6):1429-41.

Kaplan, M.S., Hinds, J.W (1977) Neurogenesis in the adult rat: electron microscopic analysis of light radioautographs. Science 197: 1092-1094.

Katz, B. and Miledi, R (1965) The effect of calcium on acetycholine release from motor nerve terminals. Proc.R. Soc. London Ser. B 161:496-503.

Kee, N.J, Preston E, Wojtowicz J.M (2001) Enhanced neurogenesis after transient global ischemia in the dentate gyrus of the rat. Exp Brain Res 136(3):313-20.

Kee, N., Sivalingam, S., Boonstra, R., Wojtowicz, J.M (2002) The utility of Ki-67 and BrdU as proliferative markers of adult neurogenesis. J Neurosci Methods. 115(1):97-105.

Kempermann, G., Kuhn, H.G. and Gage F.H (1997) More hippocampal neurons in adult mice living in an enriched environment. Nature 386: 493-495.

Khachaturian, Z.S (1984) Towards theories of brain aging. In Handbook of Studies in Old Age. Kay, D.W. & Burrows, G.D. Eds. 7-30. Elsevier. New York.

Khachaturian, Z.S (1994) The calcium hypothesis of Alzheimer's disease and brain aging. Ann N. Y. Acad Sci 747: 1-11.

Kim, H-L., Kim, H., Lee, P., King, R.G., and Chin, H (1992) Rat brain expresses an Alternatively spliced form of the dihydropyridine-sensitive L-type calcium channel α2 subunit. Pro. Nat. Sci U.S.A. 89: 3251-3255.

Kimura, S., Bassett, A.I., Furukawa, T., Furukawa, N., Myerburg, R.J (1991) Differences in the effect of metabolic inhibition on action potentials and calcium currents in endocardial and epicardial cells. Circulation 84(2): 768-77

Koch, W.J., Ellinor, P.T. and Schwartz, A (1990) cDNA cloning of a dihydropyridine-sensitive calcium channel from rat aorta. J Biol Chem 265: 17786-17791.

Komuro, H., Rakic, P (1996) Intracellular Ca2+ fluctuations modulate the rate of neuronal migration. Neuron 17(2): 275-85

Koshiyama, H., Lee, H. C., and Tashjian A.H., jr (1991) Novel mechanism of intracellular calcium release in pituitary cells. J Biol Chem 266:16985-16988.

Krinke, G.J. and Eisenbrandt, D.L (1995) Nonneoplastic changes in the brain. In Pathobiology of the Aging Rat.Mohr. Eds. U Dungworth, D.L. Capen, C.C.ILSI press. pp. 4-19.

Kuga, T., Kobayashi, S., Hirakawa, Y., Kanaide, H., Takeshita, A (1996) Cell cycle-dependent expression of L- and T-type Ca2+ currents in rat aortic. Circ Res 79(1): 14-9

Kuhn, H.G., Dickinson-Anson, H. and Gage, F.H (1996) Neurogenesis in the dentate gyrus of the adult rat: age-related decrease of neuronal progenitor proliferation. J Neurosci 16: 2027-2033.

Laemmli, U.K (1970) Cleavage of structural proteins during the assembly of the head bacteriophage T4. Nature 227: 680-685.

Landfield, P.W (1994) Increased hippocampal Ca^{2+} channel activity in brain aging and dementia. Hormonal and pharmacologic Modulation. Ann. N.Y. Acad Sci 747: 351-364.

Landfield, P.W., Pitler, T.A (1984) Prolonged Ca^{2+}-dependent after hyperpolarizations in hippocampal neurons of aged rats. Science 226: 1089-1092.

Lee, H.R, Roeske, W.R. and Yamamura H.I (1984) High affinity specific [^{3}H](+)PN200-110 binding to dihydropyridine receptors associated with calcium in rat cerebral cortex and heart. Life Science 35:721-732.

Lendon, C.L., Ashall, F., and Goate, A. M (1997) Exploring the etiology of Alzheimer disease using molecular genetics. JAMA 227: 825-831.

Llinas, R.R (1988) The intrinsic electrophysiological properties of mammalian neurons: insights into central nervous system function. Science 242:1654-1664.

Llinas, R., Sugiomori, M. and Silver, R.B (1992) Microdomains of high calcium concentration in a presynaptic terminal. Science 262: 677-679.

Lobner, D., and Lipton, P (1993) Intracellular calcium levels and calcium fluxes in the CA1 region of the rat hippocampal slice during in vitro ischemia: relationship to electrophysiological cell damage. J Neurosci 13(11): 4861-71

Lois, C. and Alvarez-Buylla A (1993) Proliferating subventricular zone cells in the adult mammalian forebrain can differentiate into neurons and glia. Proc Natl Acad Sci U.S.A 90: 2074-2077.

Losito, V.A., Tsushima, R.G., Diaz, R.J., Wilson, G.J., Backx, P.H (1998) Preferential regulation of rabbit cardiac L-type Ca2+ current by glycolytic derived ATP via a direct allosteric pathway. J Physiol 511 (Pt 1):67-78

Magavi, S.S., Leavitt, B.R., Macklis, J.D (2000) Induction of neurogenesis in the neocortex of adult mice. Nature 405(6789):951-5.

Martinez, A., Victoria, J. and Satrustegui, J (1988) Cytosolic free calcium levels increase with age in rat brain synaptosomes. Neurosci Lett 88: 336-342.

Mattson, M.P., Barger, S.W., Cheng, B., Lieberburg, I., Smith-Swintosky, VL, Rydel, R.E (1993) beta-Amyloid precursor protein metabolites and loss of neuronal Ca2+ homeostasis in Alzheimer's disease. Trends Neurosci 16(10): 409-14

McEntee, W.J. and Rook, T.H (1993) Glutamate: its role in learning, memory and the aging brain. Psycopharmacology 111: 391-401.

McEwen, B.S. (1999) Stress and hippocampal plasticity. Annu.Rev.Neurosci. **22,** 105-122.

McGraw, C.F, Somlyo, A.V., Blaustein, M.P (1980 a) Probing for calcium at presynaptic nerve terminals. Fed Proc . 39(10): 2796-801

McGraw, C.F., Somlyo, A.V., Blaustein, M.P (1980 b). Localization of calcium in presynaptic nerve terminals. An ultrastructural and electron microprobe analysis. J Cell Biol 85(2): 228-41

McNamara, J.O (1994) Cellular and molecular basis of epilepsy. J Neurosci 14(6):3413-25

Mikami, A., Imoto, K., Tanabe, T., Niidome, T., Mori, Y., Takashima, H (1989) Primary

structure and functional expression of the cardiac dihydropyridine-sensitive calcium channel. Nature 340: 230-233.

Miller, R.J (1992) Voltage - sensitive Ca^{2+} channels. J.Biol. Chem 267: 1403-1406.

Mills, L.R. and Kater, S.B (1990) Neuron - specific and state- specific differences in calcium homeostasis regulate the generation and degeneration of neuronal architecture. Neuron 4: 149-163.

Minturn, J.E., Fryer, H.J, Geschwind, D.H., Hockfield, S (1995) TOAD-64, a gene expressed early in neuronal differentiation in the rat, is related to unc-33, a C. elegans gene involved in axon outgrowth. J Neurosci 15: 6757-6766.

Mitterdorfer, J., Froschmayr, M., Grabner, M., Moebius, F.F., Glossmann, H. and Striessnig, J (1996) Identification of PK-A phosphorylation sites in carboxyl terminus of L-type calcium channel alpha 1 subunits. Biochemistry 35: 9400-9406.

Morad, M., Sander, C. and Weiss, J (1981) The inotropic actions of adrenaline on frog ventricular muscle: relaxing versus potentiating effects. J Physiol 311: 585-604.

Morad, M., and Cleemann, L (1987) Role of Ca^{2+} channel in development of tension in heart muscle. J molec Cell Cardio 19: 527-553.

Moresco, R.M., Govoni, S., Battaini, F., Trivulzio, S., and Trabucchi, M (1989) Omegaconotoxin binding decreases in aged rat brain. Neurobiol of Aging 11: 433-436.

Morris R. (1984) Developments of a water-maze procedure for studying spatial learning in the rat. J Neurosci Methods 11(1):47-60

Morris, R.G., Hagan, J.J., Nadel, L., Jensen, J., Baudry, M., Lynch, G.S (1987) Spatial learning in the rat: impairment induced by the thiol-proteinase inhibitor, leupeptin, and an analysis of [3H] glutamate receptor binding in relation to learning. Behav Neural Biol 47(3): 333-45

Moutin, M-J., Cuillel, M., Rapin , C., Miraz, R., Anger, M., Lompre, A-M., and Dupont, Y (1994) Measurements of ATP binding on the large cytoplasmic loop of the sarcoplasmic reticulum Ca(2+)-ATPase overexpressed in Escherichia coli. J Biol Chem 269: 11147-11154.

Mullen, R.J., Buck, C.R., Smith, A.M (1992) NeuN, a neuronal specific nuclear protein in vertebrates.Development116(1):201-11

Munaron, L., Antoniotti, S., Distasi, C., Lovisolo, D (1997) Arachidonic acid mediates calcium influx induced by basic fibroblast growth factor in Balb-c 3T3 fibroblasts. Cell Calcium 22(3):179-88

Nabauer, M., Morad, M (1990) Ca^{2+}- induced Ca-release as examined by photolysis of caged Ca in single ventricular myocytes. Am J Physiol 258: C189-C193.

Nacher, J., Rosell D.R., McEwen, B.S (2000) Widespread expression of rat collapsing response-mediated protein 4 in the telencephalon and other areas of the adult rat central nervous system. J Comp Neurol 424(4): 628-39.

Nacher, J., Crespo, C., McEwen, B.S (2001) Doublecortin expression in the adult rat telencephalon. Eur J Neurosci 14(4): 629-44.

Nachshen, D.A., Sanchez-Armass, S., and Weinstein, A.M (1986) The regulation of cytosolic calcium in rat brain synaptosomes by sodium-dependent calcium efflux. J Physiol 381,:17-28.

Nakamura, F., Kalb, R.G., Srittmatter, S.M (2000) Molecular basis of semaphorin-mediated axon guidance. J Neurobiol 44(2): 219-29.

Nakafuku, M., Nargeot, J., Lory, P., and Richard, S (1997) Molecular basis of the diversity of calcium channels in cardiovascular tissues. Eur Heart J 18: A15-A26.

Nakatomi, H., Kuriu, T., Okabe, S., Yamamoto, S., Hatano, O., Kawahara, N., Tamura, A., Kirino, T (2002) Regeneration of hippocampal pyramidal neurons after ischemic brain injury by recruitment of endogenous neural progenitors. Cell 110(4): 429-41.

Nichols, N.R., Zieba, M., Bye, N (2001) Do glucocorticoids contribute to brain aging? Brain Res Brain Res Rev 37 (1-3): 273-86

Niggli, E., Lederer, W.J (1990) Voltage-independent calcium release in heart muscle. Science 250:565 –568.

Nilsson, M., Perfilieva, E., Johansson, U., Orwar, O. and Eriksson, P.S (1999) Enriched environment increases neurogenesis in the adult rat dentate gyrus and improves spatial memory. J Neurobiol 39: 569-578.

Nowycky, M.C., Fox, A.P., and Tsien, R.W (1985) Three types of neuronal calcium channel with different calcium agonist sensitivity. Nature 316: 440-443.

Oh, J.H., Easton, D., Murawski, M., Kaneko, Y., and Subjeck, J (1999) The chaproning activity of hsp110. J Biol Chem 274: 15712-15718.

Ohya, Y., and Sperelakis, N (1989) Modulation of single slow (L-type) calcium channels by intracellular ATP in vascular smooth muscle cells. Pflugers Arch 414: 257-264.

O'Kusky, J.R., Ye, P., D'Ercole, A.J (2000) Insulin-like growth factor-I promotes neurogenesis and synaptogenesis in the hippocampal dentate gyrus during postnatal development. J Neurosci 20(22): 8435-42.

Ono, K., and Giles, W.R (1991) Electrophysiological effects of calcitonin gene-related peptide bull frog and guinea-pig atrial myocytes. J Physiol (Lond) 436: 195-217.

O'Rourke, B., Reibel, D.K. and Thomas A.P (1990) High-speed digital imaging of cytosolic Ca^{2+} and contraction in single cardiomyocytes. Am J Physiol 259: H230-H242,

O'Rourke, B., Reibel, D.K. and Thomas, A. P (1992a) Alpha-adrenergic modification of the Ca^{2+} transient and contraction in single rat cardiomyocytes. J Mol Cell Cardiol 24: 802-820.

O'Rourke, B., Backx, P.H., and Marban, E (1992b) Phosphorylation-independent modulation of L-type calcium channels by magnesium-nucleotide complexes. Science 257: 245-248

O'Rourke, B (1993) Ion channels as sensor of cellular energy. Mechanism for modulation by magnesium and nucleotides. Biochem Pharmacol 46:1103-1112.

Parent, J.M., Yu, T.W., Leibowitz, R.T., Geschwind, D.H., Sloviter, R.S., Lowenstein D.H (1997) Dentate granule cell neurogenesis is increased by seizures and contributes to aberrant network reorganization in the adult rat hippocampus. J Neurosci 17: 3727-3738.

Parsons, T., D., Lagrutta, A., White, R.E., Hartzell, H. C (1991) Regulation of Ca^{2+} current in frog ventricular cardiomyocytes by 5'-guanylylimidodiphosphte and acetycholine. J Physiol (Lond) 432-593.

Payat, M.D., Schanne, O.F., RuiZ-Ceretti E, Demers, J.M (1978) Slow inward and outward currents of rat ventricular fibers under anoxia. J Physiol (Paris), 74(1): 31-5.

Peltzer, S., Shuba, Y.M., Asai, T., Codina, J., Birnbaumer, L., McDonald, T.F., et al (1990) Membrane-delimited stimulation of heart cell calcium current by beta-adrenergic signal-transducing Gs protein. Am J Physiol. 259(1pt 20: H264-7.

Pencea, V., Bingaman, K.D., Wiegand, S.J., Luskin, M.B (2001) Infusion of brain-derived neurotrophic factor into the lateral ventricle of the adult rat leads to new neurons in the parenchyma of the striatum, septum, thalamus, and hypothalamus. J Neurosci 21(17): 6706-17.

Peretto, P., Merighi, A., Fasolo, A., Bonfanti, L (1999) The subependymal layer in rodents: a site of structural plasticity and cell migration in the adult mammalian brain. Brain Res Bull 49(4): 221-43

Perez-Reyes, E., X. Wei, Castellano, A. and Birnbaumer,L (1990) Molecular diversity of L-type calcium channels. J Biol Chem 265: 20430-20436.

Perez-Reyes, E., . Kim, H.S., Lacerda, A.E., Ilorne, W., Wei, X.., Rampe, D., Campbell, K.P. Birnbaumer, L (1989) Induction of calcium currents by the expression of the α1- subunit of the dihydropyridine receptorfrom skeletal muscle. Nature 340: 233-236.

Porter, N.M., Thibault, O., Thibault, V., Chen, K-C., Landfield, P. W (1997) Calcium channel density and hippocampal cell death with age in long-term culture. J Neuroscience 17: 5629-39.

Pragnell, M., De Waard, M., Mori, Y., Tanabe, T., Snutch, T.P., Campbell, K.P (1994) Calcium channel beta-subunit binds to a conserved motif in the I-II cytoplasmic linker of the alpha 1-subunit [see comments]. Nature 368(6466): 67-70.

Purves, D., Hadley, R.D., Voyvodic, J.T (1986) Dynamic changes in the dendritic geometry of individual neurons visualized over periods of up to three months in the superior cervical ganglion of living mice. J Neurosci 6(4):1051-60.

Quinn, C.C., Gray, G.E., Hockfield, S (1999) A family of proteins implicated in axon guidance and outgrowth. J Neurobiol 41(1): 158-64.

Randak, C., Roscher, A.A., Hardorn, H-B., Assfalg-Machleidt, I., Auerswald, E.A., and Machleidt, W (1995) Expression and functional properties of the predicted nucleotide binding fold of the cystic fibrosis transmembrane conductance regulator fused to glutathione-S-transferase. FEBS Lett. 363: 189-194.

Randall, A. D., and Tsien, R.W (1995) Pharmacological dissection of multiple types of calcium channel currents in rat cerebellar granule neurons. J Neurosci 15: 2995-3012.

Randall, A., Benham, C.D (1999) Recent advances in the molecular understanding of voltage-gated Ca2+ channels. Mol Cell Neurosci 14(4-5):255-72

Reynolds, J.N. and Carlen, P.L (1989) Diminished calcium currents in aged hippocampal dentate gyrus granule neurons. Brain Res. 508: 384-390.

Ringer, S (1887) J Physiol Zool 13:88-94.

Reuter, H (1974) Localization of ß- adrennergic receptors, and effects of noradrenaline And cyclic nucleotides on action potentials, ionic currents and tension in mammalian cardiac muscle. J Physiol Lond 242: 429-451.

Roses, A.D (1996) The alzheimer diseases. Curr Op Neurobiol 6: 644-650.

Rougier, O., Vassort, G., Garnier, D., Gargouil, M., Coraboeuf, E (1969) Existence and role of a slow inward current during the frog atrial potential. Pflugers Arch 308: 91-110.

Schanne, F. A. X., Kane, A.B. Young, E.E. and Farber, J. L (1979) Calcium dependence of toxic cell death. Science 206: 700-702.

Schlessinger, A.R., Cowan, W.M. and Gottlieb, D.I (1975) An autoradiographic study of the time of origin and the pattern of granule cell migration in the dentate gyrus of the rat. J.Comp Neurol. 159: 149-175.

Schmidt, J.W. and Catteral, W.A (1986) Biosynthesis and processing of the α subunit of the voltage-sensitive sodium channel in rat brain neurons. Cell 46: 437-445.

Schoenmakers, T.J., Visser, G.J., Flik, G., Theuvenet, A.P (1992) CHELATOR: an improved method for computing metal ion concentrations in physiological solutions. Biotechniques 12(6):870-4, 876-9

Scholzen, T. and Gerdes J. (2000) The Ki-67 protein: from the known and the unknown. J Cell Physiol 182: 311-322.

Scott, B.W., Wang, S., Burnham, W.M., De Boni, U., Wojitowicz, J.M (1998) Kindling-induced neurogenesis in the dentate gyrus of the rat. Neurosci Lett 248:73-76.

Seki, T., Rutishauser, U (1998) Removal of polysialic acid-neural cell adhesion molecule induces aberrant mossy fiber innervation and ectopic synaptogenesis in the hippocampus. J Neuroscience 18(10): 3757-3766.

Seki, T. and Arai, Y (1993) Highly polysialylated neural cell adhesion molecule (NCAM-H) is expressed by newly generated granule cells in the dentate gyrus of the adult rat. J Neurosci 13: 2351-2358.

Seki, T. and Arai, Y (1996) Dendritic development of newly-generated granule cells in the adult hippocampus occurs upon contact with radial glia-like cells. Soc Neurosci Abstr 22:534.

Sharpe, C., Goldstone, K (2000) The control of Xenopus embryonic primary neurogenesis is mediated by retinoid signalling in the neurectoderm. Mech Dev 91(1-2): 69-80

Siddiqui, S.S (1990) Mutations affecting axonal growth and guidance of motor neurons and mechanosensory neurons in the nematode Caenorhabditis elegans. Neurosci Res 13(Suppl): 171-190.

Siddiqui, S.S., Culotti, J.G (1991) Examination of neurons in wild type and mutants of Caenorhabditis elegans using antibodies to horseradish peroxidase. J Neurogenet 7: 193-211.

Smith, D.B., and Johnson, K.S (1988) Single-step purification of polypeptides expressed in Escherichia coli as a fusion with glutathione-S-transferase. Gene 67: 31-40.

Smith, P.A., Rorsman, P., Ashcroft, F.M (1989) Modulation of dihydropyridine-sensitive Ca^{2+} channels by glucose metabolism in mouse pancreatic beta-cells. Nature. 30, 342: 550-553.

Smith, S.J., Augustine, G.J (1988) Calcium ions, active zones and synaptic transmitter release. Trends Neurosci 11(10): 458-64

Snutch, T.P., leonard, J.P., Gilbert, M.M., Lester, H.A., and Davidson, N (1990) Rat brain expresses a heterogeneous family of calcium channels. Proc Natl Acad Sci U.S.A. 87: 3391-3395.

Snutch, T.P. and Reiner, P.B (1992) Calcium channels: diversity of form and function. Curr Op Neurobiol 2: 247-253.

Snutch, T.p., Tomlinson, W.J., Leonard, J.P. and Gilbert, M.M (1991) Distinct calcium channels are generated by alternative splicing and are differentially expressed in the mammalian CNS. Neuron 7: 45-57.

Soldadov, N.M (1992) Molecular diversity of L-type calcium channel transcripts in human fibroblasts. Proc Natl Acad Sci USA 89: 4628-4632.

Soong, T.W., Stea, A., hodson, C.D., Dubel, S.J., Vincent, S.R. and Snutch, T.P (1993) Structure and functional expression of a member of the low voltage-activated calcium channel family. Science 260: 1133-1136.

Spitzer, N.C (1995) Spontaneous activity: functions of calcium transients in neuronal differentiation. Perspect Dev Neurobiol 2(4): 379-86

Squire, L.R (1992)Memory and the hippocampus: a synthesis from findings with rats, monkeys, and humans. Psychol Rev 99(2):195-231

Stanfield, B.B. and Trice, J.E (1988) Evidence that granule cells generated in the dentate gyrus of adult rats extend axonal projections. Exp Brain Res 72:399-406.

Striessnig J., Grabner, M., Mitterdorfer, J., Hering, S., Sinnegger, M.J. and Glossmann, H (1998) Structural basis of drug binding to L Ca^{2+} channels. TiPS, 19: 108-115.

Suga, H (1990) Ventricular energetics. Physiol Rev 70:247-277.

Sunshine, J., Balak, K., Rutishauser, U., Jacobson, M (1987) Changes in neural cell adhesion molecule (NCAM) structure during vertebrate neural development. Proc Natl Acad Sci U S A. 84(16): 5986-90

Takasawa, S., Nata, K., Yonekura, H., et al (1993) Cyclic ADP-ribose in insulin secretion from pancreatic ß cells. Science 259: 370-373.

Tanabe, T., Takeshima, H., Mikami, A., Flockerzi, V., Takahashi, H., Kangawa, K., Kojima, M., Matsuo, H., Hirose, T., and Numa, S (1987) Primary structure of the receptor for calcium channel blockers from skeletal muscle. Nature 328: 313-318.

Tanabe, K., Tucker, J.S., Matsuo, M., Proks, P., Ashcroft, F. M., Seino, S., Amachi, T., and Udea, K (1999) Direct photoaffinity labelling of the Kir6.2 subunit of the ATP-sensitive K+ channel by 8-azido-ATP. J Biol Chem 274(7): 3931-3933.

Tanaka, O., Sakagami, H., Kondo, H (1995) Localization of mRNAs of voltage-dependent Ca^{2+}channels: four subtypes of α1- and ß- subunits in developing and mature rat brain. Mol Brain Res 30:1-16

Tanaka, E.M., Kirschner, M.W (1991) Microtubule behavior in the growth cones of living neurons during axon elongation. J Cell Biol 115(2): 345-63

Tanapat, P., Galea, L.A. and Gould E (1998) Stress inhibits the proliferation of granule cell precursors in the developing dentate gyrus. Int J Dev Neurosci 16: 235-239.

Tanapat, P., Hastings, N.B., Reeves, A.J. and Gould E (1999) Estrogen stimulates a transient increase in the number of new neurons in the dentate gyrus of the adult female rat. J Neurosci. 19: 5792-5801.

Tanapat, P., Hastings, N.B., Rydel, T.A, Galea, L.A, Gould, E (2001) Exposure to fox odor inhibits cell proliferation in the hippocampus of adult rats via an adrenal hormone-dependent mechanism. J Comp Neurol 437(4): 496-504.

Tang, J., Landmesser, L., Rutishauser, U (1992) Polysialic acid influences specific pathfinding by avian motoneurons. Neuron 8(6): 1031-44

Taniguchi, J., Noma, A. and Irisawa, H (1983) Modification of the cardiac action potential by intracellular in jection of adenosine triphosphate and related substances in guinea pig single ventricular cells. Circulation Research 53: 131-139.

Tank, D.W., Sugiomori, M., Connor, J.A., Llinas, R.R (1988) Spatially resolved calcium dynamics of mammalian Purkinje cells in cerebellar slice. Science 242: 773-777.

Temple, S (2001) The development of neural stem cells. Nature 414(6859): 112-7

Thibault, O. and Landfield, P.W (1996) Increase in single L-type calcium channels in hippocamal neurons during aging. Science 272: 1017-1020.

Tollefson, G.D (1990) Short-term effects of the calcium channel blocker nimodipine (Bay-e-9736) in the management of primary degenerative dementia. Biol Psychiatry 27(10): 1133-42

Towbin, H., Staehelin. T., and Gordon, J (1979) Electrophoretic transfer of proteins from polyacrylamide gels to nitrocellulose sheets: Procedure and some applications. Proc anal Acad Sci USA 76: 4350-4354.

Traut, T.W (1994) the functions and consensus motifs of nine types of peptide segments that form different types of nucleotide-binding sites. Eur J Biochem 222(1): 9-19.

Trautwein, W. and Pelzer, D (1985) Voltage-dependent gating of single calcium channels in cardiac cell membrane and its modulation by drugs. In Calcium CELL Physiology (ed. D. Marme), pp. 53-93. Springer, Berlin.

Trautwein, W. and Cavalie, A (1985) Cardiac calcium channels and their control neurotransmitters and drugs. J Am Coll Cardiol 6: 1409-1416.

Trautwein, W. and Osterreider, W (1986) Mechanisms of ß-adrenergic and cholinergic control of Ca and K currents in the heart. In cardiac Muscle, The regulation of Excitation and Contraction (ed. R.D. Nathan).

Trautwein, W., and Heschler, J (1990) Regulation of cardiac L-type calcium current by phosphorylation and G proteins. Annu Rev Physiol 52: 257-274.

Tsien, R.W., Tsien, R. Y (1990) Calcium channels, stores and oscillations. Annu Rev Cell Biol 6: 715-760.

Tsien, R.W., Bean, B.P., Hess, P.Lansman, J.B., Nilius, B., and Nowycky, M.C (1986) Mechanisms of calcium channel modulation by ß-adrenergic agents and dihydropyridine calcium agonists. J Molec Cell Cardiol 18: 691-710.

Tsien, R.W (1977) Cyclic AMP and contractile activity in heart. Adv Cyclic Nucleotide Res. 8: 363-420.

Tsien, R.W., Giles, W.R. and Greengard, P (1972) Cyclic AMP mediates the effect of adrenaline on cardiac Purkinje fibers. Nature New Biol 240:181-183.

van Praag, H., Kempermann, G. and Gage F.H (1999) Running increases cell proliferation and neurogenesis in the adult mouse dentate gyrus. Nat Neurosci 2: 266-270.

van Praag, H., Schinder, A.F., Christie, B.R., Toni, N., Palmer, T.D., Gage, F.H (2002). Functional neurogenesis in the adult hippocampus. Nature 415(6875):1030-4

Vereecke, J.G. VDH, Isenberg, G., Carmeliet, E (1981) Voltage clamp analysis of the effect of dinitrophenol on single guinea-pig myocytes. Arch Int Physiol Biochem. 89: 35P.

Verkhratsky, A. and Toescu, E.C (1998) Calcium and Neuronal Aging. TINS 21(1): 2-7.

Villalba, M. et al (1995) Altered cell calcium regulation in synaptosome and brain cells of the 30-month-old rat: Prominent effect in hippocampus. Neurobiol. Aging. 16: 809-816.

Wahler, G.M., and Sperelakis, N (1986) Cholinergic attenuation of the electrophysiological effects of forsklin. J Cyclic Nucleotide Prot Phosphorylation Res 11: 1-10.

Walker, J.E., Saraste, M., Runswick, M.J., Gay, N.J (1982) Distantly related sequences in the alpha- and beta-subunits of ATP syntethase, myosin, kinases and other ATP-requiring enzymes and a common nucleotide binding fold. Embo J 1(8): 945-951.

Walsh, K.b., Begenisich, T.B., Kass, R.S (1989) Beta-adrenergic modulation of cardiac Ion channels. Differential temperature sensitivity of potassium and calcium currents. J Gen Physiol 93(5): 841-54.

Wang, L.H., Strittmatter, S.M (1996) A family of rat CRMP genes is differentially expressed in the nervous system. J Neurosci 16(19): 6197-207

Wang, S., Scott, B.W., Wojtowicz, J.M (2000) Heterogenous properties of dentate granule neurons in the adult rat. J Neurobiol 42(2): 248-57

Weiland, G.A., Oswald, R.E (1985) The mechanism of binding of dihydropyridine calcium channel blockers to rat brain membranes. J Biol Chem 260(14): 8456-8464.

Werth, J.L., and Thayler, S.A (1994) Mitochondria buffer physiological calcium loads in cultured rat dorsal root ganglion. J Neurosci 14: 348-356.

Wier, W.G (1990) Cytoplasmic [Ca^{2+}] in mammalian ventricle: dynamic control by cellular processes. Annu Rev Physiol 52: 467-485.

Winberg, M.L., Noordermeer, J.N., Tamagnone, L., Comoglio, P.M., Spriggs, M.K., Tessier-Lavigne M, Goodman CS (1998) Plexin A is a neuronal semaphorin receptor that controls axon guidance. Cell 95(7): 903-16.

Yamada, S.,Uchida, S., Ohkura, T., Kimura, R., Yamaguchi, M (1996) Alteration in calcium antagonist receptors and calcium content in senescent brain and attenuation by nimodipine. JPET 277: 721-727.

Yamamoto, S., Nagao, M., Sugimori, M., Kosako, H., Nakatomi, H., Yamamoto, N., Takebayashi, H., Nabeshima, Y., Kitamura, T., Weinmaster, G., Nakamura, K., Nakafuku, M (2001). Transcription factor expression and Notch-dependent regulation of neural progenitors in the adult rat spinal cord. J Neurosci 21(24): 9814-23

Yokoshiki, H., Katsube, Y., and Sperelakis, N (1997) Regulation of Ca^{2+} currents by intracellular ATP in smooth muscle cells of rat mesenteric artery. Ame J Physiol. 272: H814-819.

Yoshida, H., Watanabe, A., Ihara, Y (1998) Collapsin response mediator protein-2 is associated with neurofibrillary tangles in Alzheimer's disease. J Biol Chem 273(16): 9761-8

Zhang, J.F., Randall, A.D., Ellinor, P.T., Horne, W.A. Sather, W.A., Tanabe, T., Schwartz, T.L., and Tsien, R.W (1993) Distinctive pharmacology and kinetics of cloned neuronal Ca^{2+} channels and their possible counterparts in mammalian CNS neurons. Neuropharmacol 32: 1075-1088.

Zuhlke, R.D., Pitt, G.S., Deisseroth, K., Tsien, R.W., Reuter, H (1999) Calmodulin supports both inactivation and facilitation of L-type calcium channels [see comments]. Nature 399: 159-162.